



HOMOGENOUS CATALYTIC / PHOTOCATALYTIC CO₂ CONVERSION INVOLVING VERSATILE, NON-COSTLY METAL COMPLEXES

Nassima El Aouni

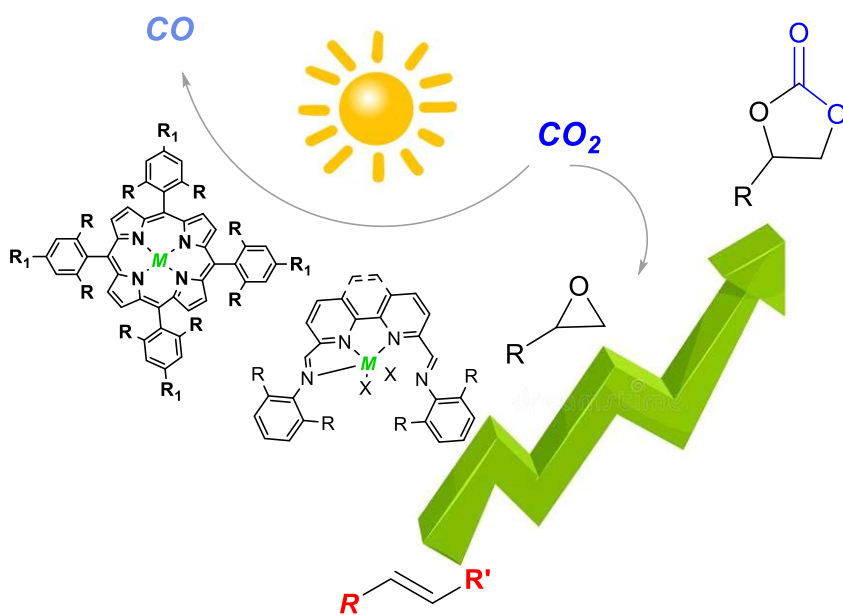
ADVERTIMENT. L'accés als continguts d'aquesta tesi doctoral i la seva utilització ha de respectar els drets de la persona autora. Pot ser utilitzada per a consulta o estudi personal, així com en activitats o materials d'investigació i docència en els termes establerts a l'art. 32 del Text Refós de la Llei de Propietat Intel·lectual (RDL 1/1996). Per altres utilitzacions es requereix l'autorització prèvia i expressa de la persona autora. En qualsevol cas, en la utilització dels seus continguts caldrà indicar de forma clara el nom i cognoms de la persona autora i el títol de la tesi doctoral. No s'autoritza la seva reproducció o altres formes d'explotació efectuades amb finalitats de lucre ni la seva comunicació pública des d'un lloc aliè al servei TDX. Tampoc s'autoritza la presentació del seu contingut en una finestra o marc aliè a TDX (framing). Aquesta reserva de drets afecta tant als continguts de la tesi com als seus resums i índexs.

ADVERTENCIA. El acceso a los contenidos de esta tesis doctoral y su utilización debe respetar los derechos de la persona autora. Puede ser utilizada para consulta o estudio personal, así como en actividades o materiales de investigación y docencia en los términos establecidos en el art. 32 del Texto Refundido de la Ley de Propiedad Intelectual (RDL 1/1996). Para otros usos se requiere la autorización previa y expresa de la persona autora. En cualquier caso, en la utilización de sus contenidos se deberá indicar de forma clara el nombre y apellidos de la persona autora y el título de la tesis doctoral. No se autoriza su reproducción u otras formas de explotación efectuadas con fines lucrativos ni su comunicación pública desde un sitio ajeno al servicio TDR. Tampoco se autoriza la presentación de su contenido en una ventana o marco ajeno a TDR (framing). Esta reserva de derechos afecta tanto al contenido de la tesis como a sus resúmenes e índices.

WARNING. Access to the contents of this doctoral thesis and its use must respect the rights of the author. It can be used for reference or private study, as well as research and learning activities or materials in the terms established by the 32nd article of the Spanish Consolidated Copyright Act (RDL 1/1996). Express and previous authorization of the author is required for any other uses. In any case, when using its content, full name of the author and title of the thesis must be clearly indicated. Reproduction or other forms of for profit use or public communication from outside TDX service is not allowed. Presentation of its content in a window or frame external to TDX (framing) is not authorized either. These rights affect both the content of the thesis and its abstracts and indexes.

Homogeneous catalytic / photocatalytic CO₂ conversion involving versatile, non-costly metal complexes

Nassima EL AOUNI



DOCTORAL THESIS

2023

Nassima EL AOUNI

***Homogenous catalytic / photocatalytic CO₂
conversion involving versatile non-costly metal
complexes***

DOCTORAL THESIS

Supervised by :Dra. Anna María Masdeu i Bultó & Dr. Ali Aghmiz

Departament de Química Física i Inorgànica



UNIVERSITAT ROVIRA I VIRGILI

Tarragona 2023



DEPARTAMENT DE QUÍMICA
FÍSICA i INORGÀNICA
Universitat Rovira i Virgili

Anna María Masdeu i Bultó, professora del Departament de Química Física i Inorgànica de la Universitat Rovira i Virgili de Tarragona,

&

Ali Aghmiz, professor del departament de Química de la Universitat Abdelmalek Essaadi de Tetouan,

FAIG CONSTAR que aquest treball, titulat:

“Homogenous catalytic / photocatalytic CO₂ conversion involving versatile- non-costly metal complexes”

Que presenta Nassima EL AOUNI per a l'obtenció del títol de Doctor, i que compleix els requeriments per poder optar a Menció Internacional, ha estat realitzat sota la nostra direcció al Departament de Química Física i Inorgànica de la Universitat Rovira i Virgili.

Tarragona, 22 de març

Directors de la tesi doctoral

Anna María Masdeu i Bultó

Ali Aghmiz

El present treball ha estat desenvolupat amb una beca FI (2019 FI_B 00784). El treball descrit en la present tesi ha estat finançat per:

- El Ministerio de Ciencia e Innovación, PID2019-104427RB-I00.
- La Generalitat de Catalunya. Direcció General de Recerca, Programa de Grups de Recerca Consolidats 2021 SGR 00163.
- El Ministerio de Economía y Competividad, CTQ2016-75016-R
- La Generalitat de Catalunya. Beca FI: 2019 FI_B 00784.



Acknowledgement / Agradecimiento / Reconnaissance

In fact, i was avoiding writing this part, since i know I'm going to start crying, ... well, I've already started crying.

Time goes fast, times is going fast, this is the famous statement of Anna María Masdeu i Bultó, and she is right, i arrived in Tarragona at the age of 24 and now I am 27, but this year is special because I will complete this stage of my life. Anna Masdeu Bultó my supervisor but also a friend, she tried to integrate here in Tarragona from the first day. She has a lot of work and a family to take care of, but she met me at the bus station, she helped me to find accommodation, she accompanied me to the bank and also to the hospital, she introduced me to her family, her husband and the beautiful daughters Andrea and Sara. Having such a good relationship with the supervisor is crucial during your PhD journey. Professionally speaking, i want to thank her for the chance she gave me to enter her lab, to learn new things, to develop my knowledge. Thank you for the moments we spent, the discussions, for your kindness, and especially your patience. My second supervisor, Ali AGHIMIZ, I don't know how to start. I still remember the first time I met Professor Ali during a practical course in the second year of my degree. He saw my curiosity to know and learn more... and he asked me if I wanted to continue my PhD studies, I had hesitations, I always perceived the PhD as huge. After the master's degree, he helped me in the process of obtaining the scholarship, as well as obtaining my visa, and it is thanks to him that I am now finishing my thesis. He always encouraged me, he helped me a lot, he believed in me even in moments of doubt. I would like to thank you on behalf of myself and my family for all the support you have given me, and I hope that one day i too will help someone get closer to their dream as you did... our university in Tetouan needs teachers like you. The work is mine and the thesis bears my name, but this could not be done without the presence of supervisors, colleagues, technicians, i start with Raquel, always smiling, her presence is crucial in the department, she manages a lot of things always keeping a smile and a good mood. She helped me

from my first day, she accompanied me for the analyses, and above all I talk to her when I don't feel well, i can never thank you enough my sweetie. in my lab, there were not many people, but at the beginning there was Yeamin but now Dr Yeamin, the days we spent together in the lab even it was not much but believe me was the best ones, thank you for being always here you and your family, to more lunches and foods together. Maria Elena, she came as an Erasmus student, but with the corona she didn't have any luck, but I was lucky to make a great friend like her, i promise you that we will travel to Italy and Morocco right after the thesis. Right after corona crisis, he came Aria, with him i spent more time in the lab, it was nice to spend time with you in the lab, wish you good luck for the next chapter of your life.

My laboratory is a little far from the other laboratories of my colleagues, but I always feel their kindness and their availability. Lola, calm, very nice to everyone, and ready to help me at any time. Thank you, you are a very nice person, I wish you the best for the few months you have left. Pol you are exceptional, thank you for our little talks and for your kindness and your availability at all times, Jessica calm, adorable and always helpful. Joris, with his beautiful smile and his good vibes, our little discussions in French were cool. Oriol, the new Dr, congratulations again, and thank you for your availability and your kindness always. Jordi, Sara, Anna, Angie, Daniel, Mireia, Paula, you were all kind and i wish you good luck for your PhD.

The physics lab friends, starting with my Tunisian friends, Sami, my best friend, but I can't believe you won't be at my defense day, good luck for your stay in Berlin, and thank you for the delicious dishes you cooked for us, see you soon, and then Ghassan, with your jokes, but you're unique, best luck in your stay in France. Antonio thank you for the time we spent and the discussion we had, and Ines thank you for the few months we spent together, Ikram and Fatemeh thanks. Of course, I would like to thank Joseph, the technician, and my neighbor in the lab, thanks for your kindness, you were always available. Thank you to the technicians of the Servei that without them this work could not be accomplished: Ramon, Sonia, Debora. Many thanks to Cyril for giving us the permission to access the Eurecat, to Laia, Emma, and Aithor. Many

thanks to the lab in Coimbra-Portugal that hosted me during the three months, Mariette Pereira, Rui, Zoe, Jussi, Vitalic and all the people there. Muito obrigada

Sara the energetic, thank you for the laughs we had together, and for the positive vibes you spread, good luck in your new job. Khadija, I already miss our meals together, good luck. Sara the energetic, thanks for the laughs we had together, good luck in your new job. Khadija, I already miss our meals together, good luck.

This is the hardest part, talking about my parents is so emotional. I thank God for giving them health to see this day, i know they are very proud of me, they have always been with me even though they are not here, I can say that it is thanks to their encouragement that I have reached this moment. My sisters Souhaila and Salma, my brother Salim. Good luck to all of you in your carrier.

My husband Saad, who accompanied me during my master and now during the PhD, thank you for bearing with my mood and nervousness, because you believe on me and on my goals. Gratitude to their parents, who are also my second parents. To the soul of my aunt who left us early. To all my family and friends in Morocco.

Thanks to all the people i met during this journey

N.EL



|

*" Le courage n'est pas l'absence de peur,
Mais la capacité de vaincre ce qui fait peur. "*

Nelson Mandela

Table of contents

| | |
|--|----|
| CHAPTER 1 : General introduction | 1 |
| 1.1. Carbon dioxide, from pollutant to chemical feedstock | 3 |
| 1.1.1. CO₂ cycloaddition to epoxides | 7 |
| 1.1.2. Olefins epoxidation | 13 |
| 1.1.3. One pot oxidative carboxylation | 16 |
| 1.1.4. Photocatalytic CO₂ reduction | 18 |
| CHAPTER 2: Objectives | 27 |
| CHAPTER 3: Zinc catalyzed cycloaddition of CO₂ to epoxides for cyclic carbonate synthesis. | 35 |
| 3.1. Introduction | 37 |
| 3.2. Experimental section | 40 |
| 3.2.1. General remarks | 40 |
| 3.2.2. Ligands and Zn complexes synthesis | 40 |
| 3.2.3. Catalysis : Reactor Preparation | 49 |
| 3.2.4. X ray structure | 50 |
| 3.3. Results & Discussion | 51 |
| 3.3.1. Synthesis of ligands and complexes | 51 |
| 3.3.2. X ray structure | 52 |
| 3.3.3. Catalysis | 55 |
| 3.3.4. Proposed mechanism of the reaction | 66 |
| 3.4. Conclusion | 69 |

| | |
|--|-----|
| CHAPTER 4: Eco-friendly, cost-effective metal-catalyzed complexes for epoxidation/cycloaddition reaction | 71 |
| 4.1. Introduction | 73 |
| 4.2. Experimental section | 76 |
| 4.2.1. General remarks | 76 |
| 4.2.2. Synthesis of the involved ligands and complexes. | 76 |
| 4.2.3. Catalysis | 82 |
| 4.3. Results and discussion | 84 |
| 4.3.1. Synthesis | 84 |
| 4.3.2. Epoxidation of alkenes | 87 |
| 4.3.3. Comparison to the previously reported work from the literature employing Fe(II) and Fe(III) as catalyst. | 91 |
| 4.3.4. Proposed mechanism of styrene epoxidation | 94 |
| 4.3.5. Cycloaddition of CO₂ to epoxides | 95 |
| 4.3.6. Attempts to Oxidative carboxylation of olefins to cyclic carbonates | 102 |
| 4.3.7. Proposed mechanism for the cycloaddition of CO₂ to epoxides. | 105 |
| 4.4. Conclusion | 106 |
| CHAPTER 5: Metal catalyzed photocatalytic CO₂ reduction towards CO/H₂ | 107 |
| 5.1. Introduction | 109 |
| 5.2. Experimental section | 113 |
| 5.2.1. General comments | 113 |

| | | |
|---|--|-----|
| 5.2.2. | <i>Synthesis</i> | 114 |
| 5.2.3. | <i>Photocatalytic experiments</i> | 117 |
| 5.2.4. | <i>Formic acid determination method</i> | 118 |
| 5.2.5. | <i>Cyclic voltammetry cell preparation</i> | 118 |
| 5.2.6. | <i>Hydroformylation experiments attempts</i> | 119 |
| 5.3. | <i>Results and Discussion</i> | 120 |
| 5.3.1. | <i>Synthetic aspects</i> | 120 |
| 5.3.2. | <i>Photocatalytic CO₂ reduction</i> | 121 |
| 5.3.3. | <i>Porphyrins as catalysts</i> | 129 |
| 5.3.4. | <i>Fe catalysts reported for photocatalytic CO₂ reduction</i> | 132 |
| 5.3.1. | <i>Sequential photoreduction/ hydroformylation</i> | 136 |
| 5.3.1. | <i>Electrochemical studies</i> | 136 |
| 5.3.2. | <i>Proposed Mechanism of the photocatalytic CO₂ reduction</i> | 138 |
| 5.4. | <i>Conclusion</i> | 141 |
| CHAPTER 6: General conclusions | | 143 |
| CHAPTER 7: Bibliography list | | 149 |
| CHAPTER 8: Appendix | | 169 |
| 8.1. | <i>Publications</i> | 171 |
| 8.2. | <i>Abbreviation lists</i> | 172 |

Abstract

The explosive industrial development and the excessive use of fossil fuels have produced a large volume of carbon dioxide in the atmosphere. The efficient conversion of this gas into useful chemicals and fuels represents an important measure towards the recycling of such a valuable input raw material released continuously into nature. Carbon dioxide (CO₂) has been anticipated as an ideal carbon building block for organic synthesis due to its noble properties, being abundant, renewable carbon feedstock, non-toxic and natural. Therefore, scientists and researchers are exploring a variety of strategies for overcoming the thermodynamic and kinetic barriers associated with CO₂ activation and conversion.

Carbon capture and utilization (CCU) and carbon capture and storage (CCS) technologies are significantly contributing to promote the use of CO₂ as a C1 chemical feedstock to obtain value-added chemicals. However, converting this gas is an uphill struggle considering the high energy input required for converting this very stable substance. Hence, it is essential to apply a suitable catalyst able to weaken the high energy C=O bonds through specific chemical interactions in order to reduce the activation energy required to transform this molecule.

In the present thesis, the application of metal complexes as catalysts for the use of CO₂ as C1 feedstock is presented. Thus, a series of zinc, iron, cobalt, and nickel complexes bearing 2,9-bis(imino) phenanthrolyl and bipyridinyl backbones have been synthesized and characterized. Attempts to synthesize macrocyclic derivatives of curcumin were as well carried out. Besides, a further set of complexes with symmetrical zinc and iron porphyrins with variable substituents was prepared during 3-months stay in Coimbra-Portugal.

The successfully synthesized and appropriately characterized compounds are being applied to diverse homogeneous catalytic processes involving CO₂ as raw material, targeting to operate in mild temperature and pressure conditions. These catalytic

routes are mainly focused on the conversion of CO₂ into other value-added chemicals. A reaction mechanism is constantly suggested for each reaction process.

In the 1st chapter of general introduction, the use of carbon dioxide in synthetic and industrial applications was targeted, together with a general discussion about strategies to recover and utilize CO₂ have presented. Which include the cycloaddition of CO₂ to epoxides to generate intermediates materials, with broad application in the chemical and pharmaceutical industries. This pathway is exposed by providing additional details on the components of the catalytic process, as well as previously proposed reaction mechanism are shown, and the achievements already obtained are given.

A second approach presented which involves the epoxidation of olefins to obtain the epoxides as intermediates, and their coupling to CO₂ to generate cyclic carbonates. General information is delivered regarding the wide use of these products. The choice of the suitable oxidant as well as the efforts already made while using inexpensive metal catalysts, and the mechanism suggested so far. The third pathway is related to the photocatalytic reduction of CO₂ to CO as the main product. Background knowledge is offered, namely the constituents of an appropriate photocatalytic setup, the mechanism that has been previously suggested, and the general research in this area up to now.

In the 2nd chapter, the overall and specific objectives for the present thesis are described in-depth.

The 3rd chapter is devoted to the preparation of zinc complexes bearing tetradentate N₄ donor ligands, and their characterization. The molecular structures of selected ones are determined by X-ray diffraction method. These complexes are applied for the catalytic cycloaddition of CO₂ to epoxide to produce cyclic carbonates, having many applications in the chemical and pharmaceutical industry. Therefore, and in order to find the optimal reaction conditions, several parameters effect are studied herein, included the reaction time, the pressure of CO₂ injected, along with the temperature, and also the ratio catalyst/co-catalyst on the reaction performance.

The 4th chapter is dedicated to the preparation of Fe, Co, Ni complexes with the previously outlined tetradentate N₄ phenanthrolyl and bipyridinyl ligands. The prepared complexes can be fully harnessed on the catalytic epoxidation of olefins to their corresponding epoxides which is of great significance. The choice of an environmentally friendly oxydant is taken into consideration. Those epoxides are valuable organic intermediates that undergo ring-opening reactions with a variety of reagents to give mono or bifunctional organic products. After that, the epoxides are coupled to the CO₂ in catalytic systems involving the same catalysts employed for the first part. A preliminary study of direct oxidative carboxylation, in order to generate cyclic carbonates from olefins are tested via the subsequential 2 steps reaction and also by the single pot process, to prove the versatility and the stability of the synthesized complexes to run different kinds of reactions.

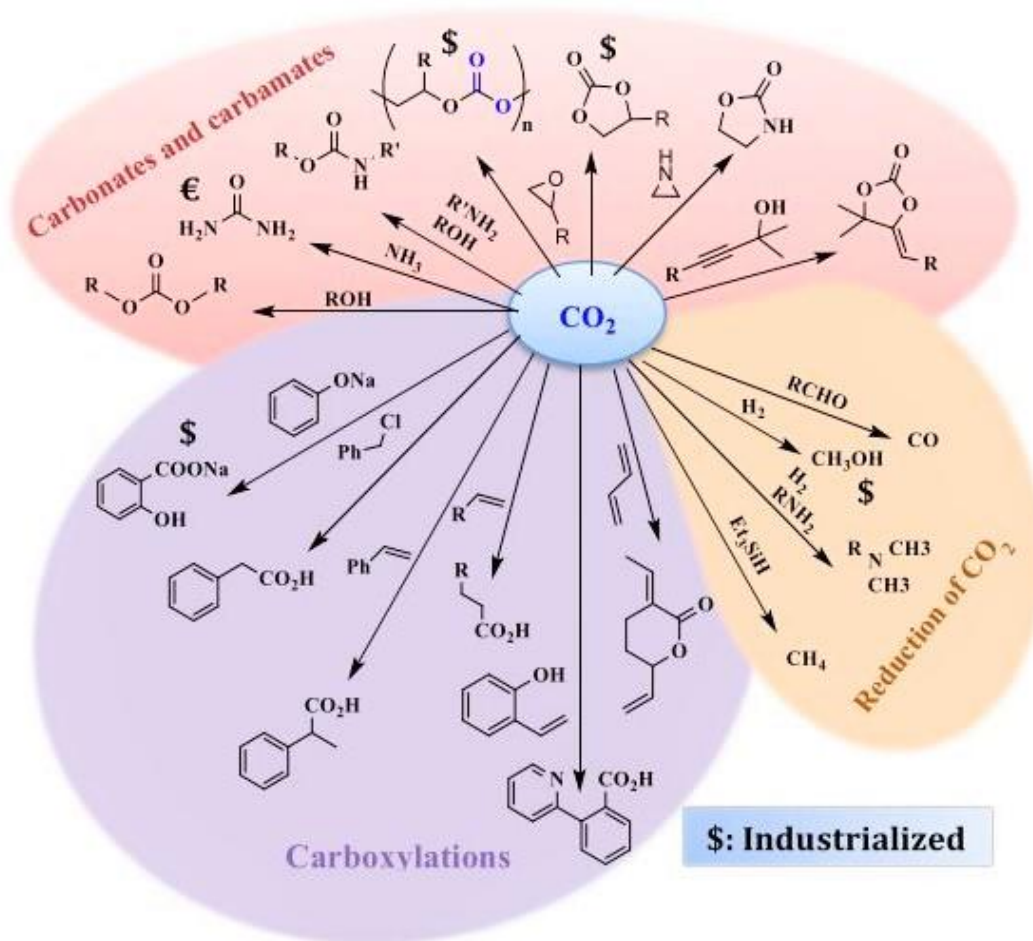
In the 5th chapter, the Fe, Co, Ni synthesized complexes, are tested for the third pathway related to the photoreduction of CO₂ to CO/H₂. Those molecular catalysts are proven their ability to catalyze the photocatalytic processes, under visible light irradiation. A comparison between the metal center of the catalyst, the substituents of the ligands, the effect of the solvent, the photosensitizer, the sacrificial donor effect along with the irradiation time is performed. Moreover, a series of symmetrical zinc(II) and iron(III) porphyrins, which were prepared during an internship at the university of Coimbra (Portugal), are tested as, photocatalysts and photosensitizers, for the CO₂ photoreduction approach. Lastly, implicating the CO/H₂ obtained upon photoreduction of CO₂ into the hydroformylation of alkenes leading to the generation of aldehydes has been additionally targeted.

*Later on , in **chapter 6**, general conclusions extracted upon the work conducted, are given there, while **chapter 7** is consecrated to appendixes.*

CHAPTER 1 : General introduction

1.1. Carbon dioxide, from pollutant to chemical feedstock

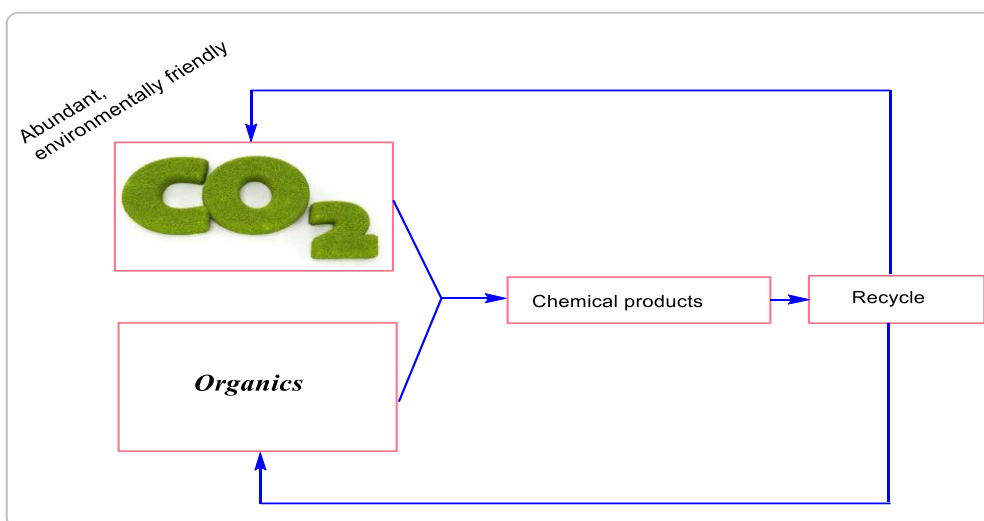
Anthropogenic activities, including fossil fuel combustion and transportation, are releasing environmentally harmful emissions,^[1] most notably CO₂,^[2] which is considered the main contributor to the greenhouse effect.^[3] The concentration of this gas was 399.89 ppm till May 2013, and in 2023, it reached up to 420.41 ppm.^[4] Furthermore, the dependency of human life on fossil resources also the uncontrolled consumption of non-renewable fuels are having detrimental consequences on earth,^[5] and resulted in an urgent need to replace the use of fossil fuels with renewable energy sources.^[6] CO₂ capture and sequestration (CCS) emerges as an attractive idea for the mitigation of emissions released,^[7] but certain technical and economic limitations are still present, such as the high requirement of CO₂ gas storage capacity in underground reservoirs, besides the underground leakage that cannot be totally excluded.^[2] This drawback has motivated researchers to explore the use of CO₂ as a source of C1 for the conversion of organic reactive molecules into fuels and high-value fine chemicals.^[8-11] Performing CO₂ conversion in a cost-effective and environmentally benign manner would be promising and remains challenging.^[12] This is due to its thermodynamic stability and kinetic inertness.^[13,14] Converting CO₂ into useful feedstock chemicals and fuels is a major strategy to reduce the overreliance to petrochemicals, and also to recycle this renewable, abundant molecule. In addition, further products can be derived from the reduction of CO₂ such as : CO, methanoic acid, methanol, methane,^[15-18] the products generated depend on the conversion technology applied, which can include, electrochemical,^[19] photochemical,^[20] thermochemical,^[21] or also radiochemical strategies.^[22] Otherwise, approximately 0.2 Gt of CO₂ are used annually by industrial activities, a small amount compared to anthropogenic emissions estimated with 34 Gt recorded in 2021.^[23] Further research into CO₂ capture, sequestration and utilization is essential to combat rising CO₂ concentration.^[24]



Scheme 1: Some possible CO₂ transformation, and the chemicals products generated, Adopted form.^[25–28]

Numerous reactions have been reported for the conversion of CO₂ into various valuable chemicals. (Scheme 1) However, the transformation of CO₂ to other chemicals is a challenging task because CO₂ is kinetically stable.^[29] Hence, catalysis is clearly one of the fundamental cornerstones for achieving the CO₂ transformation goal. Designing catalysts that activate inert feedstocks, such as CO₂, and improve reaction rates, will reduce the current reliance on toxic reagents. Similarly, adopting catalytic processes rather than using stoichiometric reagents, will improve atom economy and reduce unwanted by-products and waste treatments. The use of

renewable natural resources is the key element of a sustainable society. An easily accessible resource is carbon dioxide, which has advantages of being abundant, economic, and renewable (Scheme2).^[29-34] It's also attractive as an environmentally friendly chemical reagent. This compound is presently used as a substitute for phosgene^[35] in the chemical industry for the production of bulk chemicals, such as urea, salicylic acid, cyclic carbonates, and polypropylene carbonate.^[36] However, few industrial processes incorporate CO₂ to its fullest potential as a raw material, this is because CO₂ is the most oxidized state of carbone. The weak free energy of CO₂ ($\Delta G_f^\circ = -394.39 \text{ kJ.mol}^{-1}$) considered the major barrier to its transformation into useful chemicals.^[37] So a large energy input is required for its transformation.



Scheme 2: CO₂: green carbon resource.^[38]

Nevertheless, several strategies for overcoming the thermodynamic stability of CO₂ and transform it to relevant chemicals are proposed, including the use of high-energy starting materials such as hydrogen to methanol, unsaturated compounds to acids, and small-ring compounds to carbonates or carbamates (Scheme 1). The choice of low-energy oxidized synthetic targets such as organic carbonates. Shifting the equilibrium

to the product side, by removing a particular compound, And by providing physical energy such as light or electricity.^[38]

The selection of appropriate reactions can lead to a negative free energy of reaction (Gibbs free energy) (Figure 1).

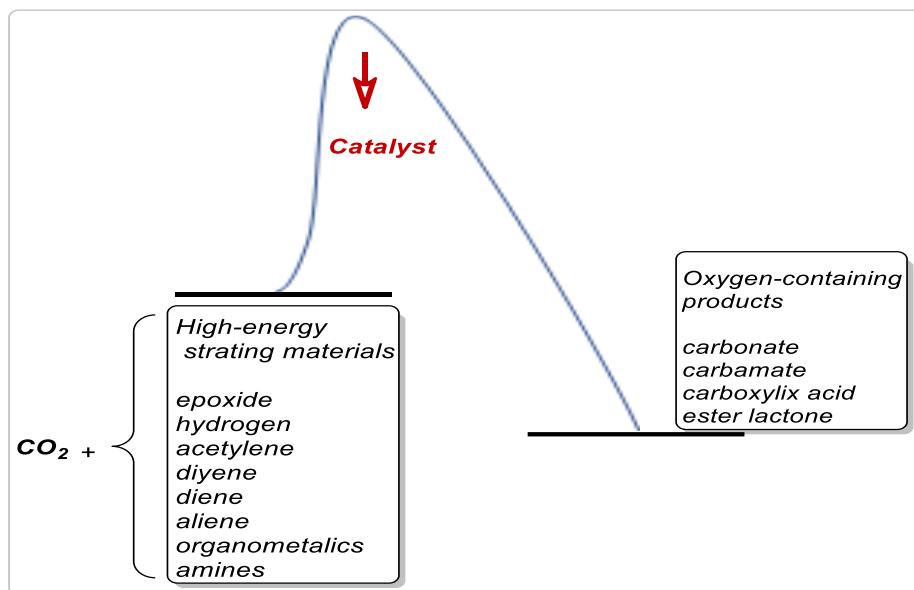
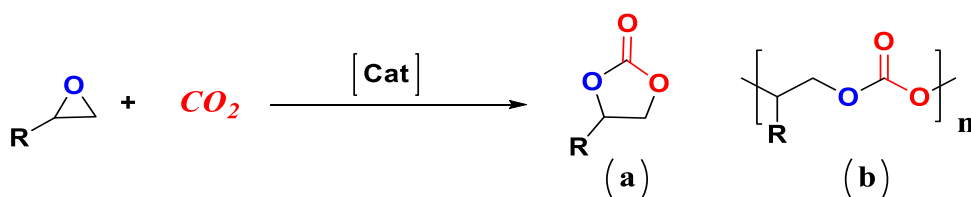


Figure 1: CO₂ fixation in different substrates. Adapted from Sakakura et al.^[38]

This thesis presented the use of carbon dioxide for carbonate synthesis by CO₂/epoxide coupling, as well as its photoreduction to generate CO/H₂. The fundamentals of these reactions are provided.

1.1.1. CO₂ cycloaddition to epoxides

The most important method to prepare organic carbonates is the phosgenation of alcohols, which involves a highly toxic substance such as carbonyl dichloride.^[39] Other possible routes such as the oxidative carbonylation of alcohols use potential explosive carbon monoxide and oxygen mixtures.^[39] The possibility of utilizing a source of carbon as an alternative to phosgene^[29] or carbon monoxide, to generate cyclic carbonates represents a highly desirable target. The greenest, cheapest and most atom-economy efficient synthesis of carbonates is the catalyzed cycloaddition of carbon dioxide to epoxides. The products generated from this reaction are cyclic (a, Scheme 2) and poly carbonates (b, Scheme 2) which are considered industrially crucial products.^[40]



Scheme 3: General reaction of cycloaddition of CO₂ to epoxides, and the possible products.

The study of the reaction coupling of aliphatic or aromatic epoxides with CO₂ to generate cyclic carbonates in a cost-effective manner, thanks to the abundance, availability, and renewability of CO₂. Cyclic carbonates have found many uses as polar solvents,^[41] electrolytic materials,^[42] and precursors^[43] for the synthesis of many fine chemicals,^[43] pharmaceutical, and medicinal products,^[44] as well as for the manufacture of polymeric materials.^[45]

One of the crucial points to be developed by researchers is carrying out this reaction in affordable economic conditions. For the synthesis of cyclic carbonates from epoxides and CO₂, organic solvents were usually necessary.^[8] The pollution risk of such solvents prompted researchers to look for solvent-free processes.^[46-48] Solventless reactions provide various benefits,^[42] including lower pollution and handling expenses through simplification of the experimental setup, working technics

and labor savings, as well as the reactor size.^[25,49] The challenge is that solventless fixation of CO₂ to carbonate often occurs under high pressure and temperature or supercritical CO₂ conditions.^[50]

Catalysts for this transformation include organocatalysts such as organic salts,^[51,52] ionic liquids,^[53,54] and hydrogen bond donor compounds.^[55,56] Metal-based catalytic systems are also used such as metal halides,^[25,57] metal oxides,^[58] or metal complexes, a large number of metal complexes, such as Al,^[59] Cr,^[60] Cu,^[61] Co,^[62] Ni,^[63] Zn,^[64] Fe,^[65] have been developed as highly active catalysts for the epoxide/CO₂ coupling reaction, with porphyrins, β -diiminate, amino-triphenolate, and bis(salicylimine) (salen) as ligands for producing cyclic carbonates and polycarbonates.

1.1.1.1. Zn-based catalysts for the CO₂/epoxide coupling

Zinc complexes have extensively been studied in catalysis for CO₂/epoxides fixation.^[64,66–76] The advantages of Zn(II) based complexes over other catalysts such as those based on chromium, cobalt and manganese include their lower toxicity^[72,77] and their higher stability towards oxidation.^[78] Zn(II) catalysts efficiently activates epoxides as a Lewis acid.^[79] Zn (II) complexes with Schiff base ligands with N₄-donor atoms have been used as catalysts for CO₂/epoxide cycloaddition^[73,74] because they are easy to prepare and thus, by modification of the structure, their stereo-electronic properties can be readily modulated. Furthermore, these complexes may adopt different coordination numbers from 4 to 6, thus, they can stabilize a wide range of geometries.^[80,81]

Previous reported Zn-based catalysts include complexes with O₄-donors,^[71,82] and N-donor polydentate ligands.^[83] Efficient and recyclable catalytic system of a ZnO₄ coordinated complex e.g., 2-hydroxypyridine N-oxide zinc(II), Zn(OPO)₂ (Zn-1, Figure2) and tetrabutylammonium iodide (TBAI) was developed for the cyclic carbonate synthesis from epoxides and CO₂ without the use of any organic solvents. This easily prepared, low-toxic Zn-1 may have a strong Lewis acidity for the activation of epoxides and exhibited high activity (TOF up to 22 000 h⁻¹) even at a

CO₂ pressure as low as 1 bar with a broad substrate scope. Furthermore, the catalyst can be easily recovered and reused five times without a significant loss of its catalytic activity. Other Zn-based catalysts also favored this reaction (e.g., ZnSO₄, ZnI₂), and also Salen-Zn which have been reported [68] but with negligible yields. Most notably, no product was detected in the absence of TBAI. Furthermore, the presence of a proper cocatalyst was vital for the eventual success of the reaction.

A series of pyrrole-based Zn (Zn-2, Zn-3, Zn-5, Zn-6, Figure 2) complexes have been reported previously [84] as a homogeneous catalyst for the CO₂ fixation to epoxides, which produce selectively the cyclic carbonates. Similar zinc (salphen) catalysts based on tetradentate NNOO-donor ligands, [76,85] (Zn-4, Zn7, Figure 2) were selective to the formation of the cyclic carbonates but their activity was rather low.

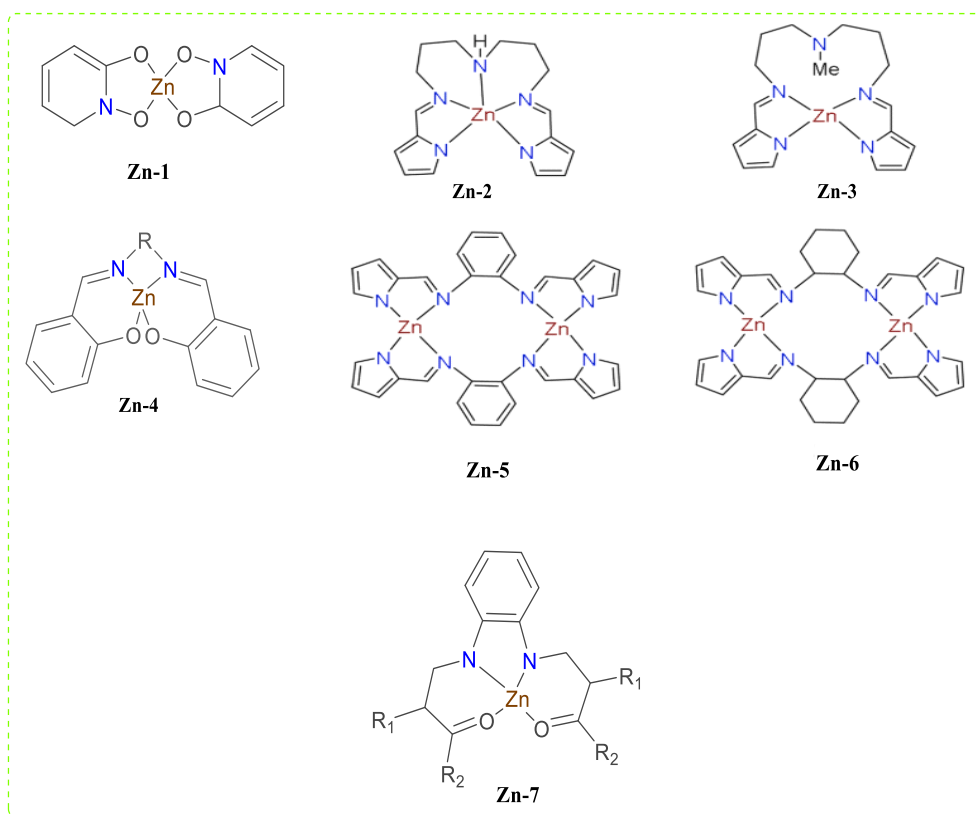


Figure 2: Zinc complexes for the production of cyclic carbonates.

1.1.1.2. Fe-based as catalysts for CO₂ coupling to epoxides.

Iron-based catalysts have received considerable attention in recent years as excellent catalysts applied in various fields. The cost effectiveness and environmental benefits, abundance in the earth, have made it an alternative to other transition metals in many cases, and make its use possible on a ton scale. However, one of its drawbacks is that it oxidizes over time in the presence of air or moisture. In recent years, a number of iron complexes active as catalysts in the chemical fixation of CO₂ with epoxides have been reported. The drawback being that difficult reaction conditions were required to be able to fix CO₂ to epoxides in good yield by applying the iron catalyst. Some examples, Dongfeng et al.^[86] reported a series of metal phthalocyanines (Fe-1, Figure 3) as catalysts for the coupling of CO₂ and terminal epoxides. The presence of a base in excess (4.5 equiv. per Fe) was required to allow the reaction to proceed. Similar to previous reports, harsh reaction conditions (140 °C, 43 bar CO₂) were employed by Jin et al.^[87] using an iron porphyrin complex as catalyst (Fe-2, Figure 3) for the coupling of propylene oxide and CO₂. This paper mainly focused on the cobalt porphyrin complexes for the same reaction, hence the iron analog was synthesized for comparison. The systems were active for the formation of cyclic carbonate at 25 °C and 7 bar CO₂ pressure in the presence of 2 equiv. phenyl trimethylammonium tribromide (TPAT). However, in comparison with the cobalt analog, the iron complexes were much less reactive, giving a conversion of only 10% after 3 hours reaction time.

A major advancement in iron-catalyzed CO₂/epoxide chemistry was achieved by Buchard et al.^[88] focused on the formation of polycarbonates. Shortly thereafter, Dengler et al.^[89] reported tetraamine and diimine-diamine iron (II) complexes active in the coupling of CO₂ and propylene oxide to form propylene carbonate (Fe-3, Fe-4, Figure 3), these complexes were active for cyclic carbonate formation without the addition of an external cocatalyst but showed higher conversion with the addition of an equiv. of TBAB. Complex Fe-4 was inactive alone but was capable of achieving >80% conversions with the addition of TBAB.

Building on this work, Sheng et al.^[90] reported similar tetraamine and diimine–diamine iron (II) complexes active towards the coupling of propylene oxide (PO), epichlorohydrin (ECH), and cyclohexene oxide (CHO) with CO₂ (Fe-5, Fe-6, Figure 2). Both complexes were highly active catalysts. and unlike that Fe-3 and Fe-5 were previously reported by Dengler et al.^[89] these complexes were active without the addition of a cocatalyst, but the conversions remained low. Nevertheless, in the presence of 1 equiv of TBAB, high activity was obtained.

In 2013, Fuchs et al.^[91] expanded to N₂O₂-iron (III) (Fe-7, Figure 3), and iron (II) (Fe-8, Figure 3) systems that were active catalysts for the coupling of propylene oxide and other substituted epoxides with CO₂ to yield cyclic carbonates. The iron (II) system was observed to be active only in the presence of a cocatalyst (TBAB) and required higher catalyst loadings to achieve high conversions. On the other hand, the iron (III) complex was active without an external cocatalyst and required lower catalyst loadings to achieve similar conversions. This complex was also screened for reactivity with a range of other epoxides, demonstrating the diverse applicability of this system.

Therefore, further developments in this area are still necessary to find more active systems under mild reaction conditions, and less catalyst loading.

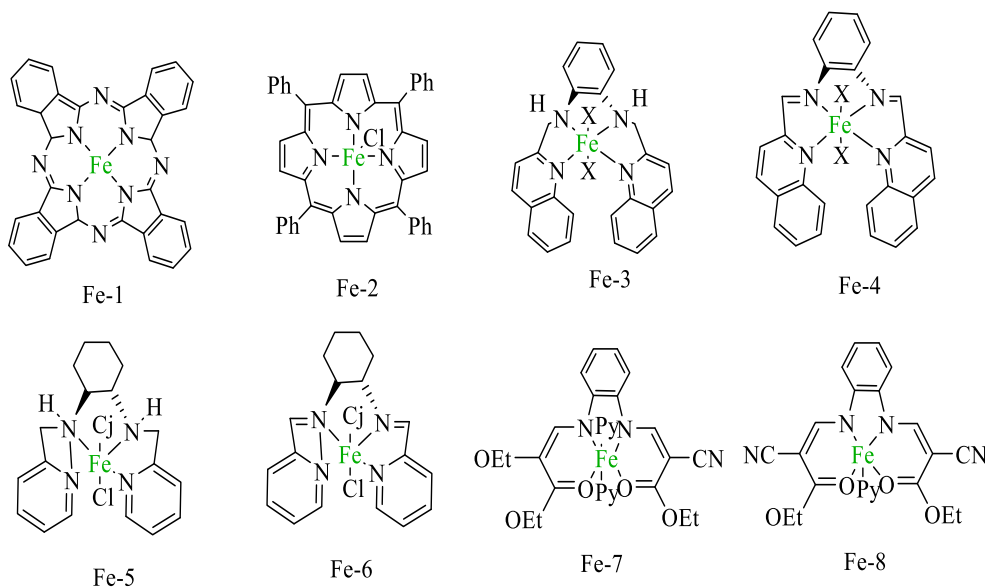


Figure 3: Fe catalysts used for the cyclic carbonate production.

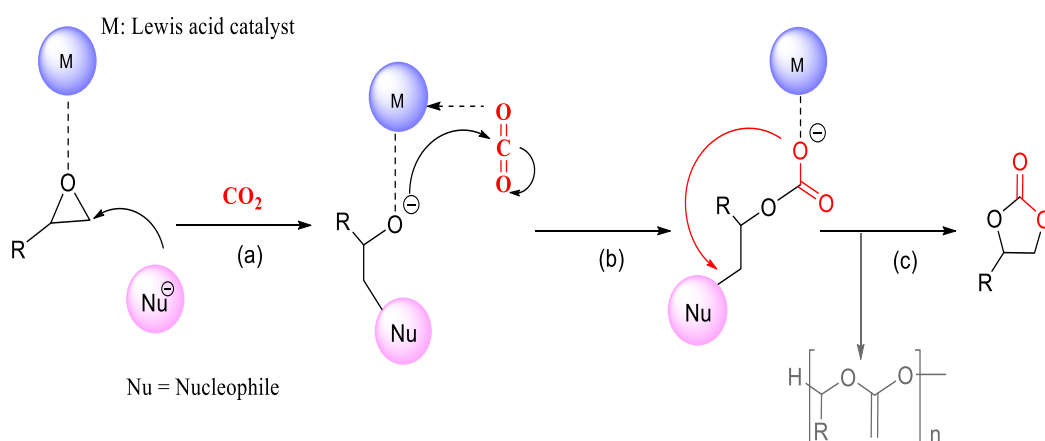
1.1.1.3. Co and Ni based-catalysts for CO₂ coupling to epoxides

Other transition metal complexes were applied as well in this approach. A series of inorganic Co and Ni complexes containing ethylenediamine and cyclam as ligands were used as catalyst in the expansion of the epoxides ring with CO₂.^[92–94] The reactions were carried out under CO₂ pressure above 5 bar and temperature above 100°C. After a reaction time between 4h and 5h, it was possible to achieve a conversion between 0 and 88%.

1.1.1.4. General mechanism of the CO₂ cycloaddition

The commonly accepted mechanism for this reaction involves, in most cases, three steps. starting with the opening of the epoxide ring, followed by the insertion of carbon dioxide and finally the ring closing step to form the cyclic carbonate (Scheme 4).^[95–99] The first step is initiated by nucleophilic attack of a Lewis base (Nu-, Scheme 4, a) to open the epoxide ring. It frequently corresponds to the highest energy barrier,

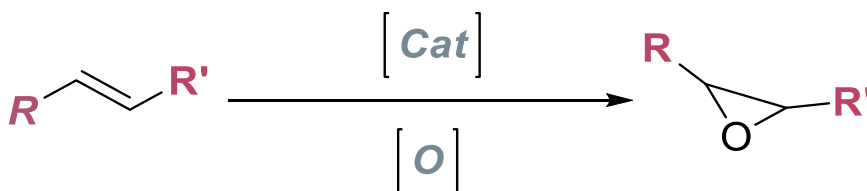
which is diminished through activation of the epoxide with a Lewis acid (LA) or a hydrogen bond donor (HBD). Next, the alkoxide formed attacks the electrophilic carbon of CO₂ to form a carboxylate species (Scheme 4, b). Finally, nucleophilic attack of the carboxylate on the chain carbon leads to the cyclic carbonate while the nucleophile is released (Scheme 4, c). Alternatively, in the last step, insertion of an epoxide molecule can occur to initiate a copolymerization sequence to form polycarbonates. The relative stability of these intermediates is crucial to selectively form the cyclic carbonates.



Scheme 4: Generally accepted mechanism for the synthesis of cyclic carbonates by a binary system Metal catalyst/Nu. Based on Martin et al.^[99]

1.1.2. Olefins epoxidation

Epoxidation reaction (Scheme5) is one of the most important organic transformations, since it provides direct access to various active epoxides, which are considered to be an attractive class of industrial products, that have been employed as chemical intermediates. The catalytic epoxidation of olefins provides an interesting production technology. Complexes of various transition-metals, such as Fe, Cr, Ru, Mn, Cu, Co, etc., have been employed in homogeneous catalytic systems for epoxidation of alkenes.^[100–104]



Scheme 5: Epoxidation reaction towards epoxides ring.

Iron-catalyzed epoxidation has been of particular appeal owing to its availability, cheap cost, and low toxicity of the iron salts. A number of different chiral iron–porphyrin complexes have been developed and applied in epoxidation reactions. In 2012, Simonneux and his co-workers^[105] developed a series of chiral Halterman iron–porphyrins (Fe-9, Figure 4), which are able to promote the epoxidation reaction in asymmetric version, using hydrogen peroxide as oxidant. The sulfonated Halterman iron porphyrin^[106] is water soluble and thus the epoxidation can be conducted under aqueous conditions. However, the substrate scope of these reactions is narrow and includes only styrene derivatives and 1,2-dihydronaphthalene. Furthermore, the products are afforded mostly with moderately good enantioselectivities.

Tetradentate nitrogen-containing iron complexes, which have electronic properties that resemble to those of porphyrin, also proved to be efficient catalysts for the Fe-catalyzed asymmetric epoxidation of olefins. For instance, Mitra et al.^[107] developed chiral Fe–amino pyridine (Fe-10, Figure 4), which is capable of promoting highly enantioselective epoxidation of diverse olefins with aqueous hydrogen peroxide as oxidant. Furthermore, the authors also discovered that the enantioselectivity of this process increased with growing steric demand of acidic additives. The same group had improved the catalytic behavior of the Fe-aminopyridine complex significantly by introducing a dimethyl amino group into the pyridine rings (Fe-11, Figure 4). The authors also employed a catalytic amount of carboxylic acid as a cocatalyst, which has the potential to improve both the yields and enantioselectivities of the epoxidation reaction through synergistic cooperation with the iron complex. The presence of catalytic amounts of a carboxylic acid has been found to enhance both the yield and

enantioselectivity in epoxide formation. After careful screening of a variety of carboxylic acids, ibuprofen turned out to be the best co-ligand. This new epoxidation method shows applicability to various substrates, including diverse enones and cis- β -substituted styrenes.

Later on, Wang et al.^[108] Designed the Fe-aminobenzimidazole complex (Fe-12, Figure 4), which found to be an effective catalyst for the hydrogen peroxide mediated enantioselective epoxidation of chalcone derivatives, providing the products in most cases with high enantio selectivities. This tetradentate N₄ ligand has also been employed in manganese catalyzed epoxidation of α,β -unsaturated ketones, giving similar results in terms of yields and enantioselectivities. Therefore, further research is desired in this area to access versatile epoxides under mild and environmentally benign reaction conditions.

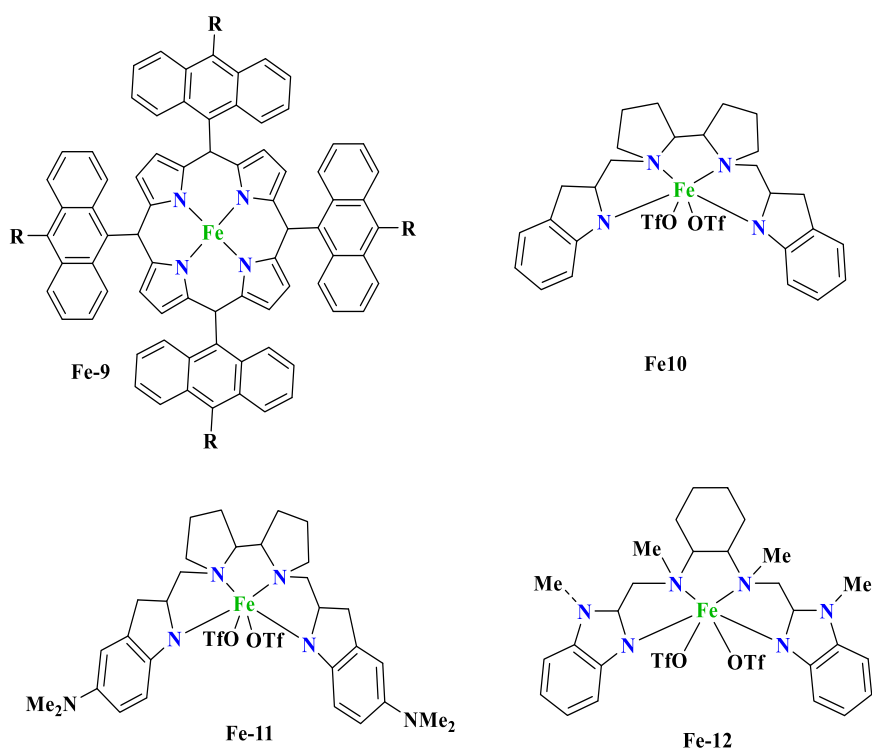


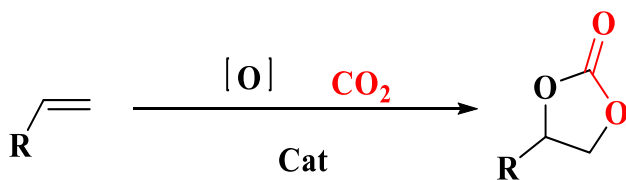
Figure 4: Fe catalysts employed for epoxidation of olefins.

1.1.2.1. Oxydant agents

The oxidant is a crucial pillar for achieving better performance on the epoxidation reaction, over the past decade, increased attention has been given to the development of more environmentally friendly and efficient epoxidation methods using environmentally friendly oxidants such as tertbutyl hydroperoxide (TBHP), hydrogen peroxide, air, or oxygen.^[109] Advantages of applying TBHP as oxidant for the epoxidation include its high good solubility in polar solvents, neutral pH reactions, safe handling, and easy separation of the tert-butanol by-product.^[110] On the other side, hydrogen peroxide has several applications as oxidants for the synthesis of value-added chemicals.^[111] Factors such as its low cost, environmentally benign nature, and ability to act as an oxidant for a number of functional groups, make it an ideal choice for the oxidation of a number of organic compounds. Another advantage of using H₂O₂ as an oxidant is that it is used as an aqueous solution at about 30-40%, which is suitable for performing oxidations of high-boiling chemicals under homogeneous and heterogeneous reaction conditions, and the only by-product of oxidations is water.^[112] The disadvantage is that this agent lacks stability at high temperatures and in the presence of an iron catalyst, it may decompose more rapidly.

1.1.3. *One pot oxidative carboxylation*

The synthesis of five-membered cyclic carbonates through metal-catalyzed oxidative carboxylation of olefins (Scheme 6) has gained considerable attention in recent years.



Scheme 6: *One -pot oxidative carboxylation.*

The strategies for this appealing synthetic approach can be typically classified into two categories: (i) two step sequential reaction consisting of oxidation followed by carboxylation and (ii) direct oxidation and carboxylation in just a single-step. An

early report outlining the utility of metal catalysts for this conversion was published by Aresta and colleagues in 2000^[113] who demonstrated that the reaction of styrene with CO₂ (45 atm) in the presence of molecular oxygen as oxidant and a catalytic amount of Niobium pentoxide (Nb₂O₅) in DMF at 120°C yielded the corresponding styrene carbonate in only 5% along with styrene oxide, benzaldehyde, and benzoic acid as by products.

Within the same context, by using a noble metal, Bai et al.^[100] had developed a one-step synthesis of carbonate from styrene, O₂ and CO₂ with ruthenium dioxo(tetraphenylporphyrine) [Ru(TPP)(O)₂] as catalyst. This catalytic system can transform the styrene to the styrene carbonate in harsh conditions with a yield of 89%. However, in the same work, and in order to compare the metal effect, Jing and coworkers had replaced the ruthenium with less expensive metal such as iron. The Fe(TPP)Cl has led to a yield of styrene carbonate of only 3.6% under the same reaction conditions.

With the attempts made so far, it has been concluded that the direct access of five membered carbonates through olefins, remains difficult to achieve, because the CO₂ insertion reaction is unfavorable under low CO₂ pressure. However, increasing the CO₂ pressure may decrease the yield and the selectivity towards cyclic carbonates, due to the dilution occurred. Further research seems to be required for the purpose to improve the conversion to the target carbonates under mild reaction conditions.

1.1.4. Photocatalytic CO₂ reduction

Among the various methods invented to convert CO₂ into useful chemicals, there is the photocatalytic CO₂ reduction.^[114] Thanks to natural photosynthesis^[115,116] carbon dioxide is transformed into biomass using sunlight,^[117] the most abundant renewable energy on earth. Mimicking the natural process of photosynthesis, artificial photosynthesis technology,^[118] which integrates the harvesting of solar energy and the chemical conversion process into a single device, holds promise as a solution to the world's energy and environmental crises.

The two processes, whether natural or man-made, follow identical physico-chemical steps, starting with a light absorption, then the separation of the charges, afterwards the separation of the water and the chemical synthesis, while the electron acceptors and charge transfer processes are distinct in detail.^[117] It is feasible to design artificial systems capable of harnessing light and oxidizing water and reducing protons or other organic compounds like CO₂ to generate useful chemical fuel source. The artificial CO₂ photoreduction concept, consists on the catalytic conversion of CO₂ assisted by sunlight, appearing to be an exciting way to produce renewable fuels as well as to take advantage of this exhausted, inexpensive, raw material emitted constantly to the environment.^[119–121] Moreover, photocatalytic reduction of CO₂ can provide access to several value-added chemical products, (Figure 5) such as CO,^[122] and CH₃OH.^[123,124] CO can be further converted to liquid fuels by the Fischer–Tropsch process.^[125,126]

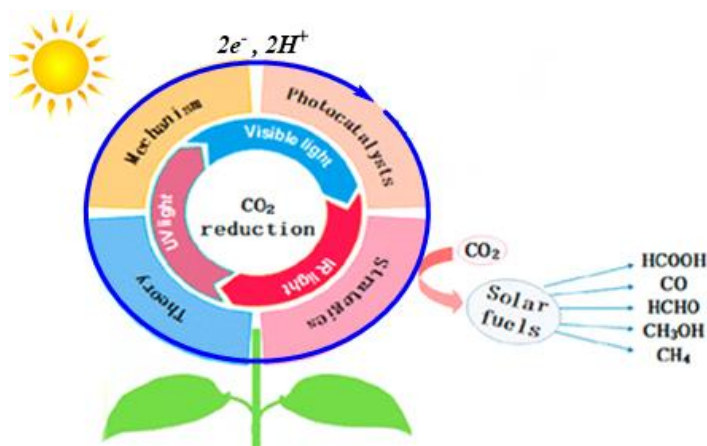


Figure 5: Products generated via the photocatalytic CO₂ reduction. Adopted from Chen et al.^[127]

1.1.4.1. Components of a photocatalytic reduction system

A photocatalytic CO₂ reduction system requires principally a photosensitizer (PS) to harvest the light, a catalyst (Cat), and a sacrificial electron donor (SD). For homogeneous processes, the PS and the Cat are mostly based on transition metals and rarely on organics.^[128] Although noble metals have shown excellent results in the field of photochemistry and electrochemistry, alternative environmentally benign systems using 3d transition metals (Mn, Fe, Co, Ni) are in demand, and electrons are derived from the ability of the photosensitizer (PS) / sacrificial donor pair to form a strong reductant by irradiation with a light source.

Photosensitizer: PS

A redox photosensitizer (PS) is the key element responsible for light harvesting and photochemical reactions,^[129] with the ability to absorb energy from a photon.^[130,131] It's the one, that should mediate electron transfer from the electron donor to the catalyst by photo-excitation in the photocatalytic reaction, transferring an electron from the occupied high orbital of the metal to the π^* orbital of the ligand.^[132] This metal-ligand charge transfer (MLCT) forms an activated PS* species. The PS* complex therefore possesses a highly energetic occupied orbital but a partially vacant

low-energy orbital as well.^[133] Typically, the PS for CO₂ reduction must exhibit the following photophysical and electrochemical properties, first of all, the PS must possess stronger absorption at an excitation wavelength than other coexisting materials, such as SD and Cat, in the lamp region employed, secondly, the PS should possess a long emission lifetime, owing to the need for an efficient reductive quenching process, then, a strong excited state as oxidant is required to catch an electron from the reductant. Precious metal-based PSs (such as Ru, Ir, and Re) have demonstrated successful activity for CO₂ reduction in recent investigations, especially, [Ru(II)(N[^]N)₃]ⁿ⁺ (N[^]N = diimines ligand, typically 2,2-bipyridine complexes (Figure 4) have been the most widely used PS in previously reported photocatalytic CO₂ reduction systems.^[134–141] However, the use of PS containing inexpensive metals such as copper,^[142] iron, and other transition metals,^[141,143–148] as well as metal free PS,^[142,148] are desirable in order to make the process environmentally friendly and also economically viable (Figure 6). This part, continues to be a persistent struggle for the research community, requiring further investigation aimed at improving the outcomes attained.

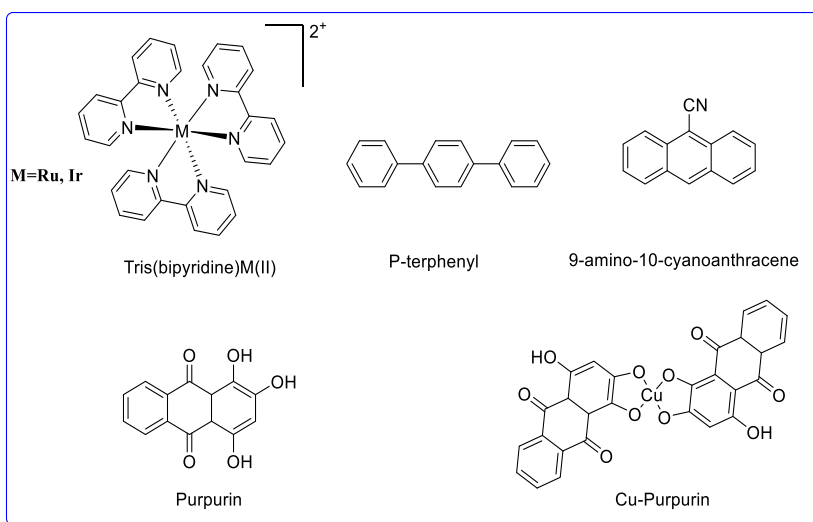


Figure 6: Selected PS employed for homogeneous photocatalytic CO₂ reduction.

Electron Donor / Sacrificial reductant

The electron donor or sacrificial reductant (SD) is a specie willing to donate electrons^[149] to fill this vacant low energy orbital on the metal and hence, create a complex with a high energy π^* orbital. Amines can be oxidized by either two or one electron processes,^[150] tertiary aliphatic amines are probably the most used sacrificial donors in the photochemical reduction reactions. Triethylamine (TEA) and triethanolamine (TEOA),(Figure 7) being among the most commonly employed SD in this context, both displays very similar features, they exhibit irreversible oxidation potentials around 0.7 V vs. SCE,^[151,152] they are used in purely organic^[153] or aqueous^[154] media, and frequently, through mixtures of water with an organic solvent (DMF, MeCN, and THF) are reported.^[149,155–157] It was noted that both the PS and SD are mostly used in excess compared to the catalyst in the purpose to insure the irreversible aminyl transformation,^[158] and to improve the overall yield of the photocatalytic system.^[159] TEA and TEOA having very similar properties, so, the use of TEA vs. TEOA is difficult to rationalize. For instance, Tinker et al.^[160] and Curtin et al.^[161] described the superiority of TEA over TEOA for their photocatalytic system typically for stability reasons.^[160] Thoi et al.^[153] observed an improved efficiency with TEA rather than TEOA, whereas Yuan et al.^[162] reported the improved reductive quenching rates with TEOA vs. TEA. Moreover, the aromatic amines, are also found to be used as sacrificial donor for CO₂ photoreduction, a number of them have been studied as potential sacrificial donors.^[163–165] Furthermore, L-ascorbic acid and related ascorbate ions are famous anti-oxidant, natural preservative agents, they are likely candidates for SDs and were successfully used in the 80s.^[162,166,167] After that, there are 1,3-dimethyl-2-phenyl-2,3-dihydro-1H-benzo-d-imidazole (BIH, Figure 7) and 1-benzyl-1,4-dihy-dronicotinamide (BNAH, Figure 7) which share common features^[168] originally used to reduce organic compounds. It has recently been applied to the photoreduction of CO₂ similar to BNAH,^[130] the BIH provides also, two electrons and one proton (hydride donor),^[169] which can react as well with the excited state of $[\text{Ru}(\text{bpy})_3]^{2+}$ as PS in a reductive quenching process, yielding PS⁻ and oxidized BIH⁺. This latter is very acidic and loses a proton to a base in the medium,

which provoke the necessity of the existence of a base such as TEOA which is supposed to accept the proton from BIH and is named proton acceptor instead of a SD as described before.^[170] This stage is crucial for limiting the electron back exchange between the reduced PS⁻ and the BIH^{•+}.^[130]

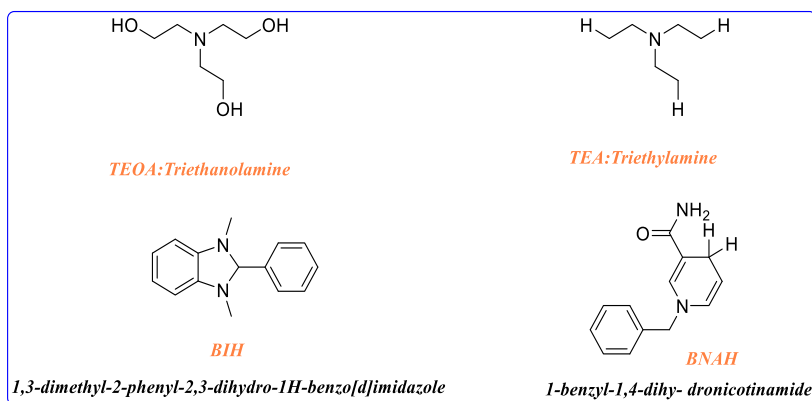


Figure 7: SD employed for CO₂ photocatalytic reduction.

Catalyst :Cat

The core reaction site of a photocatalytic system is the catalyst, it's the one that activates CO₂ and induces the reduction reaction.^[171] Therefore, a relevant molecular catalyst is required to carry out the catalytic process,^[172] this must have certain imposing characteristics, mostly, redox activity which is the ability to transfer between different oxidation states, high solubility in a wide range of solvents, the catalyst must be stable, low toxic, abundant material, as well as cost-effective.

A large number of studies have been devoted to the search for metal-based molecular catalysts for the photochemical reduction of CO₂.^[124,173,174] The majority of them, are based on noble metals such as rhenium,^[175–177] or ruthenium,^[177] and fewer systems employ abundant and more environmentally friendly catalysts such as those based on iron,^[178] manganese,^[179] cobalt,^[180] and nickel.^[181]

In 2014, Bonin et al.^[174,182] were capable of developing photochemical systems of CO₂ reduction, in an organic solvent with iron porphyrin derivatives (Fe-13, Figure8),

as homogeneous molecular catalysts under visible light irradiation. From moderate to high TON were achieved with high selectivity towards CO.

In 2016, Guo et al.^[183] were reported a quaterpyridine Fe catalyst (Fe-14, Figure 8). This complex has been efficient for both water oxidation and reduction of CO₂ under visible light using [Ru(bpy)₃²⁺] (bpy = 2,2'-bipyridine) as the photosensitizer, the BIH as sacrificial reductant. A TON for CO of 2660 after irradiation for 80 min, with a TOF of 117 min⁻¹ for the first 20 min was achieved. Within the same year. Takeda et al.^[184] were able to design a photocatalytic system involving non expensive metals in both sides catalysts and cocatalysts. CuI (dmp)(P)²⁺ (dmp =2,9-dimethyl-1,10-phenanthroline; P = phosphine ligand) were used as a redox photosensitizer and Fe(II) (dmp)₂(NCS)₂ (dmp =2,9-dimethyl-1,10-phenanthroline) as a catalyst. This system produced mainly CO with a TON up to 273 after 12h of irradiation by visible light (Fe-15, Figure 8). However, the investigations undertaken in this field to date, have focused mostly on noble metal complexes, either as catalysts or as photosensitizers, making the development of novel systems employing only low-cost, non-toxic materials a more challenging task.

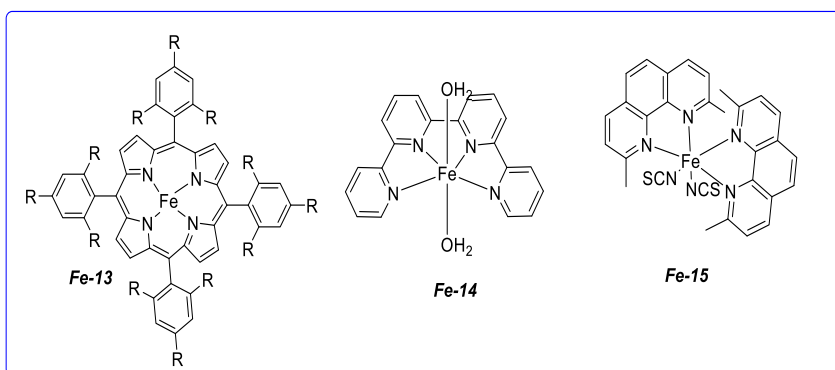


Figure 8: Selected Fe catalysts used for CO₂ photoreduction.

Solvent

The solvent equally takes a crucial part in homogeneous photocatalytic system. To dissolve all the components, a proper but also low-cost and less-toxicity, with higher

stability under irradiation conditions, is required.^[185] The common solvents used in photocatalytic systems for CO₂ reduction include dimethylformamide (DMF), acetonitrile (MeCN), methanol (MeOH) and dimethylacetamide (DMA).

1.1.4.2. Performance parameters

Turnover number : TON

To evaluate the productivity of the catalyst. Turnovers are generally useful for assessing the efficiency of single catalyst, a so-called turn over number is calculated, which can be defined as the number of reduction processes that can occur per catalyst cycle during the lifetime of the catalyst. In a further setting, it corresponds to the number of moles of substrate that one mole of catalyst can transform before being inactivated. It provides a measure of catalyst robustness.

Turnover Frequency : TOF

Other major parameter that is calculated, is the turnover frequency (TOF). This is the TON per unit of time, generally per hour

Selectivity

Selectivity in catalysis is one of the most significant factors to be controlled by researchers, In the photocatalytic reduction of CO₂, there are several products that can be formed, however in this thesis, we focused on carbon monoxide and dihydrogen as main products.

1.1.4.3. Mechanism of the photocatalytic process

Building on what already been reported in the literature, two broad mechanisms may occur, and that depend on the power of the PS employed. As mentioned above, a photocatalytic cycle system consists mainly of three processes, first of all, the PS is excited by harnessing light and convert it into a chemical potential. It is the one that

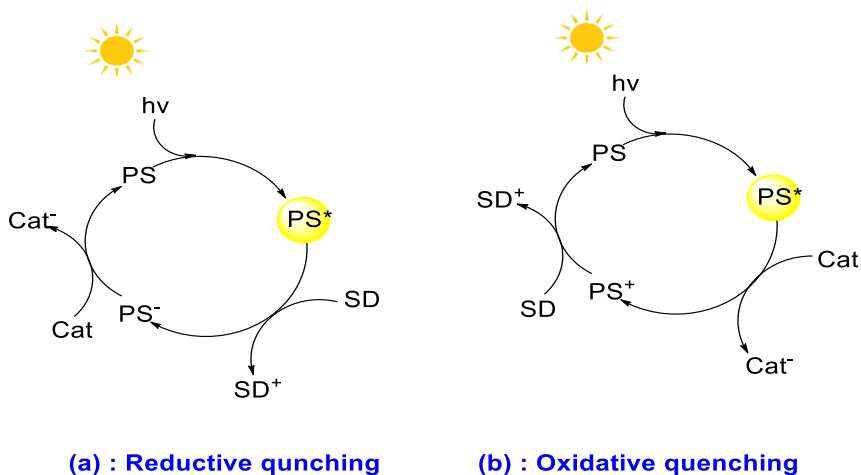
mediates the electron transfer. Secondly, the SD, supplies electrons upon photoinduced control by the PS, and thirdly, the reductive catalyst, which accumulates electrons, and activates the CO₂, then induces the reduction reaction. Once the PS is promoted to its excited state PS*, acquires at the same time enhanced oxidative and/or reductive power(s). Thermodynamically, if the PS* is strongest enough as oxydant, it could occur a reduction and gives the reduced species PS⁻, which will be a reductant stronger than the PS and the PS*. So, the PS⁻ which is a strong reductant is then oxidized to return to its ground state reducing the catalyst. The reduced catalyst will then be the species responsible for the reduction of CO₂, this pathway is the reductive quenching ((a), RQ, Scheme 5). On the other hand, in the oxidative quenching or deactivation ((b), OQ, Scheme 5), PS* is less oxidizing, and strong reductant, so, oxidation of the PS* by donating electrons and generate PS⁺ occurs together with the reduction of the catalyst to give the Cat⁻. The reduced catalyst able to reduce the CO₂. The oxidized PS (PS⁺) will be returned to its fundamental state by catching electrons from the SD. It has been reported in previous studies, that the amount of sacrificial donor may affect the pathways of reductive or oxidative quenching. The higher the concentration of SD, the higher the probability of observing the RQ vs OQ one ^[186,187] although RQ was reported to take place commonly with the [Ru(bpy)₃]²⁺ photosensitizer.^[188]

For the last stage, to obtain CO, a double reduction of CO₂ must occur, so, the catalyst must be reduced to its active state by accepting two electrons, repeatedly interacting with PS, SD, or with the evolving products of oxidized SD, which are often not only a source of electrons but also a source of the two protons necessary for the reaction. In some studies, it has been shown that the system works better when the concentration of water increases. The presence of water could favor the production of H₂,^[189] which is thermodynamically formable and competitive with CO₂ reduction, and thus decrease the selectivity towards CO.

The interaction between CO₂ and the molecular catalyst generally occurs through the insertion of CO₂ into a metal bond-either through a metal-hydride bond or through a bond to a vacancy in the metal center coordination sphere. In the first case,

electrostatic attractions occur between the C-O and M-H bonds, both polarized, placing the carbon of CO₂ which is the electrophilic center near the nucleophilic hydride. On the other side, when CO₂ occupies a vacant coordination position, a η¹-CO₂ occurs, so that the oxygens are placed in a position that favors their protonation. In general, the first type of interaction results in formic acid production while the second is more common to obtain CO.^[190]

To sum up, three important objectives should be fulfilled in homogeneous CO₂ photoreduction : (1) the development of a photosensitizer that absorbs a wide range of visible light well, is highly oxidative in the excited state, highly reductive in the reduced state, and stable in both the excited and reduced states : (2) the development of a catalyst capable of rapid CO₂ reduction with a low overpotential, weak absorption of visible light, and is stable during the photocatalytic reaction, and (3) rapid electron transfer from the reduced photosensitizer to the catalyst.^[191]



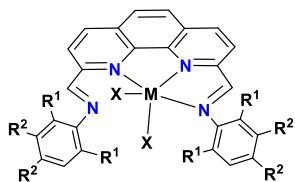
Scheme 7: Two of the possible mechanisms of deactivation of the photosensitizer: (a) by reductive deactivation and (b) by oxidative deactivation.^[191]

CHAPTER 2: Objectives

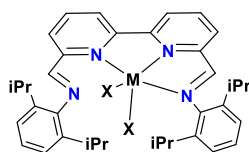
As noted in the introduction, a wide range of catalytic systems and strategies have been developed to date with the aim of converting CO₂ into valuable products, particularly through the use of noble and transition metal catalysts. Yet, additional efforts are warranted to synthesize more efficient, cost-effective, and selective catalysts to yield the target products under gentle reaction conditions.

The present doctoral thesis has been conducted with the main purpose of developing efficient, non-toxic, and cost-effective metal complexes, for chemically selective catalytic processes, that involve tetradentate N₄-donor ligands in order to convert CO₂ into industrially relevant chemical products. Based on the state of the art, the selected ligands contain phenanthroline and bipyridine bi-imine and amine. Those ligands are easily preparable, and by modification of the structure, their stereo-electronic properties can be readily modulated, allowing to enlarge the area of study.

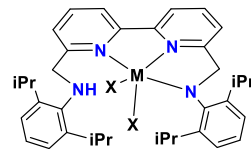
Thus, a large number of catalytic systems and strategies are being developed for the synthesis of organic carbonates from CO₂ and epoxides. However, although this process is known so far, more efficient, yet cost-effective, non-toxic, and selective catalysts are still needed for the generation of cyclic carbonates or polycarbonates under mild operating conditions. Therefore, a family of catalysts based on Zn(II) and Fe(II), Co(II) and Ni(II) will be prepared to be used for the preparation of cyclic carbonates from alkenes or epoxides (Figure 9).



Zn1 : X=Cl ; R¹=iPr ; R²=H
Zn2 : X=Cl ; R¹=Et ; R²=H
Zn3 : X=Cl ; R¹=H ; R²=OCH₃



Zn4 : X=Cl
Co4 : X=Cl
Ni4 : X=Cl



Zn5 : X=Cl

Fe1a : X=Cl ; R¹=iPr ; R²=H
Fe1b : X=OTf ; R¹=iPr ; R²=H
Fe1 : X=OTf ; R¹=Et ; R²=H

Co1 : X=Cl ; R¹=iPr ; R²=H
Co2 : X=Cl ; R¹=iPr ; R²=H

Ni1 : X=OTf ; R¹=Et ; R²=H
Ni2 : X=Br ; R¹=iPr ; R²=H

Figure 9: Phenanthroline and bipyridinyl complexes prepared in in this thesis.

The second catalytic reaction is consacred to the photoreduction under atmospheric pressure of CO₂ to CO/H₂ exploring the use of molecular catalysts into artificial photosynthetic systems working under visible-light illumination. The final goal was to use the CO/H₂ produced during the photoreduction of CO₂ for the hydroformylation of alkenes to generate aldehydes. The hydroformylation, commonly referred to as oxo synthesis or oxo process,^[192] is a well-known industrial process for the production of aldehydes from alkenes, in this process, homogeneous catalysis is often employed owing to its better performance and higher selectivity. Aldehydes are versatile compounds involved in the manufacturing processes of dyes, resins, and organic acids,^[193] they serve as chemical feedstocks in the synthesis of rubbers, plastics, and other larger molecules.^[194]

Accordingly, the specific objectives regarding the synthesized of N4 tetradentate phenanthrolyl and bipyridyl, and their application in epoxidation and CO₂ fixation to epoxides:

- ✓ To develop a family of Zn(II), Fe(II), Co(II) and Ni(II) (Figure 9) complexes bearing phenanthrolyl and bipyridyl N4 donor ligands with different substitutions and their characterization to be involved as catalysts for cycloaddition and epoxidation of olefins.
- ✓ To study the advantage of the ligand structure on the conversion of the reaction.
- ✓ To explore the substituents effect of the ligands on the catalytic activity of the catalyst.
- ✓ To achieve high reaction efficiency, while trying to lower the catalyst and co-catalysts loading, as well as performing the reaction under the mildest possible conditions.

For photocatalytic CO₂ reduction, Fe, Co, and Ni complexes with phenanthrolyl and bipyridine N4 (Figure 9) and metal porphyrins (Figure 10) with zinc and iron are involved in this field in order:

- ✓ To investigate the effect of different parameters such as the metal center, the ligand structure, towards the reactivity and the selectivity of the products obtained, besides exploring the effect of the system components regarding the photocatalytic activity.
- ✓ To find the effective metal catalyst able to show good activity and stability, and also to explore the versatility of tetradentate complexes and their ability to perform a wide range of reactions.
- ✓ To investigate the efficiency of selected metal and organic compounds as photo-sensitizers for the photocatalytic process in order to make the system as economical as possible.
- ✓ To conduct preliminary examinations involving metal porphyrins, as catalysts and as photosensitizers, as well as comparing the results to the previously explored phenanthrolyl metal complexes.
- ✓ To examine the multi-functionality of the synthesized catalysts and their potential to perform a wide range of catalytic reactions.

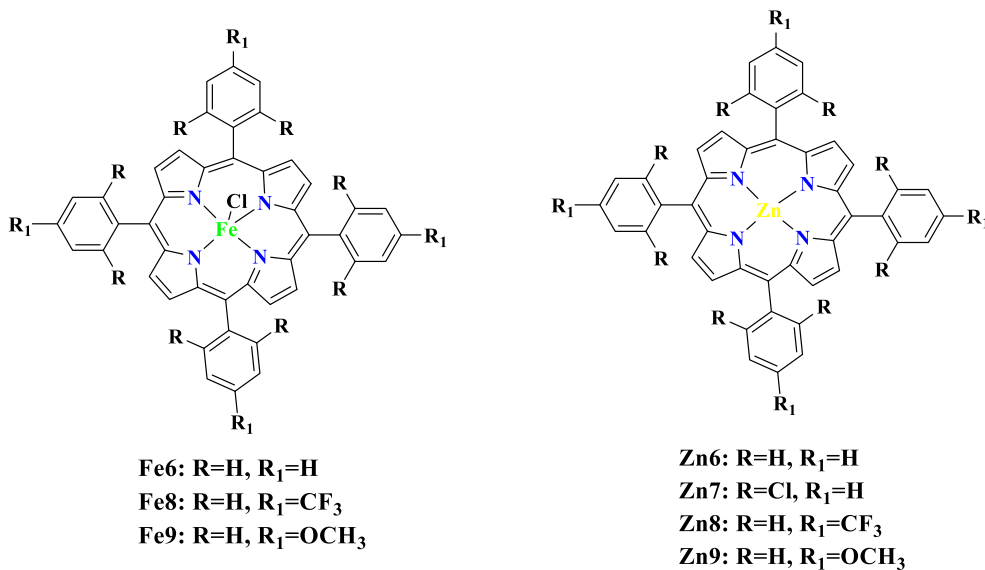


Figure 10: Structure of the porphyrins used for the photocatalytic investigations.

***CHAPTER 3: Zinc catalyzed cycloaddition
of CO₂ to epoxides for cyclic carbonate
synthesis.***

3.1. Introduction

The use of CO₂ as a building block for the synthesis of high value-added chemicals has emerged as an area of significant focus in CO₂ conversion.^[195,196] The cycloaddition of CO₂ to epoxides, which can be used even on an industrial scale for the synthesis of cyclic carbonates and polycarbonates^[197] is among the most extensively investigated classes of reactions using CO₂. Lately, a large range of homogeneous and heterogeneous catalytic systems were proposed for the chemical fixation of CO₂ to epoxides.^[198–200] Synthesis of cyclic carbonates from CO₂ is a topic of great relevance,^[198,201] especially because cyclic carbonates have a great applicability in industrial process. As already discussed in the general introduction, they are mainly employed as polar aprotic solvents, electrolytes in secondary batteries, monomers for polycarbonate-based polymers and fine chemical intermediates.^[198,201,202] On the other hand, CO₂ is a thermodynamically stable molecule, for an efficient coupling reaction to give cyclic carbonates, the use of both catalyst coupled with a cocatalyst is needed for the ring opening of the epoxide and reducing the activation energy of the CO₂ conversion.

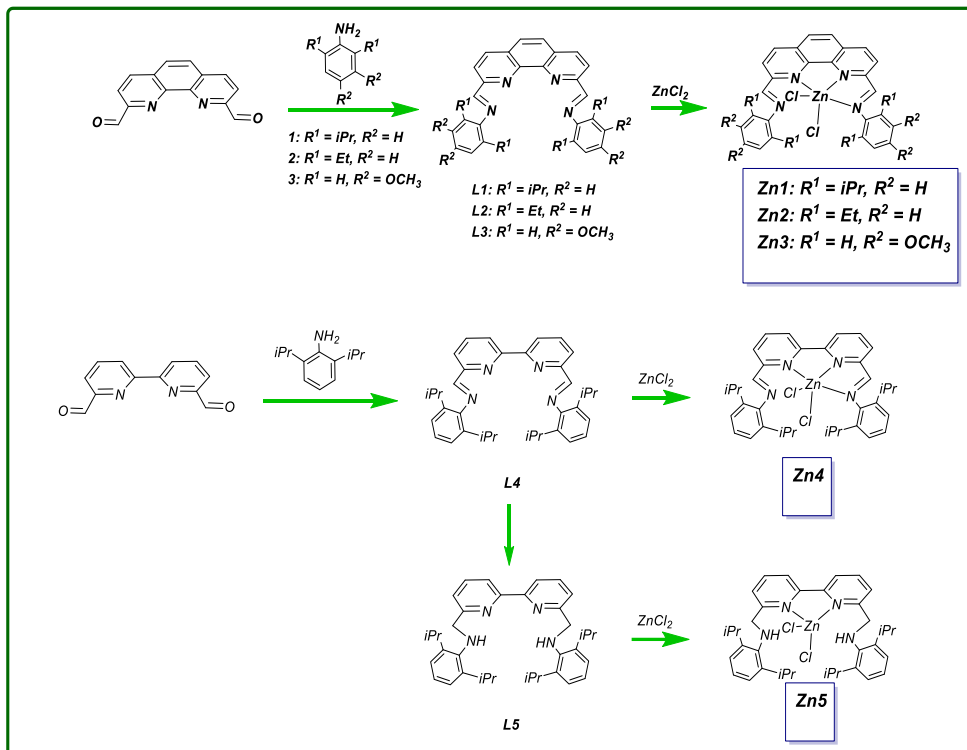
Several types of metal-free catalysts have so far been presented,^[203] such as halides containing weakly interacting cations (e.g., ammonium, imidazolium), and nitrogen donor base.^[204,205] Other catalysts comprising a hydroxy-containing electrophile phenols,^[206] glycerol,^[207] lignin,^[208] and cellulose,^[54]. A variety of affordable, abundant, and low toxic metals has attracted substantial attention and they have been tested as catalysts for this reaction (e.g., Cu, Al, Zn), showing promising performance, even under neat conditions.

Regarding the application of Zn-based complexes bearing N₄-donor ligands as catalysts for CO₂/epoxide cycloaddition, some significant examples have been reported in the literature. The authors of these works use rather high loadings of catalysts or harsh reaction conditions.

For instance, Zn halide complexes derived from the N4-donor polypodal ligand tren (N1,N1-bis(2-aminoethyl) ethane-1,2-diamine) with formula [Zn(trenR)X]X (X=Br, I) produced cyclic carbonates from terminal epoxides in 80-97% yield at 80°C under atmospheric CO₂ pressure using 1 mol% catalyst in 6h of reaction time.^[209] Other Zn-N4-donor catalysts ^[210] with a pyridine based macrocyclic ligand 3,6,9-triaza-1(2,6)-pyridine-cyclodecaphane gave quantitative yields in the cyclic carbonates using 0.5 mol% of catalyst loading at 8 bar of CO₂ pressure at 125°C at 3h reaction time. Dinuclear Zn(II) systems with N4-donor and N5-donor ligands based on pyrrole skeleton were also reported ^[210] to catalyze the cycloaddition of CO₂ to epoxides with TOF up to 232 h⁻¹ at 120°C for styrene oxide in the presence of ammonium halides.

2,2'-Bipyridine (Bipy) and 1, 10-phenanthroline (Phen), as well as substituted derivatives of bipyridine, phenanthroline and other α -diimines, have been widely adopted as ligands in analytical and preparative coordination chemistry.^[211]

As an illustration, recent reports demonstrate the incorporation of these ligand systems into macrocycles. A great deal of this work has been initiated by the current intense interest in the catalytic, redox, and photoredox properties of these ligands with various metals, particularly with ruthenium. The main feature of these nitrogenous heterocycles containing six-membered rings is their ease of access. They can be easily synthesized by the condensation reaction between carbaldehyde and aniline derivative. Moreover, several substituents can be introduced in order to modify the structure and the electronic properties of the molecule. For that, a set of zinc complexes with tetradentate donor ligands that bear a phenanthroline and bipyridine bis(aniline) backbone (Scheme 8) were synthesized and applied as catalysts for the cycloaddition of CO₂ to a variety of epoxides to generate cyclic carbonates. Preliminary studies were undertaken previously in the group,^[212,213] and here the study was completed. So, only the new results will be presented.



Scheme 8: Synthesis of ligands and zinc complexes.

3.2. Experimental section

3.2.1. General remarks

All the reactions were carried out in oven-dried glassware, connected to a line of N₂ gas to make the synthesis under inert atmosphere. The starting materials were purchased from commercial suppliers and stored carefully. Epoxides were supplied by sigma Aldrich and were stored tightly in a dry place, as they are moisture sensitive, away from oxidizing agents. CO₂ gas from the gas cylinders (99.99% pure) were purchased from Linde, Germany. The solvents used for synthesis or purification are being dried prior to utilization. Ethanol, 1-propanol, were dried over reflux in Mg/I₂ and distilled under nitrogen atmosphere, and n-butanol was dried over molecular sieves 3Å. Products characterization has been performed according to the well-known characterization techniques; nuclear magnetic resonance (NMR) spectra, were acquired at 400 MHz Varian. Chemical shifts (δ) are expressed in ppm and are measured with reference to the residual solvent as references. Deuterated solvents were purchased from sigma Aldrich and securely managed and stored. Samples for high-resolution electrospray ionization mass spectra (ESI-TOF) and elemental analysis were sent safely to be performed at the Service Techniques of Research of Girona university (Spain). The FT-IR spectra (Fourier Transformed Infrared) were recorded on a Bruker Vortex 70 spectrometer and on a JASCO 6700 FTIR equipment using the attenuated total reflectance (ATR) technique (range 4000-600 cm⁻¹).

3.2.2. Ligands and Zn complexes synthesis

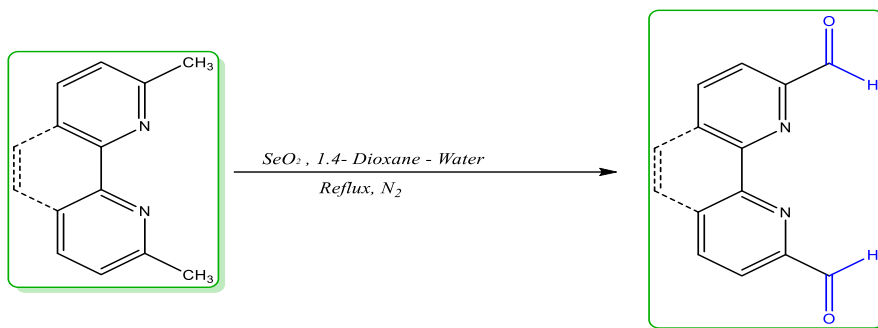
3.2.2.1. 2,9-diformyl-1,10-phenanthroline

The compound was prepared following a modified procedure from the literature. (Scheme 7) ^[214-216] In a two neck round bottom flask, selenium dioxide (3.39 g, 30.55 mmol, 2.12 equiv.) in dioxane (75 mL) and water (2 mL) was heated under reflux, and then a solution of 2,9-dimethyl-1,10-phenanthroline (3 g, 14.41 mmol, 1.0 equiv.)

in dioxane (60 mL) at room temperature was added to the first mixture dropwise for 30 minutes. The reaction mixture was heated to reflux under vigorous stirring for 2 hours. The final suspension was filtered while hot through celite, to remove the metallic selenium formed, and then the filtrate was cooled down at -30 °C. The formed yellow precipitate formed was filtered off, washed with diethyl ether thoroughly and dried under vacuum to obtain 2,9-diformyl-1,10-phenanthroline as a beige-yellowish powder. 0.97 g. Yield: 61%. ¹H-NMR (400MHz, ppm, DMSO-d₆) δ : 10.17 (s, 2H) 8.80 (d, J=8.0 Hz, 2H); 8.31 (d, J=8.0 Hz, 2H); 8.29 (s, 2H). ¹³C-NMR (126MHz, ppm, DMSO-d₆) δ:120.08, 131.41, 138.37, 129.20, 152.15, 145.23, 193.69.

3.2.2.2. 6,6'-diformyl-2,2'-bipyridine

This product was prepared by a slightly modified procedure from the literature.^[217,218] (Scheme7) In a 250 ml two-necked flask equipped with a mechanical stirrer and a reflux condenser, (0,25g, 1.5mmol) of 2,9-dimethyl-2,2'-bipyridine was placed in dioxan (5ml) and refluxed in an oil bath until completely dissolved. Then, selenium dioxide (1.5g, 13.5mmol) was added carefully to the first solution and stirred vigorously. The reaction mixture was refluxed for 72h. At the end of the reflux time, the hot solution was quickly decanted to separate the selenium. The dioxane was immediately removed with a rotary evaporator. The residue was dissolved in hot distilled ethyl acetate, filtered off to remove the remaining selenium particle, and washed 4 times with hot ethyl acetate. The product was recovered from the filtrate after evaporation of the solvent, recrystallization of the product with toluene was performed to obtain the product as a blank powder. 0.14 g. Yield: 44% . ¹H NMR (400 MHz, ppm, CDCl₃) δ : 10.19 (s, 2 H), 8.84-8.82 (dd, 2 H), 8.07-8.03 (m, 4 H).



Scheme 9: 2,9-diformyl-1,10-phenanthroline / 6,6'-diformyl-2,2-bipyridine synthesis reaction

3.2.2.3. (1,10-phenanthroline-2,9-diyl)bis(N-(2,6-diiso-propylphenyl) methanimine): L1

L1 was prepared according to a previously reported procedure.^[215] To a stirred solution under nitrogen of 2,9-diformyl-1,10-phenanthroline (0.19 g, 0.80 mmol) in dry ethanol (30 mL) with 2-3 drops of glacial acetic acid, at reflux, 2,6-diisopropylaniline (2.28 g, 12.86 mmol, 8 eq.) in dry ethanol (30 mL) were added dropwise for 30 minutes. The solution was stirred and refluxed for 5 h and turned orange. After this time, it was cooled to room temperature, reduced to half volume *in vacuo* and kept at -30 °C overnight. The yellow precipitate obtained was filtered off, washed with cold ethanol (3 x 10mL), and dried under vacuum to yield a yellow crystal. 0.30 g. Yield :70%.

¹H NMR (400 MHz, ppm, CD₂Cl₂) δ: 1.18 (d, 24 H, *J* = 6.8 Hz), 3.05 (sept, 4H, *J* = 6.8 Hz), 7.15-7.21 (m, 6H), 8.01 (s, 2H), 8.47 (d, 2H, *J* = 8.4 Hz), 8.67 (s, 2H), 8.70 (d, 2H, *J* = 8.4 Hz).

¹³C NMR (126 MHz, ppm, CD₂Cl₂) δ: 23.1, 27.9, 120.4, 122.9, 124.5, 127.8, 130.2, 137.0, 145.7, 148.4, 154.5, 163.3 ppm.

IR(cm⁻¹, ATR): 2960 (s), 2925 (w), 2871(w), 1636 (C=N,s) 1616 (w), 1583 (m), 1550 (m),.1500 (m), 1457 (m).

ESI-MS Calcd. for C₃₈H₄₂N₄ m/z: 554.3409 [M]⁺, found m/z: 555.3488 [M+H]⁺.

3.2.2.4. 1,1'-(1,10-phenanthroline-2,9-diyl)bis(N-(2,6-diethyl-phenyl)methanimine): L2

To a stirred solution under nitrogen of 2,9-diformyl-1,10-phenanthroline (0.19 g, 0.80 mmol) in dry ethanol (30 mL) with 2-3 drops of glacial acetic acid at reflux, 2,6-diethylaniline (1.91 g, 12.86 mmol) in dry ethanol (30 mL) were added dropwise during a duration time of 30 minutes. The solution was stirred and refluxed for 5 h and turned orange. After this time, it was cooled to room temperature, reduced to more than half volume in vacuum and kept at -30 °C overnight. Pentane was added to obtain a yellow precipitate, which was filtered off, and washed with cold pentane (3 x 10mL) and dried under vacuum to yield the yellow product. 0.2794 g. Yield: 71%.

¹H NMR (400 MHz, ppm, CD₂Cl₂) δ: 1.133 (t, 12 H, *J* = 7.2 Hz), 2.540 (q, 8H, *J* = 7.2 Hz), 7.05-7.15 (m, 6H), 8.010 (s, 2H), 8.48 (dd, 2H, *J* = 8.4, 0.8 Hz), 8.687 (d, 2H, *J* = 8.4 Hz), 8.687 (d, *J* = 0.8 Hz).

¹³C NMR (126 MHz, ppm, CD₂Cl₂) δ: 14.3, 24.6, 120.3, 124.3, 126.2, 127.8, 130.2, 132.6, 137.1, 145.7 149.6, 154.6, 163.5.

IR(cm⁻¹, ATR): 2961 (m), 2931 (w), 2870(w), 1722(s), 1635 (s), 1585 (m), 1550 (m), 1500 (m), 1452 (m).

ESI MS Calcd. for C₃₄H₃₄N₄ (CH₂Cl₂/MeOH) m/z: 521.2681 [M+Na]⁺, found m/z: 521.3781.

3.2.2.5. 1,1'-(1,10-phenanthroline-2,9-diyl)bis(N-(3,4-dimethoxyphenyl)-methanimine): L3

The synthesis of L3 was performed according to a previously described procedure from the literature.^[219] A solution of 2,9-diformyl-1,10-phenanthroline (0.25 g, 1.06 mmol) in dry tetrahydrofuran (50 mL) under nitrogen was refluxed for 30 minutes. To this solution was added a solution of 3,4-dimethoxyaniline (0.6 g, 2.015 mmol) in

tetrahydrofuran (25 mL) dropwise for 1 h. The resulting solution was refluxed for 6h in a Dean and Stark apparatus removing azeotropically the water produced in the reaction. The solvent was reduced to half volume, cold methanol was added to yield a red solid which was filtered off, washed with methanol, and dried under vacuum to obtain the red powder. 0.35g. Yield: 66%. The ¹H NMR data was consistent with literature values.^[219]

¹H NMR (CD₂Cl₂, ppm, 400 MHz): 3.89 (s, 6H, OCH₃), 3.93 (6H, s, OCH₃), 6.97 (2H, d, J = 8.4 Hz, Ar), 7.10 (2H, d, J = 8.4 Hz, Ar), 7.13 (2H, s, Ar), 7.94 (2H, s, phen), 8.40 (2H, d, J = 8.4 Hz, phen), 8.59 (2H, d, J = 8.4 Hz, phen), 9.09 (2H, s, N=CH).

3.2.2.6. Synthesis of 6,6'-bis(aldimino)-2,2'-bipyridine (2,6-diisopropylanil): L4

The synthesis of the L4 was performed according to a procedure already described.^[220] To a suspension of 6,6'-diformyl-2,2'-bipyridine (0.25 g, 1,27mmol) in 5ml of dry ethanol, under inert atmosphere, was added 2,6-diisopropylaniline (2.8 mmol, 0.5 g) with a catalytic amount of glacial acetic acid. The mixture was stirred and heated to 70°C for 18 h. After allowing to cool down to room temperature, the resulting precipitate was collected by filtration and recrystallized from ethanol to afford the product as a bright-yellow solid. 0.330 g. Yield : 67%. The ¹H NMR data was consistent with literature values.^[220]

¹H NMR (400 MHz, ppm, CD₂Cl₂) δ: 1.19 (d, 24 H, J = 6.8 Hz), 3.00 (sept, 4H, CH(CH₃)₃, J = 6.8 Hz), 7.12-7.18 (m, 6H), 8.01 (t, 2H, J = 7.4 Hz), 8.32 (d, 2H, J = 7.4 Hz), 8.40 (s, 2H, CH=N), 8.65 (d, 2H, J = 7.8 Hz).

3.2.2.7. Synthesis N,N'-([2,2'-bipyridine]-6,6'-diylbis (methylene) bis(2,6-diisopropylaniline): L5

The synthesis of L5 was carried out adopting a reported method from the literature.^[221] In an oven dry round bottom flask and under inert atmosphere, A suspension of LiAlH₄ (0.091 g, 2.40 mmol) in dry diethyl ether (8 mL) was added to

a solution of **L4** (0.500 g, 0.90 mmol) in dry diethyl ether (4 mL). This mixture was refluxed for 7 h. The excess of LiAlH₄ was carefully decomposed by slow addition of water keeping the reaction flask in an ice bath. The mixture was extracted with ethyl acetate (3 x 15 mL), the organic layer was dried with Na₂SO₄, filtered, and evaporated to dryness with rotary evaporation. The final solid was recrystallized from ethanol to obtain a spectroscopy pure pale-yellow product. 0,29 g. Yield: 60%.

¹H NMR (400 MHz, ppm, CD₂Cl₂) δ: 1.26 (d, 24 H, *J* = 6.7 Hz), 3.50 (sept, 4H, CH(CH)₃, *J* = 6.8 Hz), 4.26 (s, 4H) 7.03-7.13 (m, 6H), 7.33 (d, 2H, *J* = 7.6 Hz), 7.84 (t, 2H, *J* = 7.5 Hz), , 8.45 (d, 2H, *J* = 7.9 Hz).

¹³C NMR (126 MHz, ppm, CD₂Cl₂) δ: 24.4, 28.2, 56.8, 119.6, 122.5, 123.9, 124.1, 137.7, 143.0, 144.2, 155.7, 158.6.

IR(cm⁻¹, ATR): 3314(w), 2953(m), 2924(m), 2864(m), 1637(m), 1566(s), 1456(s), 1436(s), 789(s), 748(s).

ESI-MS Calcd. for C₃₆H₄₇N₄ [M+H]⁺m/z: 535.3801 , found m/z: 535.3796.

3.2.2.8. Synthesis of 2,9-bis(imino)-1,10-phenanthroline-bis-(2,6-diisopropylaniline) dichlorozinc (II): ZnI

This compound was synthesized according to a previously developed procedure.^[213] In an oven dried round flask, a mixture of ZnCl₂ (0.07 g,0.51 mmol) and dry propanol (17 mL) was refluxed under stirring until the complete dissolution of the zinc salt. Then, L1 was added (0.13 g, 0.23 mmol) and a yellow solid precipitate was formed, then the mixture was stirred under reflux for 18 h. After cooling to room temperature, the solid was filtered off, washed with cold and dry hexane (3 x 10mL) and dried in vacuum to afford a bright yellow crystals. 0.11 g. Yield: 64%.

¹H NMR (400 MHz, ppm, CD₂Cl₂) δ: 1.18 (d, 24 H, CH₃, *J* = 6.8 Hz), 3.19 (stp, 4H, CH iPr, *J* = 6.8 Hz), 7.18–7.24 (m, 6H, CH Ar), 8.19 (s, 2H, CH phen), 8.63 (d, 2H, CH phen, *J* = 8.4 Hz), 8.78 (d, 2H, CH phen, *J* = 8.4 Hz), 8.99 (s, 2H, CH—N).

¹³C NMR (126 MHz, ppm, CD₂Cl₂) δ: 23.8, 27.9, 123.3, 124.9, 125.7, 128.0, 130.8, 138.0, 140.4, 160.0. FTIR (cm⁻¹) (ATR): 2961 (s), 2921 (w), 2862 (w), 1639 (m, C=N) 1620 (m, C=N), 1587 (m), 1566 (w), 1506 (s), 1462 (s).

FTIR (cm⁻¹,ATR): 2961 (s), 2921 (w), 2862 (w), 1639 (m, C = N) 1620 (m, C = N), 1587 (m), 1566 (w), 1506 (s), 1462 (s).

Conductivity: 0.23 S.cm².mol⁻¹ at T = 23.5°C (CH₂Cl₂, 0.4.10⁻³M).

HR-MS (ESI-TOF) m/z Calcd. For C₃₈H₄₂ClN₄Zn: 653.2389 [M-Cl]⁺, found: 653.2379 (100%).

Anal. Calcd. For C₃₈H₄₂Cl₂N₄Zn.H₂O (709.1): C 64.4, H 6.2, N 7.9;found C 64.2, H 6.0, N 7.7.

3.2.2.9. Synthesis of 2,9-bis(imino)-1,10-phenanthroline-bis-(2,6-diethyl aniline) dichlorozinc (II): Zn2

In a nitrogen purged Schlenk flask, a mixture of ZnCl₂ (0.07 g, 0.51 mmol) and dry propanol (17 mL) was heated under stirring until the zinc salt dissolved. Afterwards, L2 was added (0.12 g, 0.23 mmol). A yellow solid was precipitated, and the mixture was stirred at reflux for 18 h. After cooling to room temperature, the solid was filtered, then washed with dry hexane and dried in vacuo to give a yellow crystals. 0.14 g. Yield 80%. Zn₂ crystals fit for X-ray diffraction analysis were obtained by gentle evaporation of a deuterated dichloromethane solution of the complex.

¹H NMR (400 MHz, ppm, CD₂Cl₂) δ: 1.14 (t, 12 H, CH₃, J = 7.5 Hz), 2.70 (q, 8H, CH Et, J =7.5 Hz), 7.11-7.16 (m, 6H, CH Ar), 8.18 (s, 2H, CH phen), 8.60 (d, 2H, CH phen, J = 8.3 Hz), 8.77 (d, 2H, CH phen, J = 8.3 Hz), 9.00 (s, 2H, CH=N).

¹³C NMR (126 MHz, ppm, CD₂Cl₂) δ: 14.6, 24.6, 124.9, 125.5, 126.1, 128.0, 130.9, 140.3, 141.2, 147.9, 160.4.

FTIR(cm⁻¹, ATR): 2962 (m), 2928 (w), 2870(w), 1637 (m, C = N), 1617 (m, C = N), 1583 (m), 1564(m), 1505 (m), 1450 (m), 877(s), 798(s), 762

Conductivity: $3.55 \cdot \text{S} \cdot \text{cm}^2 \cdot \text{mol}^{-1}$ at $T = 25^\circ\text{C}$ (CH_2Cl_2 , $0.4 \cdot 10^{-3} \text{ M}$).

ESI-MS Calcd. For $\text{C}_{34}\text{H}_{34}\text{ClN}_4\text{Zn}$ m/z : 597.1763 $[\text{M}-\text{Cl}]^+$, found m/z : 597.1767 (100 %).

Anal. Calcd. For $\text{C}_{34}\text{H}_{34}\text{Cl}_2\text{N}_4\text{Zn} \cdot \text{H}_2\text{O}$ (650.2): C 62.5, H 5.6, N 8.6; found C 62.4, H 5.1, N 8.5.

3.2.2.10. Synthesis of dichloro(1,1'-(1,10-phenanthroline-2,9-diyl) bis(N-(3,4-dimethoxyphenyl) methanimine)) zinc(II) (Zn3)

In a purged round flask under nitrogen, a mixture of ZnCl_2 (0.07 g, 0.51 mmol) and dry propanol (15 mL) was refluxed under stirring till the zinc salt dissolution. Then L3 was added (0.11 g, 0.23 mmol), a yellow solid precipitated and the mixture was stirred at reflux for 18 h. After cooling to room temperature, the solid was filtered off, washed with dry hexane, and dried in vacuum to give a dark pink precipitate. 0.12 g. Yield: 81%.

^1H NMR (CD_2Cl_2 , ppm, 400 MHz): 3.91 (s, 12H, OCH_3), 6.95 (2H, d, $J = 8.4$ Hz, Ar-H), 7.44 (2H, d, $J = 8.4$ Hz, Ar), 7.57 (2H, s, Ar), 8.07 (2H, s, phen), 8.50 (2H, d, $J = 8.2$ Hz, phen), 8.62 (2H, d, $J = 8.2$ Hz, phen), 9.44 (2H, s, $\text{CH}=\text{N}$).

^{13}C NMR (126 MHz, ppm, CD_2Cl_2) δ : 56.2, 106.4, 111.1, 117.2, 124.8, 127.4, 129.8, 139.5, 140.7, 140.9, 149.5, 150.1, 151.5, 152.9.

FTIR(cm^{-1} , ATR): 2965(w), 2837(w), 1609 (w, C = N), 1587(m), 1567(m), 1509(s), 1262(s), 1243(s), 1223(s), 1136 (s), 1121(s), 1017(s), 867(s), 857(s).

Conductivity: $2.10 \cdot \text{S} \cdot \text{cm}^2 \cdot \text{mol}^{-1}$ at $T = 26.3^\circ\text{C}$ (DMF, $0.4 \cdot 10^{-3} \text{ M}$).

ESI MS Calcd. For $\text{C}_{30}\text{H}_{26}\text{Cl}_2\text{N}_4\text{O}_4\text{Zn}$ m/z : 641.0695 $[\text{M}]^+$, 605.0934 $[\text{M}-\text{Cl}]^+$, found m/z : 605.0954 (100 %), 641.0707 (18%).

Anal. Calcd. For $\text{C}_{30}\text{H}_{26}\text{Cl}_2\text{N}_4\text{O}_4\text{Zn} \cdot \text{H}_2\text{O}$ (660.9): C 54.5, H 4.3, N 8.5; found C 52.0, H 3.9, N 8.1.

3.2.2.11. Synthesis of dichloro(1,1'-(2,2'-bipyridine-6,6'-diyl) bis(N-(2,6-diisopropylphenyl) methanimine))zinc(II) (Zn4)

This compound was synthesized following a previously reported procedure.^[220] By using L4 and ZnCl₂ salt. In an oven-dried flask equipped with a magnetic stir bar, was charged with ZnCl₂ (0.039 g, 0.283 mmol) in dry n-BuOH (10 mL) and the contents stirred at 100°C until the zinc salt had completely dissolved. L1 (0.039 g, 0.283 mmol) was added, and the reaction mixture stirred at 100°C overnight. After cooling to room temperature, the solvent was concentrated under reduced pressure and hexane added to induce the precipitation. Followed by filtration, washing with hexane, and drying under reduced pressure to give a yellow solid. 0.063g. Yield: 77%.

¹H NMR (400 MHz, ppm, CD₂Cl₂) δ: 1.15 (d, 24 H, J = 6.6 Hz), 3.15 (spt, 4H, CH(CH)₃, J = 6.6 Hz), 7.16 (m, 6H), 8.32 (m, 4H), 8.45 (m, 2H), 8.85 (m, 2H).

¹³C NMR (126 MHz, ppm, CD₂Cl₂): δ 23.7, 27.9, 121.7, 123.2, 124.0, 125.5, 126.6, 138.2, 141.5, 151.1, 156.2, 160.0. Conductivity: 4.23·S.cm².mol⁻¹ at T = 25°C (CH₂Cl₂, 0.4·10⁻³ M).

3.2.2.12. Synthesis of dichloro (N,N'-(2,2'-bipyridine-6,6'-diylbis(methylene))bis(2,6-diisopropylaniline))zinc(II) (Zn5)

In a nitrogen-purged Schlenk tube, a mixture of ZnCl₂ (0.07 g, 0.51 mmol) and dry propanol (17 mL) was refluxed with stirring until the zinc salt dissolved. Then L5 (0.123 g, 0.23 mmol) was slowly introduced, and the mixture was stirred at reflux for 18 h. After cooling to room temperature, the solvent was removed under reduced pressure and hexane was added to induce precipitation. The solid was filtered off, washed with cold hexane, and dried in vacuo to give yellow crystals. 0.1034 g. Yield: 67%. Zn5 crystals adequate for X-ray diffraction analyses have been obtained by gentle evaporation of a deuterated dichloromethane solution from the compound.

¹H NMR (400 MHz, ppm, CD₂Cl₂) δ: 1.14 (d, 24 H, J = 6.7 Hz), 3.09 (sept, 4H, CH(CH)₃, J = 6.7 Hz), 3.09 (d, 24 H, J = 6.7 Hz), 3.09 (sept, 4H, CH(CH)₃, J = 6.7

Hz). 6.7 Hz), 4.66 (m, 6H) 7.06-7.12 (m, 6H), 7.45 (d, 2H, J = 7.8 Hz), 8.06 (t, 2H, J = 7.6 Hz), 8.18 (d, 2H, J = 7.9 Hz).

¹³C NMR (126 MHz, ppm, CD₂Cl₂) δ: 24.4, 28.2, 56.8, 119.6, 122.5, 123.9, 124.1, 137.8, 143.0, 144.2, 155.7, 158.6 ppm.

FTIR (cm⁻¹, ATR): 3086 (w), (s), 2965 (s), 2948(m), 2879(m), 1637(m), 1600(m), 1586 (m), 1474(s), 1444(m), 1172(s), 1018(m), 796(s), 762(s), 732(m)

3.2.3. Catalysis : Reactor Preparation

Catalytic cycloaddition reactions of CO₂ with epoxides were performed in a 25 ml Parr reactor (Figure 11) system equipped with a magnetic stirring bar and heated in an oil bath. In the bulk setup, the vessel was loaded with the epoxide along with freshly prepared catalyst, cocatalyst (nucleophilic source) without any solvent. The reactor was purged with 2-3 bar of CO₂. Carbon dioxide was pressurized to the desired pressure. Then the reactor was placed in the oil bath, and the reaction was carried out under the predetermined conditions. Once the reaction was completed, the reactor was cooled to 0 °C in an ice bath and depressurized slowly to carefully release the remaining CO₂ inside the autoclave. A 30 μL sample of the crude reaction mixture was dissolved in deuterated solvent with mesitylene as the internal standard reference (15 μL) for analysis by ¹H NMR. NMR spectra of the solution were collected at 25 °C and analyzed by a spectrometer (400 MHz), Chemical shifts (δ) are expressed in ppm and are measured with reference to the residual solvent as references: 7.26 ppm for CDCl₃.

The conversion yield was evaluated on the basis of the ¹H NMR spectrum of the crude reaction mixture by integrating the ratio of the epoxide to the formed cyclic carbonate. The Turnover frequency was calculated by dividing the conversion of the reaction by the percentage of catalyst used and then by the total reaction time, the unit of TOF is (h⁻¹).



Figure 11: Reactor employed for the cycloaddition of CO₂ reaction.

3.2.4. X ray structure

Zn₂ and Zn₅ crystal structure's data were collected at 100 (2) K using an Oxford Cryotream 700+ in a Rigaku MicroMax-007HF Microfocus rotating anode X-ray tube equipped with a hybrid pixel detector PILATUS 200 K with Mo K α radiation. Software for data collection, data reduction and absorption correction: CrysAlisPro 1.171.40.35a.^[222] Empirical absorption correction using spherical harmonics, implemented in SCALE3 ABSPACK ^[222] scaling algorithm. Software for data solution SIR2019.^[223] Software for data refinement SHELXL-2018/3 ^[224] under the shelXle interface.^[225] Crystallographic data are collected in tables 1, 2 . The resolution of these structures was performed at the ICIQ-Institut Català d'Investigació Química.

3.3. Results & Discussion

3.3.1. Synthesis of ligands and complexes

Ligands derived from 1,10-phenanthroline bis(imine) L1-L3 (Scheme 6) and 2,2'-bipyridine bis(imine) L4 (Scheme) ligands were prepared by condensation of 2,9-diformyl-1,10-phenanthroline,^[214-216] and 6,6'-diformyl-2,2'-bipyridine,^[217,218] with the corresponding aniline derivative as previously reported.^[215,220] The 2,2'-bipyridine bis(amine) ligand L5, was prepared by reduction of L4 with LiAlH₄ as reported for related imines.^[221] The reaction of the ligands L1-L3 and L5 with anhydrous ZnCl₂ in 1-propanol led to the corresponding Zn(II) complexes Zn1-Zn3 and Zn5 in good yields (64-81%). Complex Zn4 was previously reported in the literature and was prepared accordingly.^[220] The new complexes Zn1-Zn3 and Zn5 were characterized by high-resolution electrospray time of flight mass spectrometry (HRMS ESI-TOF), elemental analysis and FTIR and NMR spectroscopies. X-ray diffraction structures were obtained for Zn2 and Zn5. Complex Zn1 was previously characterized.^[213]

The ESI-TOF mass spectra of the new complexes Zn2, Zn3 and Zn5 presented peaks at *m/z* corresponding to [M-Cl]⁺ fragments (Experimental Section) and the elemental analysis were in concordance with [Zn(L1-L5)Cl₂] formula. Confirmation of the neutral nature of the coordination entities was obtained by the low values of the conductivity in solution (values < 5 S.cm².mol⁻¹). Which confirm that the chloride ions remain mostly coordinated in solution with small constant dissociation. Evidence of the ligand coordination was obtained by the FTIR and NMR spectra. For Zn2. The FTIR spectra of the imine complexes, signals at ca 1635 cm⁻¹ attributed to the stretching C = N vibration confirm the presence of the coordinated ligand. These signals slightly shifted (2–3 cm⁻¹) to higher frequencies indicating a poor back bonding from the metal. It could not be distinguished if both imine groups were coordinated since there was overlapping with signals from the phenanthroline skeleton (1600–1400 cm⁻¹).^[226]

The ¹H NMR spectra presented a symmetrical pattern in which the phenanthroline and bipyridine proton's signals appear as equivalents in the δ 7.4-8.9 ppm region. The aniline proton signals were observed in the δ 7.0-7.5 ppm region, and the CH=N imine signal was detected in the δ 8.4-9.0 ppm interval for the Zn₂-Zn₄ complexes. The ¹H NMR spectrum of L5 does not show the CH-N signal at δ 8.40 ppm and a new singlet at δ 4.26 ppm corresponding to the new methylene group -CH₂-NH confirms the reduction of the imine. The ligand's signals for Zn₂-Zn₅ suffer a shielding to higher chemical shifts confirming the coordination to the metal center. Furthermore, only one imine signal was observed in the ¹H NMR spectra of Zn₂-Zn₄ although, as will be discussed in the next section, the X-ray diffraction structure of Zn1^[213] and Zn₂ indicates that the ligand was acting as tridentate coordinating to the metal through the phenanthroline and one imine.

3.3.2. X ray structure

Yellow crystals of the phenanthroline diimines derivatives Zn₂ and Zn₅ suitable for X-ray diffraction analysis have been achieved from deuterated chloroform and dichloromethane solutions. The crystals of Zn₁ were previously obtained. The ORTEP patterns for Zn₂ and Zn₅ are shown in the (Figure 10), (Figure 11) respectively, and the selected bond distances and angles of Zn₂, Zn₅ are listed in the Table 1, and Table 2 respectively.

3.3.2.1. Zn 2 complex

The Zn₂ complex presented a 5-coordinated environment (Figure 12), similarly to Zn₁.^[213] The Zn metal is bound to the ligand by 3 bonds, and equally bound to two Chlorides, thus it makes it a neutral molecule, thus the ligand acts as a 3N, N, N tridentate donor with one of the imino groups unbound (exo) giving an endo-exo overall configuration of the imine groups. The Zn-N and Zn-Cl bond distances are in the range of the ones reported for the related complexes containing L1.^[215,227]

The Zn-N1 distance (2.1007(7) Å) corresponding to the central donor atom in the tridentate ligand is significantly shorter than the Zn-N1 and Zn-N3 bond lengths

(2.366(11) and 2.307(9) Å respectively). The imine C = N bonds retain their double bond character^[220] but the relative longer distance in the coordinate imine indicates a weak back donation from the metal confirming the IR data. The relative orientation of the imine groups is in both cases trans and the aryl substituents of the imino groups are ca orthogonal to the plane defined by the N-coordinated ligand. The relative disposition of the two aryl moieties is slightly disrotated (not parallel aromatic planes) as reported for a similar Zn(II) complex.^[220]

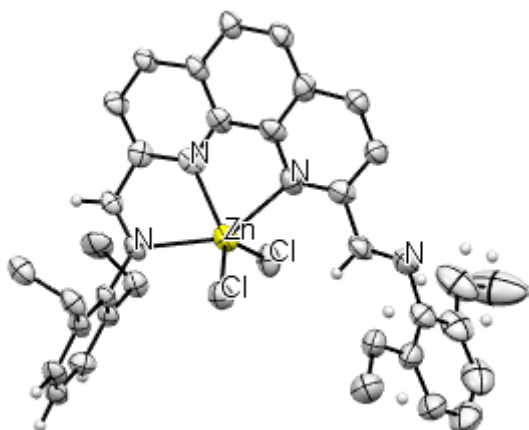


Figure 12: ORTEP drawing of complex of Zn2. All hydrogen atoms and solvent molecules are omitted for clarity. Thermal ellipsoids are drawn at the 50 % probability level.

Table 1: Selected bond lengths (Å) and angles (°) for Zn2

| Bond | Zn2 | Angle | Zn2 |
|------------------------|-----------|------------|-----------|
| Zn-Cl1 | 2.2210(8) | Cl1-Zn-Cl2 | 120.51(3) |
| Zn-Cl2 | 2.2247(8) | N2-Zn-N3 | 74.4(3) |
| Zn-N3 | 2.307(9) | N1-Zn-N2 | 72.7(3) |
| Zn-N2 | 2.100(7) | N2-Zn1-Cl2 | 114.0(4) |
| Zn-N1 _{coord} | 2.366(11) | N2-Zn1-Cl1 | 125.5(4) |
| N1-Cl1 | 1.272(7) | N3-Zn1-N1 | 146.9(4) |
| N4-C24 | 1.22(2) | Cl1-Zn1-N3 | 100.1(6) |

3.3.2.2. Zn5 complex

Zn5 (Figure 13). The bipyridine-bis(amine) zinc complex Zn5 presents a four-coordinate structure with pseudo-tetrahedral geometry in which L5 acts as a bidentate ligand with the free amine groups located outside the coordination sphere (exo), similar to reported examples. The relative positions of the aryl and pyridyl groups are in a disordered conformation. The higher flexibility of the bipyridyl structure and the steric repulsion created by the two **ortho** isopropyl substituents may account for the formation of the lower coordination number isomer.

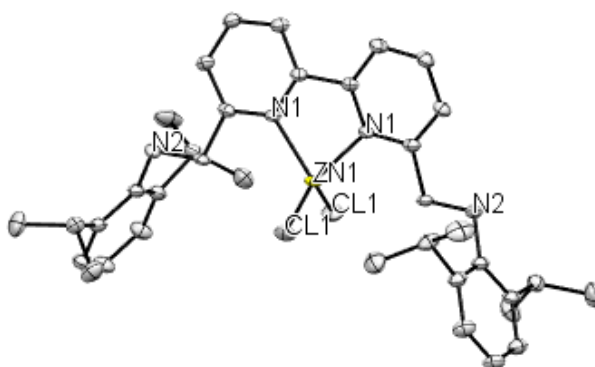


Figure 13: ORTEP drawing of complex of Zn5. All hydrogen atoms and solvent molecules are omitted for clarity.

Table 2: Selected bond lengths (Å) and angles (°) for Zn2

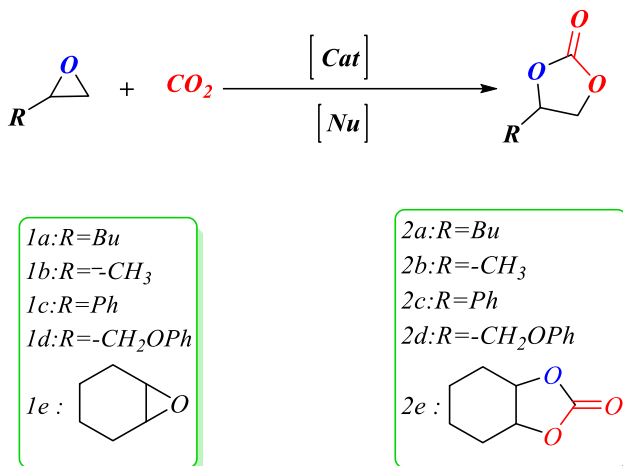
| <i>Bond</i> | <i>Zn5</i> | <i>Angle</i> | <i>Zn5</i> |
|----------------|------------|-------------------|------------|
| <i>Zn1-N1</i> | 2.058(3) | <i>N1 Zn1 N1</i> | 81.43(14) |
| <i>Zn1-Cl1</i> | 2.2114(9) | <i>N1 Zn1 Cl1</i> | 114.16(8) |
| <i>N1-C7</i> | 1.346(4) | <i>C7 N1 Cl1</i> | 120.2(3) |
| <i>N1-Cl1</i> | 1.351(4) | <i>C7 N1 Zn1</i> | 113.2(2) |
| <i>N2-C4</i> | 1.440(4) | <i>Cl1 N1 Zn1</i> | 126.4(2) |
| <i>N2-C3</i> | 1.458(4) | <i>C4 N2 C3</i> | 115.3(3) |
| <i>N2-H2N</i> | 0.78(4) | <i>C4 N2 H2N</i> | 108(4) |

3.3.3. Catalysis

The catalytic activity of zinc phenanthroline-bis(imine) (**Zn1**-**Zn3**), bipyridine-bis(imine) (**Zn4**) and bipyridine-bis(amine) (**Zn5**) concerning the cycloaddition of CO₂ to epoxides in order to generate the corresponding cyclic carbonates (Scheme 10) was studied. First of all, it was examined the cycloaddition of CO₂ to the benchmark substrate 1,2- epoxyhexane (**1a**, Scheme 10) with the complex **Zn1** at a catalyst loading of 0.1 mol% using the epoxide in a free solvent medium. The influence of the addition of a nucleophile (Nu), the reaction time, the temperature, the ratio cat/Nu, and the CO₂ pressure were examined. The aim is to operate under mild conditions, (temperature <100°C, pressure:1-30bar).

The main distinction between the **Zn1**, **Zn2** and **Zn3** complexes resides in the substitution of the aniline group, as the phenanthroline core is unchanged, whereas in **Zn4** the core is modified to a bipyridine, while **Zn5** is a bipyridine diamine rather than a diimines in **Zn4**, the scheme 6 illustrates all of these relevant points.

Tetrabutylammonium bromide has chosen to act as a nucleophile (Nu) in all performed experiments, owing to several advantages. Lately, tetrabutylammonium bromide (TBAB) has attracted considerable focus as an effective nucleophile for the CO₂ coupling to epoxides reaction. TBAB is an environmentally benign, non-volatile, non-flammable, non-corrosive, inexpensive, commercially available ammonium salt with high thermal and chemical stability.^[228] The TBAB salt can dissolve in most organic solvents^[229] as well as in the epoxides used herein under solvent free conditions.^[230,231] Furthermore, it was observed that the addition of a catalytic amount of TBAB as co-catalyst was effective in increasing the reaction rate as well as at the product yield.^[232-235]



Scheme 10: Cycloaddition of CO₂ to selected epoxides to form cyclic carbonates.

3.3.3.1. Reaction conditions optimization

The catalytic activity of Zn1 was found to be very modest under the following conditions. 30 bar CO₂ and 80 °C (only 9% yield after 20 h of reaction, entry 1, Table 3). Most probably, the chloride coordinated to the zinc center does not dissociate enough free ions to act as a nucleophile to initiate the reaction process through the ring opening of the epoxide. Indeed, Zn1 in solution has a low conductivity corresponding to a neutral molecular species. We therefore decided to add tetrabutylammonium bromide (TBAB), a commonly used nucleophile (Nu)^[51] in a 1:2 molar ratio with respect to Zn1 catalyst. The binary system Zn1/TBAB (1:2) under 10 bar of CO₂ at 80 °C, in a reaction time of 3h, generated an increase in the conversion up to 61% (entry 2, Table 3) corresponding to an average turnover frequency (TOF) of 207 h⁻¹. Only the cyclic carbonate product was detected by ¹H NMR.

Under the exact same conditions, TBAB, well-known to be an active catalyst for this type of transformation^[51] provided a lower conversion (entry 3, Table 1), confirming that the complex and the nucleophile work cooperatively. It is therefore crucial to couple the two components (catalyst and nucleophile) in a binary system, in order to obtain a high and constant conversion towards the desired products. Increasing the

Zn1/TBAB ratio from 1:2 to 1:5 increased the conversion to 75% (entry 5, Table 3) but in this case the reference experiment using only TBAB provided a similar conversion (entry 4, Table 3).

On the other hand, based on previous literature reviews, the effect of the temperature on the reaction conversion was analyzed by lowering the temperature from 80°C to 60°C. The conversion obtained demonstrated a clear drop upon the decrease of the temperature (entry 6, Table 3).

Table 3: Catalytic activity of Zn1 and TBAB in the cycloaddition of CO₂ to 1,2-epoxyhexane (1a).^a

| Entry | Cat | Nu | Zn/Nu(mol%) | P (bar) | T(°C) | t(h) | Conv ^b (%) | TOF ^c (h ⁻¹) |
|-------|-----|------|-------------|---------|-------|------|-----------------------|-------------------------------------|
| 1* | Zn1 | - | 0.1/- | 30 | 80 | 20 | 9 | 4 |
| 2 | Zn1 | TBAB | 0.1/0.2 | 10 | 80 | 3 | 61 | 207 |
| 3 | - | TBAB | -/0.2 | 10 | 80 | 3 | 45 | - |
| 4 | Zn1 | TBAB | -/0.5 | 10 | 80 | 3 | 73 | - |
| 5 | Zn1 | TBAB | 0.1/0.5 | 10 | 80 | 3 | 75 | 250 |
| 6 | Zn1 | TBAB | 0.1/0.2 | 10 | 60 | 3 | 22 | 73 |

^a General conditions: 20 mmols of 1a, catalyst (0.02 mmol 0.1 mol%), TBAB (0.04-0.1 mmol)
*: Entry conducted previously.^[213] ^b Conversion determined by ¹H NMR using mesitylene as internal standard. ^c TOF averaged turnover frequency = mols of 1a converted per mol of Zn complex per hour.

3.3.3.2. Salt incorporation effect

In an attempt to improve the conversion of the reaction using the Zn1 catalyst, without the recourse to add more nucleophile, but also to facilitate the dissociation of the chloride from the complex, thus allowing it to participate in the epoxide ring opening, we added a soluble salt, sodium tetrakis-[3,5-bis(trifluoromethyl)phenyl]borate (NaBARF), which contains a weak coordinating anion. Using Zn1 as a catalyst in the presence of 2 equivalents of NaBARF, the reaction was inhibited (entry 1, Table 4), probably because the NaCl thus formed is not soluble in the reaction medium, since we are operating in a free solvent. The Zn1/2NaBARF system in the presence of TBAB was also not active (entry 2, Table 4), probably because of the same issue.

When increasing the concentration of the nucleophile TBAB, (entries 3,4, Table 4) free Br⁻ was present in the reaction medium, and the catalytic activity reach 33% in the presence of 0.2mol% of TBAB. While achieving 63% in the presence of 0.4mol% of TBAB similar to the one obtained with Zn1/2TBAB without the NaBARF salt.

Table 4: Incorporation of the salt and its effect on the reaction conversion.^a

| Entry | Cat/Nu (mol%) | Cat/NaBarF (mol %) | Conv (%) ^e |
|----------------|---------------|--------------------|-----------------------|
| 1 | 0.1 / - | 0.1/0.2 | 0 |
| 2 ^b | 0.1 / 0.1 | 0.1/0.2 | 4 |
| 3 ^c | 0.1 / 0.2 | 0.1/0.2 | 33 |
| 4 ^d | 0.1 / 0.4 | 0.1/0.2 | 63 |

^a General conditions: 20 mmols of 1a, Cat (Zn1, 0.02mmol, 0.1mol%). P=10bar, T=80°C, Reaction time = 3h. ^b: Nu (TBAB, 0.02mmol, 0.1mol%). ^c:Nu (TBAB, 0.04mmol, 0.2mol%). ^d:Co-cat (TBAB, 0.08mmol, 0.4mol%). ^e:Conversion determined by ¹H NMR using mesitylene as internal standard.

To confirm this hypothesis, the species formed in the mixture of Zn1 with NaBARF, TBAB, and epoxide were monitored by ¹H and ¹⁹F NMR spectroscopies. When two equivalents of NaBARF were added to a suspension of Zn1 (0.02 mmol) in deuterated dichloromethane (2 mL), dissolution of Zn1 was observed as well as the appearance of a cloudiness resulting from the precipitation of NaCl. The ¹H NMR of this sample shows a shift of the signals confirming that a new complex was generated (Figure 12, b).

Further addition of 2 equivalents of TBAB resulted in a shift in the ligand signals (Figure 12, c) and partial precipitation of a yellow solid, possibly the bromide coordinated to form [Zn(L1) Br]⁺ or [Zn(L1) Br₂].

Additional injection of 5 equivalents of 1,2-epoxyhexane failed to produce any change in the spectra nor a shift in the epoxide signals,(Figure 14, d) indicating that the epoxide does not interact with the zinc complex. ¹⁹F NMR did not show any evidence of BarF⁻ coordination in any of the experiments (Figure 15). Therefore, it was confirmed that the addition of NaBARF favored the dissociation of the chlorine ligands that were probably replaced by bromine in the presence of TBAB forming an inactive species.

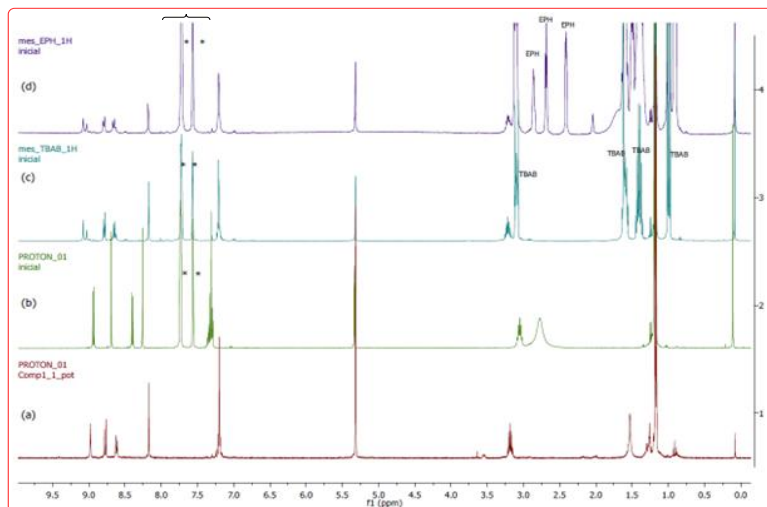


Figure 14: ¹H NMR spectrum in CD₂Cl₂ of a) **Zn1**, b) **Zn1** with 2 equivalents of NaBARF, c) **Zn1** with 2 equivalents of NaBARF and 2 equivalents of TBAB, d) **Zn1** with 2 equivalents of NaBARF, 2 equivalents of TBAB and 5 equivalents of 1,2-epoxyhexane.

As the ¹⁹F NMR spectra exhibited a chemical shift at -62.84 ppm (Figure 13) corresponding to free NaBARF, therefore, most likely [Zn(L1)][BarF] was formed.

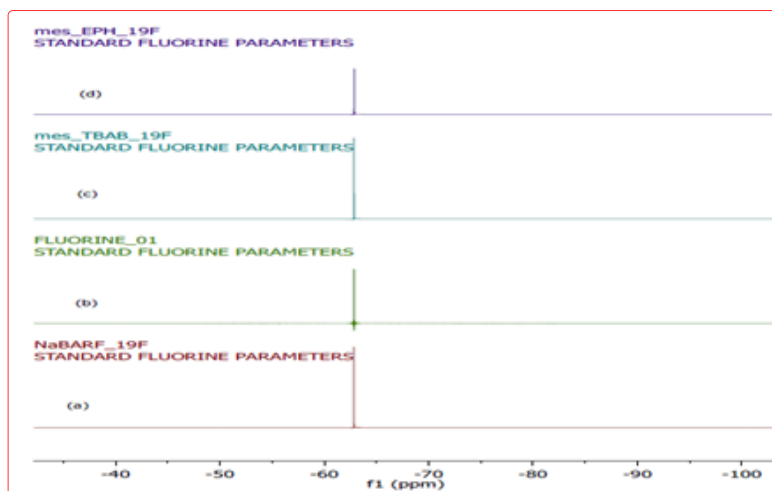


Figure 15: ¹⁹F NMR spectrum in CD₂Cl₂ of a) NaBARF, b) **Zn1** with 2 equivalents of NaBARF, c) **Zn1** with 2 equivalents of NaBARF and 2 equivalents of TBAB and d) **Zn1** with 2 equivalents of NaBARF, 2 equivalents of TBAB and 5 equivalents of 1,2-epoxyhexane.

3.3.3.3. Pressure effect

In order to assess the influence of the pressure of carbon dioxide introduced into the reactor, we chose the Zn1/TBAB molar ratio of 1:2 and a reaction temperature of 80°C. The results are shown in Figure 14. We observed that increasing the pressure from 10 bar to 20 bar and then to 30 bar and up to 40 bar, resulted in a decrease in the reactivity. A possible explanation is that a higher pressure leads to dilution of the substrate and a decrease of the catalytic activity. A test was performed by decreasing the pressure to 1 bar, the system was still active with an initial TOF of 53 h⁻¹ (Figure 16) and a high conversion (77%) was obtained after 24 h. Remarkably, under these conditions, the reference experiment using only TBAB as a catalyst produced only 26% conversion, and then a 50% increase in conversion was obtained by combining the Zn1 complex with TBAB, confirming the positive effect of using the zinc complex and nucleophile together to work cooperatively.

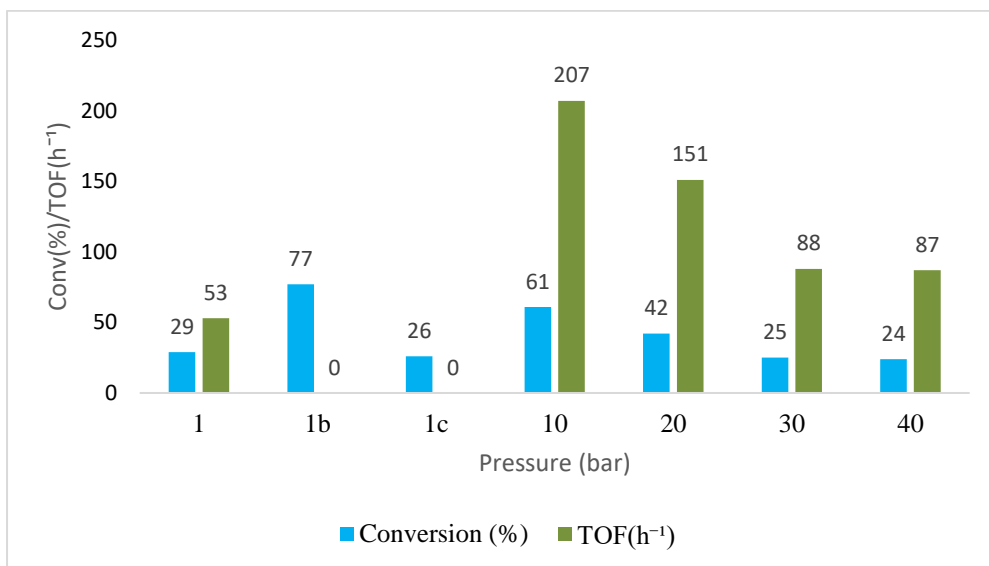


Figure 16: Effect of pressure on the cycloaddition of CO₂.^a

^a:Reaction conditions: 20 mmols of 1a, Zn1 0.02 mmol (0.1 mol%), TBAB (0.04 mmol, 0.2 mol%), temperature: 80°C, 3h. Conversion and TOF determined by ¹H NMR using mesitylene as internal standard. **b**:Zn1/TBAB (0.13/0.2 mol%), 24 h. **c**:Only TBAB (0.2 mol%), 24 h.

3.3.3.4. Catalyst effect

Once the optimized conditions were established, the effect of the Zn(II) center environment was investigated by comparing the activity of the Zn1-Zn5/TBAB catalyst systems. The catalytic reactions were carried out under the optimized conditions (pressure : 10bar, temperature : 80°C, ratio : 1:2 cat/Nu) using the epoxyhexane as substrate. The TOF values achieved for a reaction time of 3 hours are presented in Table 5. It was found that the catalytic activity increased with the steric occupancy of the orto substituent in the aniline ring (entries 1,2,3, Table 5). The order of conversion was Zn1/TBAB > Zn2/TBAB > Zn3/TBAB.

In addition, the complexes with a more flexible bipyridine backbone, Zn4 and Zn5, produced lower conversion than the phenanthroline analogs under the same conditions (entries 4,5, Table 5). Interestingly, the amino derivative Zn5 produced twice the conversion of the zinc bis (imine) analog system (entry 5, Table 5). In this case, the free amine groups may participate in CO₂ activation as previously reported with other amines.^[236]

Table 5: Cycloaddition of CO₂ to 1a using Zn1-Zn5/TBAB as catalytic system.^a

| Entry | Cat/Nu (mol%) | Cat (Zn(n)) | Conv (%) ^b | TOF(h ⁻¹) ^c |
|-------|---------------|-------------|-----------------------|------------------------------------|
| 1 | 0.1 / 0.2 | Zn1 | 61 | 207 |
| 2 | 0.1 / 0.2 | Zn2 | 53 | 173 |
| 3 | 0.1 / 0.2 | Zn3 | 26 | 87 |
| 4 | 0.1 / 0.2 | Zn4 | 25 | 86 |
| 5 | 0.1 / 0.2 | Zn5 | 54 | 177 |



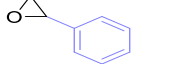
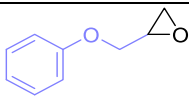
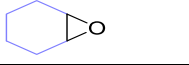
^a:General conditions: 20 mmols of 1a, catalyst (0.1 mol%), TBAB (0.2 mol%); 10 bar CO₂, T: 80°C; 3 h. ^b: Conversion determined by ¹H NMR using mesitylene as internal standard. ^c: TOF turnover frequency = mols of (1a) converted per mol of Zn complex per hour.

3.3.3.5. Scope of epoxides

The scope of the reaction was analyzed by employing alternative terminal and internal benchmark epoxides (1b-1fe Scheme 10) at 10-20 bar CO₂ pressure, 80°C using the Zn1/TBAB catalytic system (Table 6). Cyclic carbonates were also obtained as the

only products detected by ¹H NMR. The average TOF obtained from the cycloaddition of CO₂ to propylene oxide and 1,2-epoxy-3-phenoxypropane (1b and 1d, entries 2, 4, Table 6) was slightly higher than for the epoxyhexane (1a) as expected, due to the larger steric hindrance of them. Slightly lower TOF was obtained in the cycloaddition of CO₂ with styrene oxide (1c, entries 3, Table 6). For a bulkier disubstituted epoxide such as cyclohexene oxide 1e (entry 5, Table 6) the conversion was lower as expected, nevertheless, a significant TOF of 72 h⁻¹ was achieved. In this case, only cis-2e was detected by ¹H NMR.

Table 6: Catalytic activity of Zn1/TBAB in the cycloaddition of CO₂ to epoxides 1a-1e. ^a

| Entry | Substrate | Conv (%) ^b | TOF(h ⁻¹) ^c |
|----------------|--|-----------------------|------------------------------------|
| 1 |  1a | 61 | 207 |
| 2 |  1b | 82 | 208 |
| 3 |  1c | 58 | 145 |
| 4 |  1d | 84 | 228 |
| 5 ^d |  1e | 28(cis-2e) | 72 |

^a Reaction conditions: 20 mmols epoxide (1b-1f); Zn1 0.026 mmol (0.13 mol%); TBAB 0.04 mmol, (0.2 mol%), 10 bar, 80 °C, 3 h. ^b %Conversion in the cyclic carbonates (2b-2e). ^c Averaged TOF (h⁻¹). ^d 20 bar.

3.3.3.6. System stability

The stability of the catalytic system Zn1/TBAB under the reaction conditions were studied by adding the fresh epoxide in successive runs. The propylene oxide (1b) was elected as the reference substrate for this experiment. To do so, after 6 h of catalytic run, the pressure was carefully released, a sample for ¹H NMR analysis was taken and fresh 1b epoxide was added to reach the initial amount considering the conversion. The sample was repressurized and the reaction was run again. The

analysis by ¹H NMR of the contents after each run showed a constant value of ca 82–84% of carbonate 2b in the crude. Taking into consideration that fresh 1b was added in each run to achieve the initial value of 30 mmol and the carbonate accumulated in the crude, the composition of the crude indicates that the catalyst was stable and active in the consecutive runs. Indeed, at the end of one of the catalytic experiments Zn1 complex was partly recovered by precipitation after the addition of EtOH and the ¹H NMR spectra confirmed the presence of the complex (Figure 17). Nevertheless, the partial conversion for each run decreased from 84 to 57% (Figure 18). This may be related to the dilution effect caused by the 2b accumulated in the reaction media although the partial decomposition of the Zn complex in the reaction media cannot be ruled out.

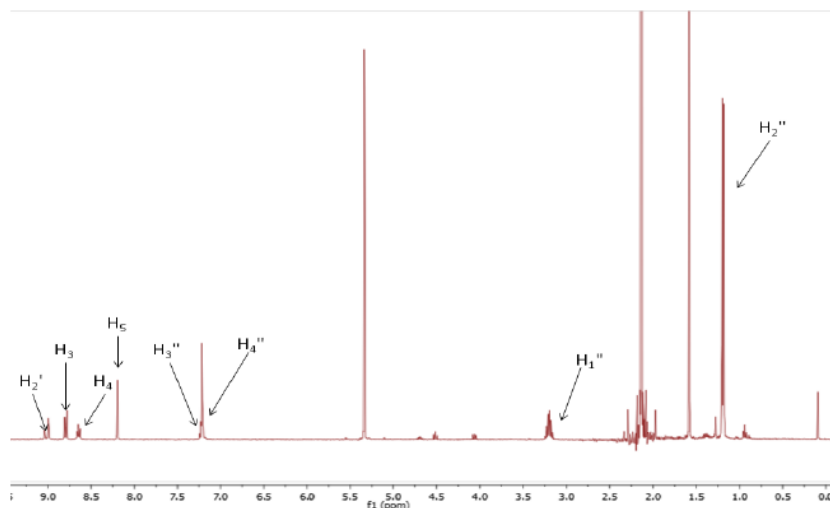


Figure 17: ¹H NMR spectrum in CD₂Cl₂ of Zn1 recovered after catalytic cycloaddition experiment.

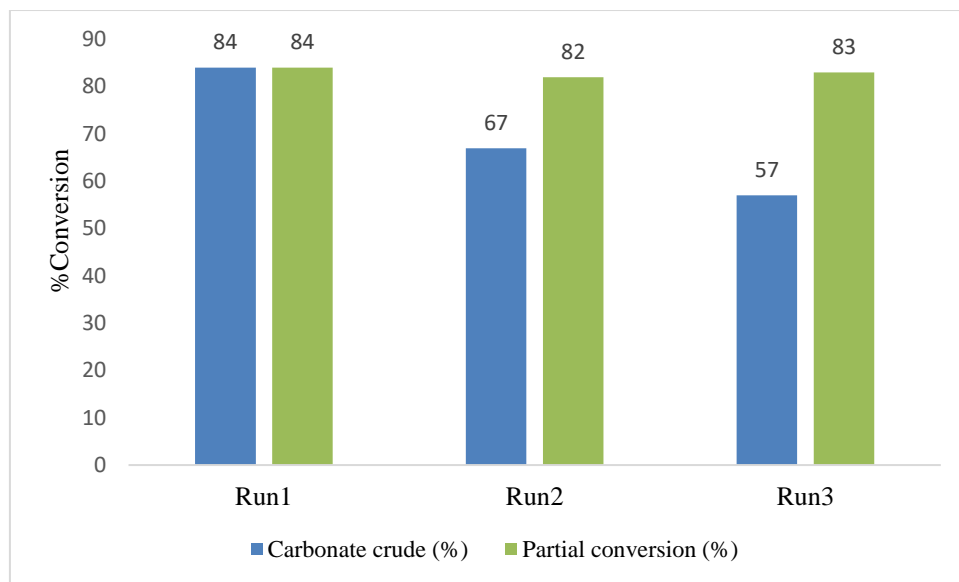


Figure 18: Conversion in 2b obtained using Zn1/TBAB catalytic system. Reaction conditions: 30 mmols 1b; Zn1 0.03 mmol (0.1 mol%); TBAB 0.06 mmol, (0.2 mol%), 10 bar, 80 °C, 6 h.

3.3.3.7. Comparison to the results reported in the literature

The obtained results were compared to selected similar catalysts previously reported in the literature. For the systems combining simple Zn(II) salts with tetrabutyl ammonium halides, the activities obtained under mild conditions are modest (Entries 1-3, Table 7), with averaged TOF between 6-64 h⁻¹,^[237] and only under high pressure (80 bar, entry 4, Table 7) the activity reached a high TOF (966 h⁻¹).^[238]

The Zn1/TBAB catalytic system provided an averaged TOF of 32 h⁻¹ for the epoxide (1a) at atmospheric pressure (entry 13, Table 7). Zn1/TBAB is a better catalytic system than the previously reported Zn(II) catalyst with NN'O-donor ligands (C1), which showed modest TOF of 25h⁻¹ during a reaction time of 24h, for 1a (entry 1, Table 8) and it decomposed after the catalytic reaction. Considering the Zn catalysts with N-donor ligands C2-C6 (entries 2-6, Table 7), Zn1/ TBAB system presented in this work, presents a higher catalytic activity even at low pressure with a TOF up to 206 h⁻¹. Although is remarkable the robustness reported for system C4/TBAI which

remains active for 4 days and for C6/TBAI which allows recycling the catalyst in 5 runs with small loss in the conversion.

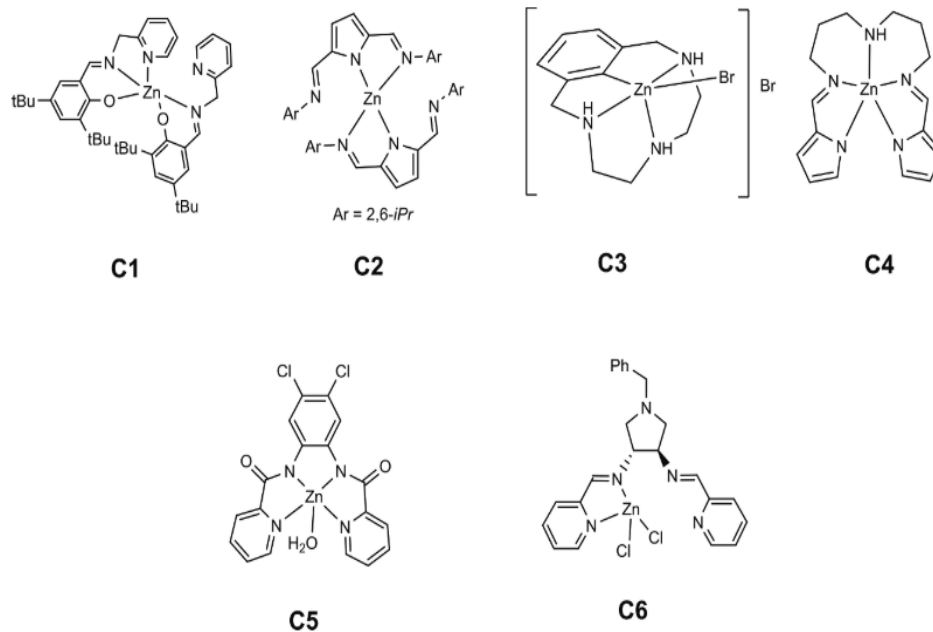


Figure 19: Zn catalysts employed in the literature for CO₂/epoxide coupling.

Table 7: Results reported in the literature using Zn salts. *

| Entry | Cat/Co-cat (mol%) | Epoxide | P(bar) | T(°C) | T(h) | Conv(%) <i>/</i> Y | TOF (h ⁻¹) | Ref |
|-------|-------------------------------------|---------|--------|-------|------|--------------------|------------------------|-----------|
| 1 | ZnCl ₂ /TBAI (4/16) | 1b | 1-1.2 | r.t. | 3.5 | 90/- | 64 | [237] |
| 2 | ZnCl ₂ /TBAI (0.2/0.8) | 1c | 1-1.2 | r.t. | 24 | 37/- | 8 | [237] |
| 3 | ZnCl ₂ /TBAI (0.2/0.8) | 1d | 1-1.2 | r.t. | 24 | 27/- | 6 | [237] |
| 4 | ZnBr ₂ /TBAI (0.14/0.56) | 1d | 80 | 80 | 0.5 | 69/- | 966 | [238] |
| 1 | C1/TBAB (0.14/0.2) | 1a | 50 | 80 | 24 | 87/- | 25 | [239] |
| 2 | C2/TBAB (2.5/5) | 1a | 1 | 25 | 18 | -/79 | 1.76 | [240] |
| 3 | C3/- (0.5/-) | 1a | 8 | 125 | 3 | 99/93d | 66 | [210] |
| 4 | C4/TBAB (1/3) | 1a | 10 | 100 | 18 | -/87 | 4.8 | [84] |
| 5 | C5/TBAB (0.2/0.2) | 1a | 50 | 80 | 20 | 40/- | 10 | [73] |
| 6 | C6/TBAI (0.025/0.125) | 1a | 30 | 80 | 16 | 60 | 150 | [74] |
| 7 | Zn1/TBAB (0.066/0.1) | 1a | 30 | 80 | 1 | 61/- | 565 | [212] |
| 12 | Zn1/TBAB (0.1/0.2) | 1a | 10 | 80 | 3 | 38/- | 206 | This work |
| 13 | Zn1/TBAB (0.13/0.2) | 1a | 1 | 80 | 24 | 77/- | 32 | This work |

* Conditions: Epoxides: see Scheme 14, P: Initial pressure; Conversion (Conv) and yield (Y); Averaged TOF (h⁻¹) estimated from reported data. rt: Room temperature.

3.3.4. Proposed mechanism of the reaction

The above experimental results, along with the X-ray structures of the catalysts, with the computational stability calculations performed by Mar Reguero research group [212] and the previously reported data, have led to suggest a possible cooperative mechanism between the Zn complex and the nucleophile TBAB. There are two possible pathways depending on the catalyst precursor. The first route consists of the **Zn1** to **Zn4** catalyst as they share the same pentacoordinate structure, while a second pathway involves the tetracoordinated **Zn5** based system.

The reaction is initiated by the Zn complex, which activate the epoxide by coordination, resulting in a less stable hexacoordinate intermediate species in the case of the imine complexes (Zn1-Zn4). The addition of the epoxide is not favored since it leads to a hexacoordinate species according to the DFT calculation performed.^[212] The relative stability of the hexacoordinate species compared to the pentacoordinate species depends on the substituents in the orto position of the aniline ring. Hexacoordinated species are relatively less stable than the pentacoordinate ones for the voluminous orto substituents. So, the lower the stability of the intermediate, the more inactive the system is. However, this observation is not consistent with the experimental findings, that demonstrate that the efficiency increases when the steric encumbrance of the aniline substituent in orto position increases. The initial hypothesis can therefore be discarded.

The hypothesis that the activity increases with the steric bulk of the substitution in the orto position of the aniline, fits the results achieved in the experimental results, for the pentacoordinate complexes. To improve the stability of the hexacoordinated species after the epoxide association, the metallic center may dissociate a chloride to keep the pentacoordinate more stable than the hexacoordinated species, matching the experimental results.

Alternatively, for the tetrahedral **Zn5** complex, the pentacoordinate species can be formed by coordination of the epoxide without dissociation of the chloride ligand giving place to more active system than its analogous **Zn4**.

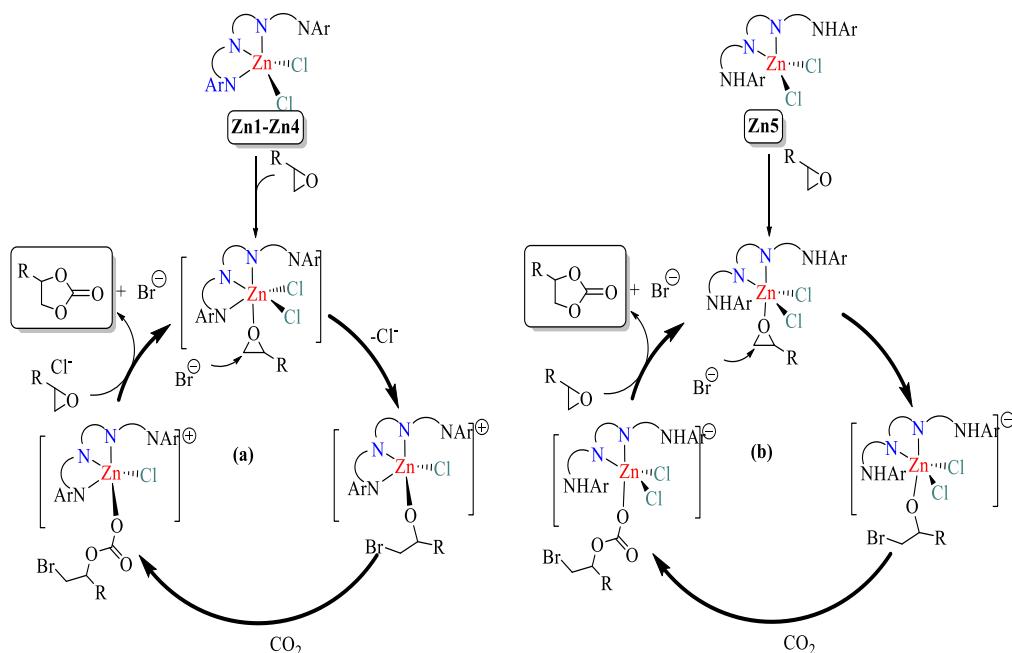
Additionally, the zinc-phenanthroline backbone (**Zn1-Zn3**) provides higher rigidity than the bipyridine one, potentially helping to control the equilibrium towards the formation of certain specified isomers, thus promoting the reactivity of the intermediates.

Nevertheless, the bipyridine systems **Zn4** and **Zn5**, which have relatively more flexible framework, can yield to more isomers, giving place to fewer active systems. Although, for the bipyridine amine derivative **Zn5**, an interaction of the free amine

with CO₂ cannot be excluded, explaining its higher activity than that of the bipyridine imines.

Based on the explanations above, the experimental and theoretical studies have revealed to propose a mechanism which is similar to both pentahedral and tetrahedral compounds, with the exception that in pentahedral a chloride is released to keep the pentacoordinate of the metal after the coordination to the epoxide, whereas in the tetrahedral case, the epoxide could corrode the metal center without losing any of the chloride. DFT calculations are currently in progress to confirm this hypothesis.

The following illustration (Scheme 11) outlines the mechanism proposed of this approach.



Scheme 11: Proposed CO₂/epoxide cycloaddition mechanisms for (a) Zn1-Zn4/TBAB and (b) Zn5/TBAB catalytic systems.

3.4. Conclusion

Zn(II) complexes with easy-modifying N₄-donor ligands derived from phenanthroline and bipyridine-bis (aniline) have been successfully synthesized and characterized by spectroscopic methods, X-ray diffraction in solid state.

The catalytic performance of Zn complexes bearing 2,9-bis(imino)-1,10-phenanthroline, and bipyridine bis (aniline) ligands in the coupling reaction of epoxides with CO₂ under gentle conditions had been scarcely studied, The systematic study of the structural parameters and the nature of the functional groups allowed identifying the best catalyst (those with the phenanthroline skeleton and with bulky substituents in the orto-aniline position). The catalyst is an air-stable, easily synthesized, and environmentally safe metal complex. It is found to be active in producing cyclic carbonates in a free solvent system. They show high selectivity as catalysts towards cyclic carbonates from the addition of CO₂ to terminal epoxides. moreover, the catalytic system is stable under catalytic conditions and can be used in a semi-batch process for several cycles adding fresh epoxide and CO₂. Although, the recovery of the catalyst still requires further exploration, together with the activity.

The polar solvents first considered necessary for this reaction are poisonous and toxic, operating free solvents has proven to be efficient and highly suitable for green chemistry processing and synthesis.

The results of this combined experimental-computational work provide an essential information to be able to design better catalytic systems, although further knowledge about the mechanism of the reaction is still necessary.

***CHAPTER 4: Eco-friendly, cost-effective
metal-catalyzed complexes for
epoxidation/cycloaddition reaction***

4.1. Introduction

In the preceding chapter, the main objective was the synthesis of cyclic carbonates by the reaction of cycloaddition of CO₂ to epoxides, this process having the advantage to produce an organic compound with utilities in various fields, and also to harness the plentiful CO₂ feedstock to generate value-added products. However, no reflection was carried out on the source of the epoxide employed, most often involving costly and poisonous reactants as well as necessitating chemical separation.^[241]

Epoxides represent a versatile and key category of organic compounds. Their chemistry is particularly interesting due to the fact that various alternative functional groups can be easily prepared from them. They are highly important intermediates that have many applications in organic synthesis and fine chemical manufacturing.^[112]

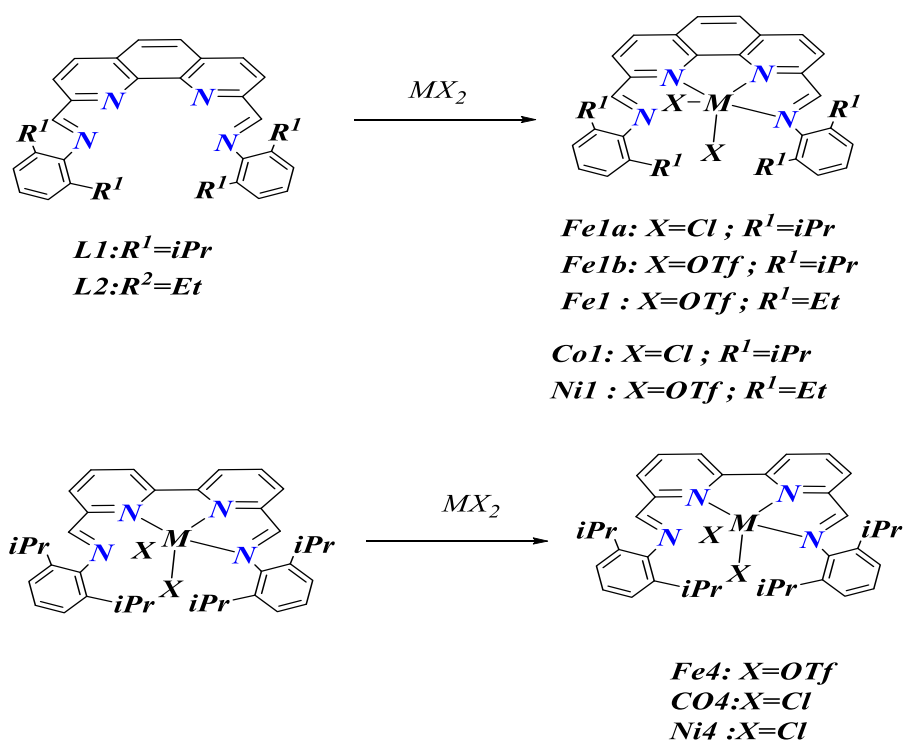
Olefin catalytic oxidation has proven to be a potent strategy for epoxides synthesis. Therefore, considerable focus has been devoted towards achieving higher efficiency with less expensive and environmentally benign catalysts and oxidants, as well as applicability to a variety of substrate classes.^[242] Among the various useful methods, the development of an iron-catalyzed epoxidation should provide us with many advantages, as iron is the most abundant transition metal on earth and relatively non-toxic.^[243,244] Iron complexes with N donor ligands are widely used in homogeneous catalysis. Undoubtedly, one of the most important applications of these complexes is the use as catalysts for the oxidation of organic compounds.^[245]

The aim of this chapter is to utilize the same catalytic system for both the epoxidation of alkenes and for CO₂ fixation in epoxides to obtain cyclic carbonates.

Iron (II) complexes with phenanthroline and bipyridyl rings, bearing N₄ donor ligands have been synthesized and characterized to be utilized as a catalyst for both the olefin epoxidation process, and for subsequent CO₂/epoxide cycloaddition.

Metal (II) complexes have been used previously for this type of reaction, however compounds bearing phenanthrolyl or bipyridyl N4 tetradentate was not applied for this particular study. Moreover, designing two reactions in one process: from olefins to epoxides, followed by coupling with CO₂ to obtain cyclic carbonates, seems to be challenging, especially that this work being performed under gentle conditions.

The further distinction between the complexes of phenanthrolyl framework, lies in the steric hindrance of the aniline ring substitution, the first one is an isopropyl substitution while the second one is a diethyl substitution as indicated in the Scheme 12 hereunder.



Scheme 12: Synthesis of metal complexes.

Firstly, and aiming to find the appropriate conditions for the epoxidation reaction, iron complexes, mainly with phenanthrolyl, are used as catalysts. The second part of this chain reaction, which is the cycloaddition of CO₂ to epoxides, was carried out using Fe, Ni and Co complexes as catalysts. Finally, the feasibility of converting the double bonds of olefins directly to their appropriate cyclic carbonates has been addressed applying certain complexes as catalysts for both, epoxidation, and CO₂ fixation to epoxides.

4.2. Experimental section

4.2.1. General remarks

All manipulation involving air-and/or moisture-sensitive compounds were performed under purged nitrogen atmosphere. The starting materials were purchased from commercial suppliers and stored carefully. The solvents used for synthesis or purification were being dried prior to utilization. Epoxides were supplied by sigma Aldrich and were stored tightly in a dry place, as they are moisture sensitive, away from oxidizing agents, CO₂ gas from the gas cylinders (99.99% pure) were purchased from Linde, Germany.

The compounds **Fe1a**,^[215] **Co1**,^[215] **Ni1**,^[215] and **Ni4**,^[220] (Scheme 12) were prepared as reported. Samples for high-resolution electrospray ionization mass spectra (ESI-TOF) and elemental analysis were sent safely to be performed at the Service Techniques of Research of Girona university (Spain), and in the Institut Català d'Investigació Química Tarragona. The FT-IR spectra (Fourier Transformed Infrared) were recorded on a Bruker Vortex 70 spectrometer and on a JASCO 6700 FTIR equipment using the attenuated total reflectance (ATR) technique (range 4000-600 cm⁻¹). The Magnetic susceptibility was measure in a Mohr balance MSB-MKI.

4.2.2. Synthesis of the involved ligands and complexes.

4.2.2.1. Synthesis of dichloro bis(1,1'-(1,10-phenanthroline-2,9-diyl)bis(N-(2,6-di-isopropyl phenyl)-methanimine))iron(II): (Fe1a)

The preparation of this compounds was previously described in the literature.^[215] A solution of 2,9-diformyl-1,10-phenanthroline (2,6-diisopropylanil) (L1) (197 mg, 0.33 mmol) in THF (10 mL) was added dropwise at 60 °C to a solution of FeCl₂·4H₂O (60 mg, 0.30 mmol) in THF (5 mL) to yield a green solution. After stirring at 60°C for 18h, the reaction mixture was allowed to cool to r.t. The reaction volume was concentrated, and diethyl ether (10 mL) was added to precipitate the product as a

green power, filtered, and subsequently washed with diethyl ether (3 x 10 mL), and dried in vacuo to afford a dark green powder. 135mg. Yield: 65%.

Anal. Calcd. for C₃₈H₄₂Cl₂FeN₄Fe·H₂O (699.5): C 65.2, H 6.3, N 8.0; found C 64.7, H 6.0, N 7.9. HRMS (ESI-TOF) m/z Calcd. for C₃₈H₄₂ClN₄Fe: 645.2436 [M-Cl]⁺, found: 645.2447 (100 %). FTIR(cm⁻¹) (ATR): 3441 (w), 2963 (w), 2868 (w), 1633(w, C=N), 1503(m), 1461 (s) cm⁻¹.UV-Vis (MeCN, 0.4.10⁻³M): 255.0nm (ε1810 L.cm.mol⁻¹), 300,0nm (ε1390 L.cm.mol⁻¹). Molar magnetic susceptibility $\chi_M = 9.7.10^{-3}$, $\mu_B = 4.81$ BM.

4.2.2.2. Synthesis of bis(1,1'-(1,10-phenanthroline-2,9-diyl)bis(N-(2,6-diisopropylphenyl)-methanimine))iron(II) triflate (Fe1b)

In the glove box, a solution of Fe(OTf)₂ (0.24 mmol, 0.088 g) in 1.5 mL of acetonitrile was added to a solution of L1 (0.25 mmol, 0.13 g) in 1.5 mL of acetonitrile under nitrogen. The mixture was stirred at room temperature for 18 h. After this time, it was filtered through celite, and 10 mL of diethyl ether and 0.5 ml of hexane were added. The mixture was kept at -25°C overnight. The product formed was filtered and washed three times with hexane and vacuum dried to obtain a dark green product Fe1b. 0.077 g. Yield: 42%.

Anal. Calcd. for C₄₀H₄₂F₆FeN₄O₆S₂·H₂O (908.7): C 51.8, H 4.8, N 6.1; found C 50.1, H 4.9, N 5.8. HRMS (ESI-TOF) m/z Calcd. for C₃₉H₄₂F₃FeN₄O₃S: 759.2279 [M-OTf], found: 759.2259. FTIR(cm⁻¹) (ATR): 3398 (w), 2963 (w), 2927 (w), 2869 (w), 1637 (w, C=N) 1616 (m), 1509 (m), 1536(m) 1463(m), 1442(w) 1385(w), 1363 (w), 1308(m), 1281(m), 1252(m), 1232 (s) 1213(s), 1160(s), 1024 (s), 864 (m), 806 (m), 762 (m), 634 (s), 572(m), 516(m). UV-Vis (MeCN, 1.51.10⁻⁴ mol/L): 250.0 nm (ε1800 L.cm.mol⁻¹), 299.0 (ε 1388 L.cm.mol⁻¹). Molar magnetic susceptibility $\chi_M = 8.5.10^{-3}$ $\mu_B = 4.24$ BM. Conductivity (CH₃CN, 1.54.10⁻⁵ mol/L): 0.25 S.cm².mol⁻¹. Conductivity (CH₂Cl₂, 4.04M): 20 S.cm².mol⁻¹ at T = 25°C .

4.2.2.3. Synthesis of bis(1,1'-(1,10-phenanthroline-2,9-diyl)bis(N-(2,6-dirthyphenyl)-methanimine))iron(II) triflate (Fe2)

A solution of Fe(OTf)₂ (0.24 mmol, 0.088 g) in 3 mL of acetonitrile was added to a solution of 2 (0.25 mmol, 0.12 g) in 2.5 mL of acetonitrile. The mixture was stirred at room temperature for 18 h. After this time, it was filtered through celite, and diethyl ether was added. The mixture was kept at -30°C overnight. The product formed was filtered off, washed three times with anhydrous hexane and vacuum dried to obtain a dark green product of Fe2. 0.1 g. Yield: 45%.

Anal. Calcd. for C₃₆H₃₄F₆FeN₄O₆S₂.CH₃CN (893.7): C 51.1, H 4.2, N 7.8; found C 51.1, H 4.5, N 7.5. HRMS (ESI-TOF) m/z Calcd. for C₃₅H₃₄F₃FeN₄O₃S: 703.1653 [M-OTf], C₆₈H₆₈Cl₂N₈Fe 526.2458 [Fe(2)₂]²⁺ found: 526.2454. FTIR(cm⁻¹) (ATR): 3109 (s), 2965 (s), 2879 (w), 1731(m), 1710(m) 1634 (m, C=N) 1619 (m), 1606(m) 1558 (w), 1536 (w), 1508 (m), 1536(m) 1448(m), 1388(w), 1358 (m)1301(w), 1259(s) 1045 (vs) 1029 (vs) 866 (vs), 805 (s), 758 (s), 634 (s). Molar conductivity (ACN, 0.26 10⁻³ M): 1.91S.cm².mol⁻¹ at T = 25°C . UV-Vis (ACN, 0.26 10⁻³ M): 249.6 nm (ε 1351 L.cm.mol⁻¹), 299.0 (ε 1885 L.cm.mol⁻¹). Molar magnetic susceptibility (Mohr balance) $\chi_M = 9.97 \cdot 10^{-3} \mu_B = 4.84 \text{ BM}$.

4.2.2.4. Synthesis of dichlorobis(1,1'-(1,10-phenanthroline-2,9-diyl)bis(N-(2,6-diisopropylphenyl)-methanimine)cobalt(II) : (Co1).

The preparation of Co1 was performed in accordance with an existing synthesis.^[215] A suspension of L1 (179 mg, 0.30 mmol) in ethanol (6 mL) was added dropwise at 60°C to a solution of CoCl₂ (0.30 mmol) in ethanol (5 mL) to give a blue solution. After agitation at 60°C for 8h, the mixture was allowed to cool to r.t. The reaction volume was concentrated, and 10 mL of diethyl ether was added to induce the precipitation of the product as light green powder, which was filtered, then washed with diethyl ether (3.10 ml), and vacuum dried to give the product Co1 as a light green. 135mg. Yield: 66%

Elemental analysis: Calc. for C₃₈H₄₂N₄CoCl₂: C, 66.67; H, 6.18; N, 8.18. Found: C, 66.22; H, 5.71; N, 8.10. HRMS (ESI-TOF) m/z Calcd. For C₃₈H₄₂ClCoN₄: 648.2430 (M-Cl), found 648.2429 (100%). Molar Conductivity (CH₃CN, 3,94.10⁻⁴ M) : 4.41 S.cm² mol⁻¹.

4.2.2.5. Synthesis of dichlorobis(1,1'-(1,10-phenanthroline-2,9-diyl)bis(N-(2,6-diethylphenyl)-methanimine))cobalt(II) : (Co2)

By following the above procedure for the synthesis of complex Co1, adding (0.33mmol, 0.16g) of L2, to (0.30mmol, 0.07g of CoCl₂.6H₂O), gave the product as a light green powder of Co2. 0.138g. Yield: 67%

Elemental analysis: Calc. for C₃₈H₄₂N₄CoCl₂: C, 66.67; H, 6.18; N, 8.18. Found: C, 66.22; H, 5.71; N, 8.10. Mass spectra analysis : HRMS (ESI-TOF) m/z Calcd. For C₃₄H₃₄ClCoN₄: 592.1804 (M-Cl), found 592.1806(100%). FTIR(cm⁻¹) (ATR): 3109.65, 2879.20 (s), 1634.38, 1619.91, 1606.41, 1558.20 (s), 1508.06, 1448.28 (s) cm⁻¹). Molar Conductivity (CH₃CN, 1.65.10⁻⁴ M) : 8,40 S.cm².mol⁻¹ at T 25°C.

4.2.2.6. Synthesis of dibromobis(1,1'-(1,10-phenanthroline-2,9-diyl)bis(N-(2,6-diisopropylphenyl)-methanimine))nickel(II) (Ni1)

The synthesis of this compound was already described in the bibliography.^[215] NiBr₂ (77 mg, 0.25 mmol) and 2,9-diformyl- 1,10-phenanthroline(2,6-diisopropylanil) (L1) (179 mg, 0.30 mmol) were combined in a Schlenk flask under N₂ atmosphere. Dichloromethane (10 mL) was then introduced, after which the reaction mixture was gently stirred at room temperature for 18 h. The reaction solution was subsequently concentrated by evaporation to half volume, and diethylether (10 mL) was next added to induce the precipitation of the product, which was further washed with 10ml of diethylether 3 times, then filtered and dried to give the final product as an orange powder 0.181g. Yield: 80%.

Mass spectra analysis: HRMS (ESI-TOF) m/z Calcd. For C₃₈H₄₂N₄Ni: 693(M-Br), found 693(100%). Molar Conductivity (CH₃CN, 1,42.10⁻⁴ M) : 8,52 S.cm².mol⁻¹ at T 25°C.

4.2.2.7. Synthesis of dibromobis(1,1'-(1,10-phenanthroline-2,9-diyl)bisN-(2,6-diethylphenyl)-methanimine))nickel(II) (Ni2)

Following the previously detailed procedure in the preparation of Ni1. The reaction of L2 (0.30mmol,0.15g) and NiBr₂ (0.25mmol,0.054g) gave the product as an orange powder. 0.128g. Yield: 60%.

HRMS (ESI-TOF) m/z Calcd. For C₃₄H₃₄BrN₄Ni: 635(M-Br), found 635(100%). FTIR(cm⁻¹) (ATR): IR(KBr): 3342(Br), 2962 (s), 1636, 1605, 1583 (s), 1500, 1447 (s) cm⁻¹). Molar Conductivity (CH₂Cl₂, 0.58.10⁻⁴ M) : 1.97 S.cm². mol⁻¹ at T 25°C.

4.2.2.8. Synthesis of 1,10-bipyridine-2,9-diyl)bis(N-(2,6-diisopropylbis) methanimine))Fe(OTf)₂ : (Fe4)

A suspension of 2,9-diformyl-1,10-bipyridine(2,6- diisopropylaniline) (0,1g, 0,33 mmol) in 5 mL acetonitrile was added to 50 mL round bottom flask. To the resulting slurry we added (0.0637g, 0.076mmol) of Fe(OTf)₂ in acetonitrile solution (1.5 mL) dropwise for 15min. After stirring at r.t. for 18 h, the reaction mixture was filtered through celite, after which, diethyl ether (10ml) was added to precipitate the product. After an overnight at -30°C, a dark green powder was recovered which was then filtered, washed with diethyl ether (3 x 10 mL), and dried in vacuo to give Fe4 as dark green powder. 0.08g. Yield: 50%.

Anal. Calcd. for C₃₈H₄₂F₆FeN₄O₆S₂.3H₂O (884.7): C 48.7, H 5.0, N 6.0; found C 47.2, H 4.8, N 5.9. HRMS (ESI-TOF) m/z Calcd. for C₃₈H₄₂F₆FeN₄O₆S₂: 735.2279 [M-OTf]⁺, found: 735.2278 (100 %). FTIR(cm⁻¹) (ATR) 3399 (w), 2966 (w), 2871 (w), 1629 (w, C=N) 1596 (m), 1524(m) 1464(m), 1437(m) 1386(w), 1365 (w), 1277(s), 1245(s), 1224 (s), 1166(s), 1026 (s), 797 (m), 633 (s), 573(m), 514(m). Conductivity

(CH₃CN, 4.36.10⁻⁵ mol/L): 0.124 S.cm².mol⁻¹ at T = 25°C. UV-Vis (CH₃CN, 4.36 10⁻⁵ M): 291.0 nm (ε 7828 L.cm.mol⁻¹), 324 (ε 4702 L.cm.mol⁻¹). Molar magnetic susceptibility $\chi_M = 1.263.10^{-2}$, $\mu_B = 5.46$ BM

4.2.2.9. Synthesis of dichloro (N,N'-(2,2'-bipyridine-6,6'-diylbis (methylene))bis(2,6-diisopropylaniline))cobalt(II) : (Co4)

In a round bottom flask of 50ml CoCl₂ (0.0899g, 0.378mmol) in 10ml of n-butanol, under reflux at 100°C till its dissolution. Then L4 (0.189mmol,0.1g) was added to the mixture stirred for 18h under reflux. A green mixture was obtained, that was evaporated, and hexane was added to induce the precipitation. The solid was filtered off, washed with hexane, and vacuum dried to yield the product as a green powder. 0.082g. Yield : 66%.

Anal. Calcd. for C₃₆H₄₂Cl₂CoN₄·3H₂O (759.6): C 56.9, H 6.0, N 7.4; found C 57.7, H 5.9, N 7.0. HRMS (ESI-TOF) m/z Calcd. for C₃₆H₄₂ClCoN₄: 624.2430 [M-Cl]⁺, found: 624.2424 (100 %). FTIR(cm⁻¹) (ATR) 3425 (w), 2959 (m), 2868 (w), 1632 (w, C=N) 1593 (m), 1463(m), 1435(m) 1383(w), 1362 (w), 1327(w), 1171(s), 1100 (m), 1028 (m), 799 (s), 767 (m) 738 (m), 646 (w). Conductivity (CH₃CN, 7.11 10⁻⁵ mol/L): 0.21 S.cm².mol⁻¹ at T = 25°C. UV-Vis (CH₃CN, 3.4 10⁻⁴ M): 207.0 nm (ε 7772 L.cm.mol⁻¹), 277.0 nm (ε 1980 L.cm.mol⁻¹), 323 (ε 1495 L.cm.mol⁻¹). Molar magnetic susceptibility $\chi_M = 1.67.10^{-3}$: $\mu_B = 1.99$ BM.

4.2.2.10. Synthesis of dichloro(N,N'-(2,2'-bipyridine-6,6'-diylbis (methylene))bis(2,6-diisopropylaniline)) nickel(II) : (Ni4)

Using the approach outlined in the literature ^[220] using anhydrous NiCl₂ (0.025g, 0.377 mmol) and L1 (0.05 g, 0.189 mmol) in n-butanol as solvent, the reaction mixture was refluxed for 18h. Then the solvent was evaporated, and hexane was added to induce the precipitation of the crude as red orange. The solid was filtered of, washed with hexane, and vacuum dried. The Ni4 was obtained as orange-red. 0.093g. Yield : 75%.

HRMS (ESI-TOF) m/z Calcd. for C₃₆H₄₂ClN₄Ni: 623.24 [M-Cl]⁺, found: 623.24 (100%). FTIR(cm⁻¹) (ATR): 2924 (m), 1639 (m, n(C=N)), 1590 (w), 1573 (m), 1462 (s), 1434 (m), 1361 (w), 1262 (w), 1167 (m), 1109 (m), 1012 (w), 799 (vs), 769 (s) and 737 (s).

4.2.3. Catalysis

4.2.3.1. Typical epoxidation reaction

In a purged Schlenk tube connected to N₂ gas, equipped with a magnetic stirrer bar, the metal catalyst was introduced (0.0043 mmol) in 2.2 mL of previously deoxygenated acetonitrile and stirring was initiated gently. After that, the olefinic substrate (0.4349 mmol) was introduced, and the solution was stirred for 5 min, before the addition of mesitylene as a reaction standard (0.16 M, 60 μL). The concentration of the substrate was analyzed by gas chromatography. Then, the oxidant (1.07 mmol) was immediately inserted into the reaction solution, the mixture was kept under reflux at 60°C for 24h. Samples were picked up after 6h and 24 h to be analyzed by GC for styrene and cyclohexene or dried under vacuum to be analyzed by ¹H NMR for Cis and Trans stilbene, Trans-β-methyl stilbene and 1,2-dihydronaphthalene. Oxidation products yields based on the starting substrate concentration were quantified by comparison with mesitylene internal standard. Catalytic reactions were carried out in duplicate, in order to ensure the consistency of the results.

4.2.3.2. Standard cycloaddition reaction

A 25 mL Parr reactor was loaded with a stirring bar, the substrate (20 mmol), the catalyst (0.02 mmol) together with the nucleophile source (0.04 mmol). The autoclave was purged with 2-3 bar CO₂ and pressurized with the desired CO₂ pressure, then heated to the specific temperature. After the reaction time. The vessel was cooled with an ice bath and carefully depressurized. The % conversion was determined by ¹H NMR of the crude mixture as an integral ratio between epoxide and cyclic

carbonate, the yield was measured using an internal standard. For that, 30 μ L of the crude sample, then 15 μ L of the mesitylene and 0.5mL of deuterated chloroform were analyzed by ¹H-NMR. The Turnover frequency was calculated by dividing the conversion of the reaction by the percentage of catalyst used and then by the total reaction time, the unit of TOF is (h⁻¹). The runs of cycloaddition performed under atmospheric pressure were done by using the Schlenk instead of the reactor. As always, the experiments were performed in duplicate, to ensure the reproducibility of the results.

4.2.3.3. Oxidative carboxylation of olefins

- Two step oxidative carboxylation: The catalysts Fe1a (0.00294 mg, 0.0043 mmol), TBHP (195 μ L) as oxidant, all mixed in dry acetonitrile solution (2.2 mL) and under N₂, were heated to 60 °C. TBAB was added (0.0056 g, 0.017 mmol) to the reaction medium, and CO₂ gas was inserted through the balloon. The reaction was left under stirring at 60 °C for further 24 hours. The formation of the cyclic carbonate was analyzed by means of ¹H-NMR analysis, the experiments were conducted in duplicate, in order to guarantee the repeatability of the results.
- One pot oxidative carboxylation: Simultaneously, the catalysts Fe1a (0.00294 mg, 0.0043 mmol), TBAB (0.0056 g), TBHP (195 μ L) as oxidant, together with CO₂ 1 bar pressure, through the balloon were inserted in a Schlenk, and dissolved in dry acetonitrile solution (2.2 mL). Then the mixture was heated to 60 °C. The reaction was left under stirring for 24 hours. The crude was analyzed by means of ¹H-NMR analysis, the experiments were conducted in duplicate, in order to guarantee the repeatability of the results.

4.3. Results and discussion

4.3.1. Synthesis

The ligands 2,9-bis(imino)-1,10-phenanthrolyl L1, L2, L4 employed in this section of the work have been produced in reasonable yields by the condensation reaction of two equivalents of the appropriate aniline with one equivalent of 2,9-dialdehyde-1,10-phenanthroline (Scheme 8), affording pale yellowish products upon being purified by recrystallization from ethanol. The synthesis and the characterization have been discussed in chapter 3.

The complexes employed as catalysts (**Fe1a**, **Fe1b**, **Co1**, **Co2**, **Ni1**, **Ni2**, **Fe4**, **Co4**, **Ni4**) (Scheme 12) were prepared by reaction of the corresponding salts with the appropriate ligand (L1, L2, L4). They were recovered as solid powders with moderate to good yields (42-80%). The resulting compounds were fully characterized by the known characterization methods. The mass spectrometry ESI-TOF showed an intense fragments upon the removal of one or two halides or triflate, and elemental analysis agree with the $M(L_n)X_2$ formulation. FT-IR shows the presence of the stretching of the imine (ca 1635 cm^{-1}) and the aromatic amine frequencies (ca 1620 cm^{-1}). Conductivity measurement of the complexes (Fe2, Co1, Co2, Ni1, Ni2, Fe4, Co4) was recorded as a solution in acetonitrile solvent. The values of molar conductivities of these complexes were lower than $10\text{ S.cm}^2.\text{mol}^{-1}$, revealed that they are non-electrolytes.^[81] Interestingly, the conductivity Fe1b was recorded in acetonitrile and in dichloromethane and showed higher value in dichloromethane of $20\text{ S.cm}^2.\text{mol}^{-1}$, and lower value in acetonitrile of $0.25\text{ S.cm}^2.\text{mol}^{-1}$. These variations may be related to the different polarities and densities of the solvents. These solvent properties are responsible for the differential ionization and movement of counter ions in a complex. The value of conductivity in CH_2Cl_2 of Fe1b indicate that the triflate anions may dissociated from the Fe1b. But in CH_3CN the Fe1b show low conductivity value, meaning that the triflate anions dissociated from the Fe1b and CH_3CN coordinate in its place. On the other hand, the magnetism at room temperature points to high spin

systems as reported for similar complexes.^[246] Magnetic measurements are widely used in studying transition metal complexes.^[247] The magnetic property is due to the presence of unpaired electrons in the partially filled d-orbital in the outer shell of these elements.^[247] The magnetic moment value of the complexes was between 1.99 and 5.46 B.M. which referred as paramagnetic.

The crystals of the novel complexes couldn't be grown, however the X-ray diffractions structures and studies of similar complexes found in the literature could help understanding the geometry of the compounds.

The geometry of the complexes depends on the denticity of the L1-L3 ligands. The X-ray structure of **Co1**, and **Ni1** bearing phenanthroline ligand have been previously described in the literature,^[215] and they consist of a metal atom surrounded by one ligand acting as tridentate N,N,N-donor and two halides, forming a pentacoordinate geometry.

The X-ray diffraction structure of **Ni4** bearing the bipyridyl backbone, was also reported in the literature^[220] consisting of a five-coordinate metal center surrounded by two chloride ligands and a chelating dipyriddy unit from L4 with the second imino group pendant to give an overall endo-exo configuration of the imine groups.

Further example from the literature,^[248,249] reported on a Fe(II) complex in which a substituted phenanthroline reacted with FeBr₂, acting as tridentate ligand in a five-coordinate structure with 2 bromides and three bonds to the ligand.

There are further phenanthroline and bipyridine-(bis)imine ligands in the literature acting as tetra ligands. For instance, Thenarukandiyil et al.^[250] provided the X-ray diffraction structure of a related system with a mesitylene group, showing an octahedral geometry with the ligand acting as a tetradentate. Also, Begum et al.^[227] reported complexes of Fe(II) and Ni(II) with phenanthroline bis(benzothiazolate) derived ligands with octahedral structure.^[227] Instead, the chloride analogous of Fe4 with a mesitylene group, presents a five-coordinate iron center with the ligand acting as tridentate.^[246] Furthermore, the coordination of Zn to the L1, L2 have been

described in the (Chapter 3) and show the pentacoordinate of the phenanthroline ligands to the Zn metal center, forming two bonds with the halides and 3 bonds to the N,N,N of the ligands.

Without obtaining the X-ray diffraction data for the Fe novel complexes, some DFT calculations to predict the more stable geometrical structure of the complexes, were performed thanks to a collaboration with the Professor Mar Reguero from the university Rovira i Virgili. They revealed that the most stable structure for **Fe1b** was an octahedral geometry structure with the **L1** ligand acting as an in-plane tetradentate ligand and the triflate ions coordinating in the relative trans-position.

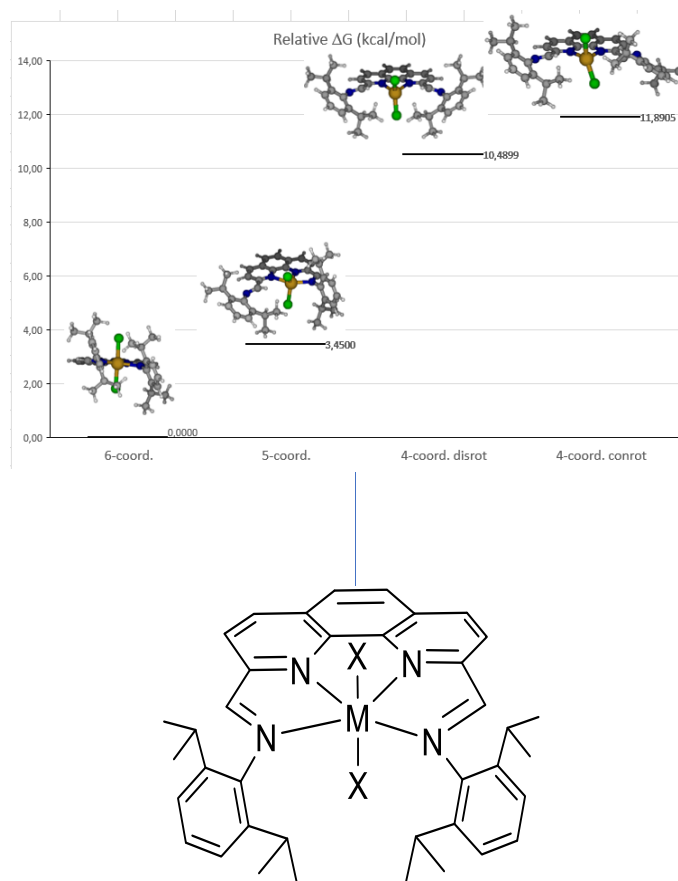
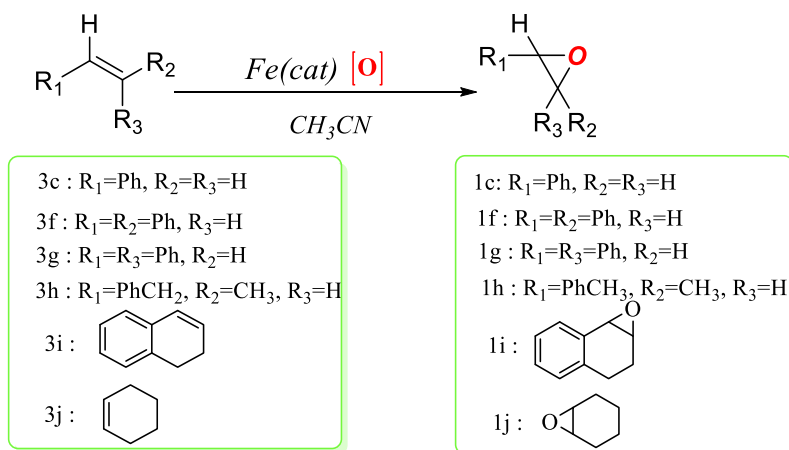


Figure 20: *Fe1b* structure by DFT calculations.^[251]

4.3.2. Epoxidation of alkenes

With the purpose of establishing the optimum operating conditions for the epoxidation, a benchmarking study was first carried out involving styrene as a reference substrate, (3c, Scheme 13) with **Fe1a** then **Fe1b** as catalysts. Building on what is previously outlined in the literature, tertbutylhydroperoxide (TBHP) and hydrogen peroxide (H₂O₂) were chosen to act as oxidants. The election of TBHP as an oxidant for epoxidation is related to the advantages it presents. First of all, the latter shows good solubility in polar solvents,^[252] reactions at neutral pH, safe handling, and easily separated from the tert-butanol by-product.^[110,252] The hydrogen peroxide is a safe and cheap oxidant as well, and easy to handle. However, it generates water as by product.^[110,253] This requires catalysts sufficiently stable in the presence of water.



Scheme 13: Epoxidation reaction process with Fe catalysts.

Comparing the results obtained (entry 1, entry 3, Table 8) using the **Fe1a**, **Fe1b** as catalysts and TBHP as oxidant. The reaction was monitored by GC, or ¹H NMR. Samples were collected after 6h and then after 24h. The best conversion and yield were obtained with **Fe1a** as catalyst. Then, it was selected to proceed with, for the rest of the study. An increase of the temperature from 40°C to 60°C was convenient in that case.

4.3.2.1. Catalyst and oxidant effect

With the aim of investigating the oxidizing agent effect on the conversion, the selectivity as well as the yield of the epoxidation, while remaining always in a non-toxic and cheap compound, the decision fell on the tertbutyl hydroperoxide and the hydrogen peroxide. The screening of the two selected oxidants was performed at 60°C, 24h and using acetonitrile as solvent. The catalyst loading and the catalyst-substrate relationship were exactly the same as before, the oxidant concentration was equally for both. (entry 1 vs entry 2, Table 8) and (entry 3 vs entry 4, Table 8). After the experiments, it was clearly shown that the best results were done by the tertbutyl hydroperoxide, both while coupling it with the Fe1a catalyst, or with the Fe1b as well.

Table 8: Fe catalyst and oxydant effect in the styrene epoxidation. ^a

| Entry | Cat | Conv(%) | Selectivity (%) | Oxydant | Yield (%) |
|-------|------|---------|-----------------|-------------------------------|-----------|
| 1 | Fe1a | 93 | 45 | TBHP | 43 |
| 2 | | 8.5 | 14 | H ₂ O ₂ | 4 |
| 3 | Fe1b | 45 | 22 | TBHP | 8.5 |
| 4 | | 32 | 16 | H ₂ O ₂ | 0.2 |

^a: Conditions: 3c: Styrene :0.43mmol. Cat:0.0043mmol. Reaction time=24h.

Temperature=60°C. Oxydant=2mmol, Analysis by GC and mesitylene as the internal standard.

As reported in the literature.^[118,252] The best results obtained with TBHP, may be related to the fact that the tertbutyl hydroperoxide is more stable as well as more soluble in organic solvent at high temperature, while the hydrogen peroxide decomposes rapidly in the presence of iron complexes and presents less solubility in organic solvents.^[107]

4.3.2.2. Catalyst loading effect

To reveal the significant role of the catalyst in olefin catalytic oxidation, a blank run evidenced that the conversion of the substrate to the products was negligible in the absence of the catalyst. Only 15% of the styrene was converted, (entry 1, Table 9)

and the selectivity was too poor, suggesting that the presence of the catalyst during the reaction is essential and that neither TBHP nor capable of carrying out the oxidative transformation.

On the other side, the results showed a moderate catalytic activity of the epoxidation when the Fe1a was introduced as catalyst, a conversion rate up to 93% of the styrene was recorded, and the formation of 47% of the styrene oxide, with a moderate selectivity of 49% to the styrene oxide (entry 2, Table 9). The GC-MS analysis had demonstrated that the major by-product formed was the benzaldehyde.

Table 9: Epoxidation of styrene without/with catalyst using TBHP oxydant. ^a

| Entry | T (°C) | Catalyst | Conv(%) | Selectivity(%) |
|-------|--------|----------|---------|----------------|
| 1 | 60 | - | 15 | 12 |
| 2 | 60 | Fe1a | 93 | 45 |

^a:General conditions: time:24h. Temperature:60°C. Solvent:CH₃CN. Styrene: 3c :0.43mmol. Fe1a :0.0043mmol. Oxydant:TBHP:2mmol. Conversion of styrene and selectivity of epoxide were determined by GC analysis using mesitylene as internal standard.

4.3.2.3. Temperature effect

The temperature impact on the chemical yields and selectivity of styrene epoxidation was examined for Fe1a. Decreasing the temperature from 60°C (entry1, Table 10) to 40°C (2, Table 10), resulted in a drop in the conversion and the selectivity of the reaction.

Table 10 : Temperature effect on styrene epoxidation using Fe1a catalyst. ^a

| Entry | T(°C) | Conv(%) | Select(%) | Yield(%) |
|-------|-------|---------|-----------|----------|
| 1 | 60 | 93 | 45 | 43 |
| 2 | 40 | 62 | 12 | 8 |

^a:Reaction conditions: Styrene 3c:0.43mmol. Catalyst: Fe1a:0.0043mmol. Oxydant:TBHP:2mmol. Time:24h. Conversion of styrene and selectivity of epoxide were determined by GC analysis with mesitylene as the internal standard.

4.3.2.4. Reaction time effect

Besides temperature, there are several factors that can affect the conversion and selectivity to the product, such as the reaction time. Therefore, a monitored experiment was conducted to study the reaction time on the conversion of olefin, samples were collected after 2 hours, 4 hours, 6 hours and finally 24 hours. By monitoring the conversion and selectivity over time, the stability of the catalytic system can be assessed too.

The results are shown in the graph (Figure 21). It can be clearly observed, the huge increase in the conversion of styrene occurred during the first 2 hours of the reaction, reaching 72% of conversion after 2h. The conversion grows constantly slower to reach 89 after 6h and 93% after 24h. Regarding the selectivity towards the target product, which is styrene oxide, there was an increase between 2h and 4h. As can be seen, after 2h the selectivity was 10% then after 4h of reaction the selectivity reached 45% and 49% after 6h, but there was a slight drop in selectivity after 24h of reaction, to return to 45% of 4h.

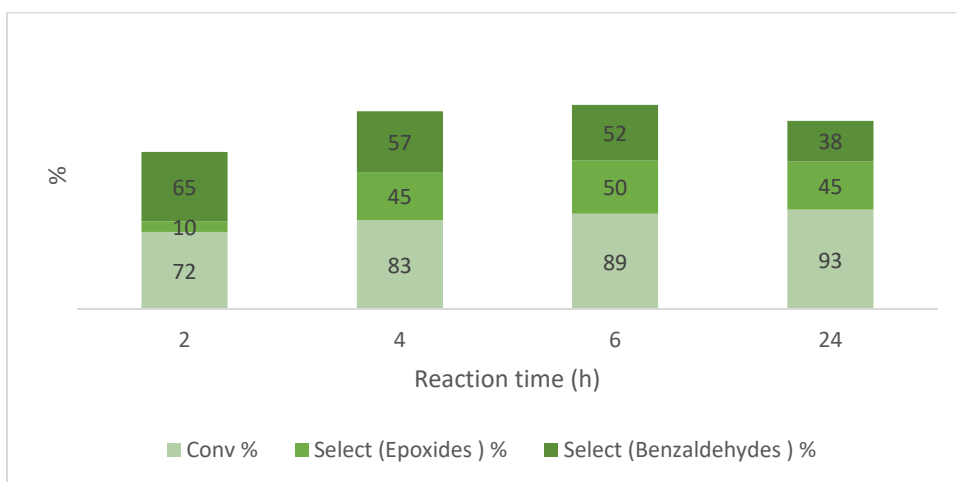


Figure 21: Reaction time effect on styrene epoxidation conversion.^a

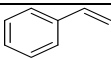
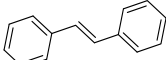
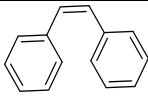
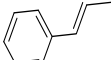
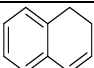
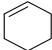
^a:Reaction conditions: Styrene 3c:0.43mmol. Catalyst: Fe1a:0.0043mmol.

Oxydant:TBHP:2mmol. Conversion of styrene and selectivity of epoxide were determined by GC analysis with mesitylene as the internal standard.

4.3.2.5. Substrate scope

With the initial screening in the epoxidation of styrene, we next examine the substrates scope using a range selected of aromatic substrate alkenes under the previously agreed conditions (T:60°C, 24h) with the FeIa as catalyst and tertbutylhydroperoxide (TBHP) as oxidant agent. **Cis**-stilbene and **trans**-stilbene exhibited interesting results. The **cis**-stilbene oxide was formed in 50% yield, with a selectivity of (**trans** / **cis**, 75: 25), (entry 2, Table 11). On the other hand, **trans**-stilbene, yielded 39% of stilbene oxide, (**trans** /**cis**: 83:13) (entry 3, Table 10).

Table 11: Epoxidation of various substrates by using FeIa as a catalyst. ^a

| Entry | Substrate | Conv(%) | Yield(%) | Selectivity(%) |
|-------|--|---------|---------------------------------|-----------------------------------|
| 1 |  3c | 93 | 43 | 45 |
| 2 |  3f | 70 | 62 | 99 |
| 3 |  3g | 61 | 39 <i>trans</i> 6 <i>cis</i> | 91% <i>Trans</i> 8% <i>Cis</i> |
| 4 |  3h | 100 | 13 | 17 |
| 5 |  3i | 100 | 74 | 18 |
| 6 |  3j | 95 | 30 | 13 |

^a:Reaction conditions: Substrate: 0.43mmol. Catalyst: FeIa:0.0043mmol.

Oxydant:TBHP:2mmol. Conversions and selectivities were determined by ¹H NMR spectroscopy by using internal standard mesitylene. Except for styrene and cyclohexene, the conversion and selectivity were determined by GC.

4.3.3. Comparison to the previously reported work from the literature employing Fe(II) and Fe(III) as catalyst.

Catalytic systems in which Fe(II) is coupled to TBHP or H₂O₂ as oxidant source for olefin epoxidation in homogeneous medium are scarcely explored. It was found in the literature that Li et al.^[254] studied the epoxidation of styrene using Fe(II)

complexes consisting of four N atoms in a reaction time of 30min. In order to explore the effect of the complex, three similar ligands were chosen and H₂O₂ was selected as oxidant agent with the bipyridine carboxylic acid as auxiliary ligand. The complexes had shown different reactivities. When 2,2-bipyridine was employed as ligand, the Fe(II) complex (C7, Figure 22) showed low catalytic activity, only 8.3% of styrene was oxidized and the product was 100% benzaldehyde.^[254] (entry 1, Table 12) On the other side, another Fe(II) complex bearing N4 symmetrical bioxazole ligand was used as coordination groups, the iron complex (C8, Figure 22) showed moderate catalytic activity (entry2, Table12). However, the Fe(II) complex containing the heterozygous ligand of 2-(pyridin-2-yl)-4,5-dihydrooxazole as ligand coordinated Fe(II) complex (C9, Figure 22) exhibited excellent catalytic ability for the epoxidation of styrene and resulted in 97.5% conversion of styrene and 89.8% selectivity of styrene oxide.^[254] (entry3, Table 12).

In another styrene oxidation system containing iron (III) complex with tridentate pyridine-imine-phenolate ligand (C10, Figure 22),^[65] using the TBHP as oxydant during 24h reaction time and 60°C, the catalytic system showed that only 24% of styrene could be oxidized.

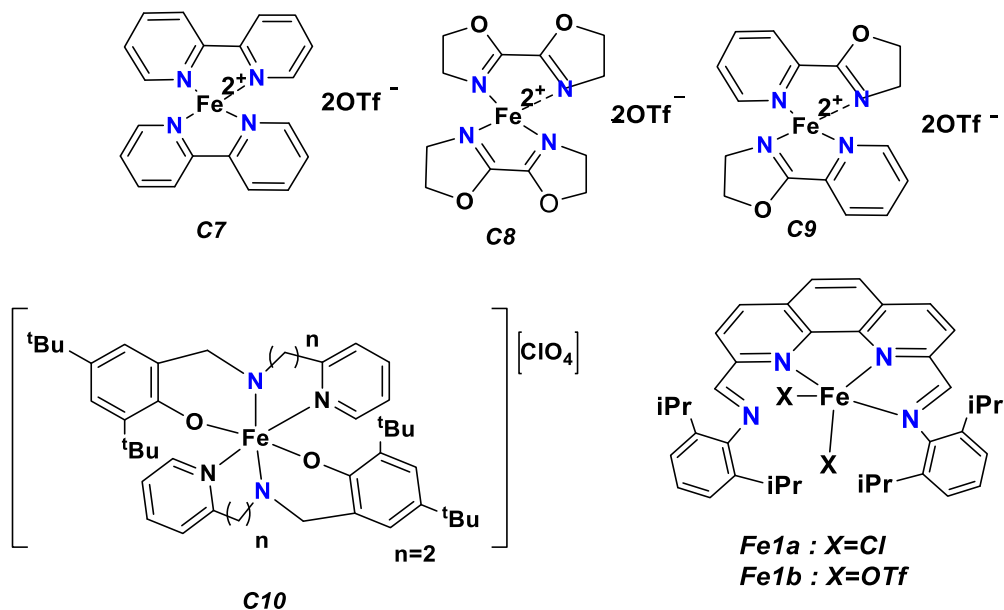


Figure 22: Selected Fe catalysts reported for olefins epoxidation.

Table 12: Comparative results of styrene epoxidation using different Fe catalysts.*

| Entry | Cat | Oxydant | Conv(%) | Selectivity(%) | T°C | Ref |
|----------------|------|-------------------------------|---------|----------------|-----|-----------|
| 1 ^a | C7 | H ₂ O ₂ | 8.3 | 0 | 25 | [254] |
| 2 ^a | C8 | H ₂ O ₂ | 49.2 | 76.8 | 25 | [254] |
| 3 ^a | C9 | H ₂ O ₂ | 97.5 | 89.8 | 25 | [254] |
| 4 ^b | C10 | TBHP | 24 | - | 60 | [65] |
| 6 ^c | Fe1a | TBHP | 93 | 45 | 60 | This work |

*:Conditions: ^a: styrene (0.1 mmol), Cat (5.0 mol%), pyridine-2-carboxylic acid (5.0 mol%), oxidant (2 equiv), CH₃CN (5 ml), 30 min. Conversion was determined by GC analysis. ^b: CH₃CN (5 ml); catalyst: 3.3 mol % respect to Styrene; TBHP (5.5 M in decane), 24h, Conversion determined by GC analysis. ^c: CH₃CN (2.2ml); Styrene (0.43mmol), Cat (1% respect to the styrene, Oxydant(5.5 M), 24h. Conversion determined by GC.

Besides, it was found that the catalytic system designed in this part of the work could also oxidize further substrates. Compared to the results found in the literature for the alkenes **trans**-stilbene (3f) and **cis**-stilbene (3g) (Scheme 14) when using (C10, figure22) with TBHP,^[65] the results obtained are close to the outcomes obtained herein when using 3f (entry4, Table13). However, our catalytic system shows more activity with 3g (Entry5, Table13) compared to C10 found in the literature.^[65] Additionally, the complex (C9, figure22) from the literature^[254] shows no activity in 3f (Entry 3, Table 13) while having H₂O₂ as oxidant in various conditions.

Table 13: Comparison of the epoxidation of further epoxides.*

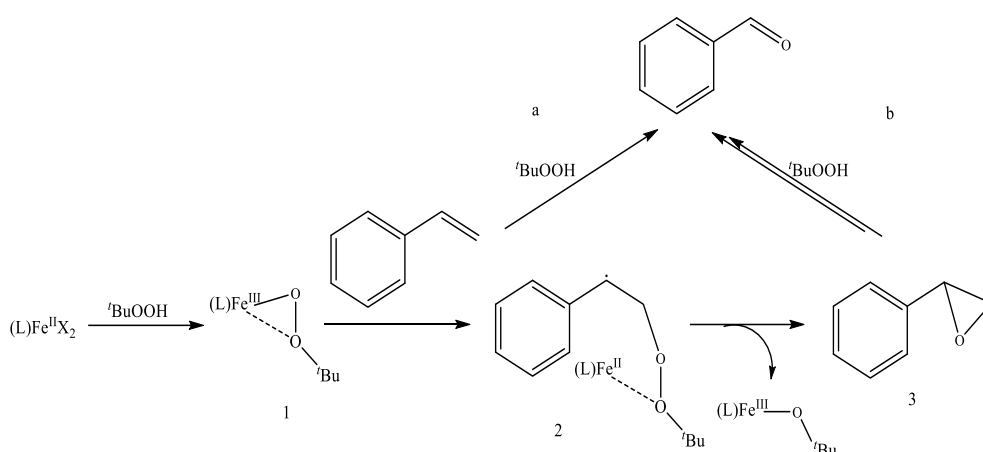
| Entry | Substrate | Cat | Oxydant | t(h) | Conv(%) | Yield(%) | Select(%) | Ref |
|----------------|-----------|------|-------------------------------|------|---------|----------|---------------------|-----------|
| 1 ^a | 3f | C10 | TBHP | 24 | 88 | n.r | 99 | [65] |
| 2 ^a | 3g | C10 | TBHP | 24 | 23 | n.r | 99 | [65] |
| 3 ^b | 3f | C9 | H ₂ O ₂ | 0,5 | - | - | - | [254] |
| 4 ^c | 3f | Fe1a | TBHP | 24 | 71 | 39 | 99 | This work |
| 5 ^c | 3g | Fe1a | TBHP | 24 | 61 | 50 | 91(trans 8(cis)) | This work |

*Conditions: **a:** CH₃CN (5 ml); catalyst: 3.3 mol % respect to Styrene; TBHP (5.5 M in decane). Conversion determined by ¹H NMR. **b:** styrene (0.1 mmol), Fe1 (5.0 mol%), pyridine-2-carboxylic acid (5.0 mol%), oxidant (2 equiv), CH₃CN (5 ml), Conversion was determined by ¹H NMR. **c:** CH₃CN (2.2ml); Styrene (0.43mmol), Cat (1% respect to the styrene, TBHP(5.5 M). Conversion determined by ¹H NMR. n.r. : Not reported.

4.3.4. Proposed mechanism of styrene epoxidation

The reaction mechanism of styrene epoxidation in the case of TBHP as oxidizing agent, according to various studies reported in the literature.^[255–257] Firstly, the metal catalyst is coordinated with TBHP to form complex comprising a higher valence transition metal-oxo compound. Secondly, the complex transforms from Fe(III)-oxo to Fe(III)-peroxo under TBHP. Moreover, according to the evidence gained from the results, a plausible general mechanism involving these N₄ donor complexes could be proposed. Considering that the selectivity towards the target product is about 50% implies that two consecutive reactions may occur as shown in the Scheme 14. Initially, Fe catalyst was coordinated with the TBHP to form a peroxo-active species

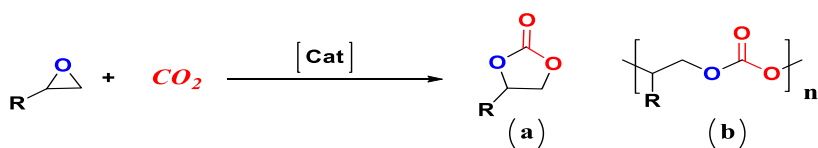
(1, Scheme 14), afterwards, the active oxygen of (1) subsequently interacts with the double bond of the styrene molecule to form the cyclic intermediate (2, Scheme 14). Lastly, the epoxide, simultaneously accompanied by the regeneration of the Fe catalyst was released. In parallel, The formation of benzaldehyde may be occurred directly by oxidation of styrene by TBHP, (a, Scheme 14). Another way to form benzaldehyde from styrene is by oxidation reaction to form styrene oxide, which further forms benzaldehyde in the presence of peroxide (b, Scheme 14).



Scheme 14: Proposed mechanism of epoxidation of styrene using TBHP and Fe(L) as catalyst.

4.3.5. Cycloaddition of CO₂ to epoxides

Having identified the optimum conditions for the epoxidation reaction, the catalytic activity of the iron (II) complex with the L1 ligand in the CO₂/epoxide coupling (Scheme 15) was undertaken. The catalytic activity of their cobalt and nickel analogues were also investigated for comparison. Given the fact that in the first part of the epoxidation, the optimization of the conditions was accomplished by employing the styrene as a substrate to yield the styrene oxide, so, in this second section the styrene oxide was picked to act as a substrate. In all experiments conducted, the metal center effect, the ligand structure, the solvent effect, and the reaction time were explored.



Scheme 15: Reaction of coupling of CO₂ to epoxides for the production of cyclic carbonate.

4.3.5.1. Solvent and solventless reaction effect

The primary screening was carried out using Fe1a complex as catalyst, a nucleophilic source which was tetrabutylammonium bromide (TBAB), the temperature and duration of the reaction were similar to those of epoxidation (24h, 60°C), the pressure of CO₂ was 10 bar, under solvent free medium. Under these conditions, a blank with only TBAB (entry1, Table 14) were conducted and gave a conversion up to 42%.

Table 14: Fe1a catalyst for the CO₂ cycloaddition to 1c with / without solvent .^a

| Entry | Solvent | Pressure (CO ₂) | Cat /Co-cat mmol % | Conv (%) | TOF(h ⁻¹) |
|-------|---------------------------|-----------------------------|--------------------|----------|-----------------------|
| 1 | Free | 10 | -/0.2 | 42 | 17.5 |
| 2 | Free | 10 | 0.1/0.2 | 53 | 22 |
| 3 | CH ₃ CN(2.2ml) | 10 | 0.1/0.2 | 36 | 15 |
| 4 | Free | 1 | 0.1/0.2 | 30 | 12.5 |
| 5* | CH ₃ CN(2.2ml) | 1 | 2/4 | 34 | 14 |

^a:Conditions de reaction : T: 60°C ; Reaction time : 24h ; Substrate : Styrene oxide: 1c: 20mmol ; Nu: TBAB. * (Cat/Nu:1 / 2 : mmol%)) ; Substrate: 0.43mmol .Conv: obtained by ¹H NMR with mesitylene as the internal standard.

The addition of the Fe1a catalyst increased modestly the conversion to 53% (entry 2, Table 14). An experiment using CH₃CN as a solvent was performed, yet in this case the system was active despite the fact that the conversion dropped to 36% (entry 3, Table 14). On the other hand, decreasing the CO₂ pressure to 1 bar in a solvent-free medium maintained the conversion at 30 (entry 4, Table 14). Finally, using the

identical catalyst loading as for the epoxidation reaction, with the exception of the presence of oxidant, a conversion of 34% was achievable (entry5, Table 14).

4.3.5.2. Influence of the complex and the metal in the CO₂/epoxides coupling.

Firstly, a test run without the catalyst using TBAB as nucleophile additive was performed to reach a conversion of 44% during 24h reaction time (Entry 1, Table 15). Next, a screening of the catalyst was performed with Fe1a, Ni1, Co1, and Fe4 (Scheme 12) in the (styrene oxide) and CO₂ coupling. In this section, a comparison was made not only according to the metal center but also according to the ligand structure. The results obtained reveal that phenanthroline based systems showed better performance than the bipyridine based ones, as already observed with the Zn based catalysts in (Chapter 3). Among the phenanthroline complexes, under the same conditions, the Ni1 complex (entry 4, Table 15) gave the highest conversion up to 88% in 24h with a TOF of 35h⁻¹, while the second conversion was achieved using Fe1a (entry 2, Table 15) as a catalyst with a value of 53% and a TOF of 22h⁻¹. The Co1 (entry 5, Table 15) provided the lowest conversion of 43%. Nevertheless, the Fe1b complex showed lower conversion than its Fe1a analog, which might be correlated to the fact that the triflate of the Fe1b complex, being more labile than the chloride halides of Fe1a, the bromide ion from TBAB might be coordinate to the Fe center avoiding the epoxide activation. On the other hand, the bipyridine triflate Fe4 complex (entry 6, Table 15) was able to achieve a rather low conversion of 17% compared with the entries (2-5, Table 15) for the same reasons.

Table 15: Results of the catalyst effect on the CO₂/ coupling. ^a

| Entry | Catalyst/Nu | Conv (%) | TOF(h ⁻¹) |
|-------|-------------|----------|-----------------------|
| 1 | Fe1a/- | 44 | - |
| 2 | Fe1a/TBAB | 53 | 22 |
| 3 | Fe1b/TBAB | 30 | 13 |
| 4 | Ni1/TBAB | 84 | 35 |
| 5 | Co1/TBAB | 43 | 22 |
| 6 | Fe4/TBAB | 17 | 7 |

^a:Conditions: Reaction time :24h ; Pressure:10bar ; Substrate: Styrene oxide,1c 20mmol ; Nu:TBAB:0.04 mmol. Cat:0.02mmol. Reaction time:24h. results given by ¹H-NMR with mesitylene as the internal standard

Then, it was clearly noticed that the NiI complex provided the most favorable performance (entry 1, Table 16) . The reaction time of the NiI catalyst was reduced to 3h, in order to assess the initial TOF of the reaction. At 3h reaction time, a TOF of 100h⁻¹ was attained at 30% conversion (entry 2, Table 16). Interestingly, a blank without TBAB was performed using only NiI as catalyst leaded to lower but significant conversion of 20% which indicate that a dissociation of the bromide ion of the catalyst takes place, to act as nucleophile and activate the epoxide (entry 3,Table 16).

Table 16: Time effect on CO₂/1c cycloaddition catalytic activity with NiI catalyst.*

| Entry | Cat | Time(h) | Cat/Nu | Conv (%) | TOF(h ⁻¹) |
|----------------|-----|---------|---------|----------|-----------------------|
| 1 | NiI | 24 | 0.1/0.2 | 84 | 35 |
| 2 ^a | NiI | 3 | 0.1/0.2 | 30 | 100 |
| 3 | NiI | 24 | 0.1/- | 20 | 8 |

*Conditions: Substrate: Styrene oxide (1c): 20mmol; Cat: 0.02mmol; Nu: TBAB 0.04mmol; T:60°C. t:24h, P (CO₂):10bar. ^a: Time =3h.

4.3.5.3. Reaction time effect on the conversion of 1c to 2c using NiI or FeIa catalyst

Furthermore, NiI exhibited modest activity at the lowest CO₂ pressure of 1bar (entry 1, Table 17), the catalytic system with NiI could achieve a 64% conversion after 48h reaction time (entry 2, Table 17).

Table 17: CO₂/1c coupling reaction with FeIa and NiI catalysts under 1bar CO₂ pressure. ^a

| Entry | Cat | Time(h) | Conv(%) | TOF(h ⁻¹) |
|-------|------|---------|---------|-----------------------|
| 1 | NiI | 24 | 34 | 14 |
| 2 | NiI | 48 | 64 | 13 |
| 3 | FeIa | 24 | 30 | 12 |
| 4 | FeIa | 48 | 60 | 12 |

^a:Conditions:Substrate (1c): Styrene oxide :20mmol ; TBAB : 0.04mmol ; Cat : 0.02mmol ; T=60°C, P (CO₂) : 1bar. Results obtained with mesitylene as the internal standard.

The catalytic system FeIa/TBAB achieved a 60% conversion under the same reaction conditions (entry 4, Table 17). Moreover, the steady increase in the conversion over 48h, indicate that these systems are stable under the catalytic conditions.

4.3.5.4. Comparison with previously reported catalytic CO₂/epoxides fixation

The application of iron-based catalysts in CO₂/epoxide cycloaddition has been scarcely investigated,^[258] since the reaction of CO₂ and epoxides to produce cyclic carbonates or polycarbonates has been dominated by metal-based catalysis particularly systems based on Cr, Co, and Zn.

Several systems using Fe(III)-based catalysts for the CO₂/epoxide reaction have shown the ability to produce significant conversion to cyclic carbonates or polycarbonates. Ji et al.^[86] reported a series of Fe(II) phthalocyanines (C11, Figure 20) as catalyst for the coupling of CO₂ and terminal epoxides. The presence of tributylamine as base in excess (4.5 equiv. per Fe) was required, for the reaction to occur and harsh reaction conditions (140 °C, 43 bar CO₂) were used (Entry1,Table 18). After that in 2007, Jing and coworkers,^[87] reported an iron porphyrin complex (C12, Figure 20) for the coupling of propylene oxide and CO₂. The reaction was conducted at 25°C and 7bar CO₂ in the presence of 2 equiv. of phenyl trimethylammonium tribromide (TPAT). The iron complex C12 was less reactive, yielding a conversion of only 10% after 3 h (entry 2, Table 18). In another study, performed by Dengler et al.^[89] reported iron (II) tetraamine and diimines-diamines

complexes with chloride and triflate halides (C13,C14,C15, Figure 23), were active for the coupling of CO₂ to propylene oxides to form propylene carbonate. Complexes diamines C13 and C14 (Figure 23) were active for cyclic carbonate formation even without the addition of an external cocatalyst but showed higher conversion with the addition of one equiv. of TBAB. However, the (C13, Figure 23) with chloride halides gave double conversion than the one with Triflates. Complex (C15, Figure 23) with diimines ligand was inactive alone but could achieve >80% conversions with the addition of TBAB. under Conditions: 1 mol% catalyst, 1 mol % co-catalyst, 100 °C, 15 bar CO₂ , 1 h reaction time (Entries 3,4,5, Table 18)

Later on, in 2019 Kamphuis et al.^[260] reported a formazanate ferrate (II) (C16, Figure 23) with different halides and without the addition of the cocatalyst, in the case of styrene oxide using the Fe(II) with bromides halides (Entry 6, Table 18) gave a conversion up to 70% in 18h under 90°C temperature. Instead, our system with the styrene oxide as substrate employing NiI catalyst (Figure 23) in the absence of TBAB could gave a conversion up to 20% in 24h under 1 bar pressure and 60°C (Entry 11, Table 18) and by the insertion of TBAB, the catalytic system could reach 30% conversion in 3h with a high TOF of 100h⁻¹ (Entry 8, Table 18). Moreover, the system kept activity to reach 82% conversion in 24h under 60°C temperature (Entry 9, Table 18). However, the Fe1a (Figure 23) analog system a conversion of 53% could be achieved in 24% (Entry 10, Table 18). Moreover, Chen et al.^[261] were also able to develop a series of bis-pincer iron (II) complexes with an unsymmetric pyridine bridge (C17, Figure 23) as catalysts for the cycloaddition of CO₂ and epoxides. At room temperature, the combined use of iron complexes with iodine ions and tetrabutyl ammonium bromide (TBAB) provided an efficient catalyst system for the synthesis of cyclic carbonates under CO₂ pressure (0.5 MPa) and without solvent. (Entry 7, Table 18).

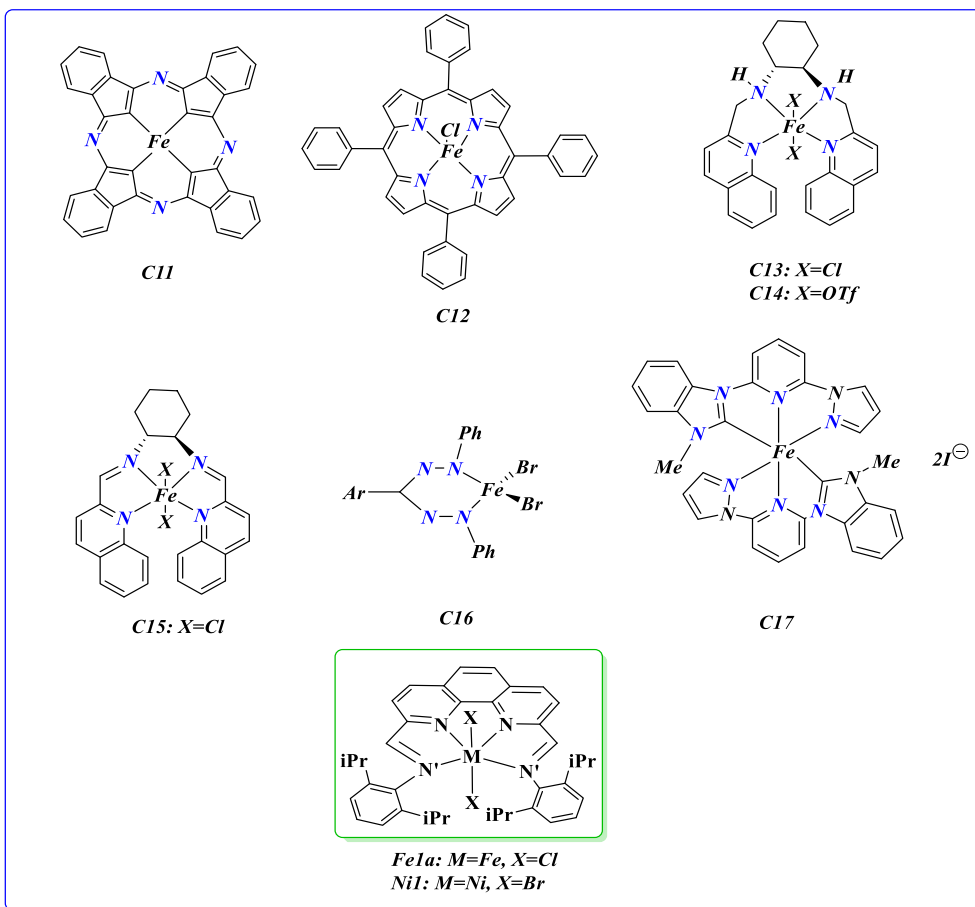


Figure 23: Selected Fe catalysts employed for the cycloaddition of CO₂ to epoxides.

Table 18: Comparison of the results obtained with the literature.*

| Entry | Catalyst | P(bar) | T(°C) | t(h) | Conv(%) | TOF(h ⁻¹) | Ref |
|-----------------|----------|--------|-------|------|---------|-----------------------|-----------|
| 1 ^a | C11 | 43 | 140 | 5 | 6 | n.r. | [259] |
| 2 ^b | C12 | 7 | 25 | 3 | 10 | n.r. | [87] |
| 3 ^c | C13 | 15 | 100 | 2 | 100 | n.r. | [89] |
| 4 ^c | C14 | 15 | 100 | 2 | 41 | n.r. | [89] |
| 5 ^d | C15 | 15 | 100 | 2 | 82 | n.r. | [89] |
| 6 ^e | C16 | 12 | 90 | 18 | 70 | 15 | [260] |
| 7 ^f | C17 | 10 | 25 | 24 | 53 | n.r. | [261] |
| 8 ^g | Nil | 10 | 60 | 3 | 30 | 100 | This work |
| 9 ^g | Nil | 10 | 60 | 24 | 84 | 35 | This work |
| 10 ^g | Fe1a | 10 | 60 | 24 | 53 | 22 | This work |
| 11 ^g | Nil | 1 | 60 | 24 | 20 | 14 | This work |

*Conditions: **a** :Substrate: 1b:PO. **b** : Substrate : PO. **c** : Substrate : PO, without TBAB. **d** : Substrate: PO, Co-cat: TBAB. **e** : Substrate: 1c, no Co-cat. **f** : substrate: PO Co-cat:TBAB: 1.5mol%. **g** : Substrate : 1c Styrene oxide : 20mmol ; Cat : 0.02mmol ; TBAB : 0.04mmol , P(CO₂)=10bar.Conversion calculated by ¹H NMR, using mesitylene as internal standard. **b**: Substrate : styrene oxide: 24.9mmol; Cat: 2.5.10⁻⁵ mol ; TBAB: 1.25.10⁻⁴ mol P(CO₂)=10bar. Conversion determined by ¹H NMR, with mesitylene as internal standard. n.r. : Not reported.

4.3.6. Attempts to Oxidative carboxylation of olefins to cyclic carbonates

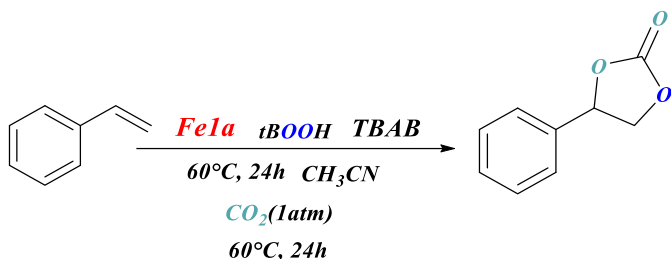
According to the results that have emerged from previous investigations in the area regarding the direct obtention of cyclic carbonates from alkenes, the majority of reactions to generate cyclic carbonates from olefins have been carried out as a one-pot oxidative carboxylation with simultaneous addition of all reactants. Few studies have been carried out by the subsequent reactions of olefins to epoxides followed by epoxidation to olefins in the same reactor.

In 2004, Arai and coworkers [262] reported that direct oxidative carboxylation of styrene-to-styrene carbonate was possible in the absence of the catalyst using molten tert-butylammonium bromide (TBAB), with tert-butyl hydroperoxide (TBHP) as an oxidant. This system led to 74% conversion, and 33 % yield to styrene carbonates (entry 1, table 19). In a different system, employing Fe porphyrin (a, Figure 24), Bai et al. [100] performed aerobic one-pot synthesis of styrene carbonate from styrene in

mild conditions, CO₂ (11bar) and O₂ (5 bar) at 30 °C. The styrene carbonate was obtained in 3.3% yields in 48h reaction time (entry 2, Table 19).

On the other hand, Ramidi et al.^[263] reported that styrene carbonate could be obtained from styrene over a manganese(III) complex of an amido-amine ligand as catalyst (b, Figure 24) with 2 equiv. of TBAB as cocatalyst. They carried out the epoxidation of olefin with TBHP and the conversions of olefins to cyclic carbonates were moderate (styrene yield = 43%) in 2.5ml of dry acetonitrile (entry 3, Table 19).

Based on that, we decided to run a preliminary test of the oxidative carboxylation using Fe1a as catalyst, using the two different approaches: the one pot process and the two-step process. The two steps system was prepared by introducing into the Schlenk, the catalyst, styrene substrate, as well as the oxidizing agent, TBHP, all dissolved in CH₃CN. After 24h, TBAB was introduced inside the Schlenk and CO₂(1atm) was inserted through a balloon and let the reaction for further 24h, at the temperature of 60°C. However, in the one pot system : the styrene olefin, the catalyst together with the TBAB, the oxydant (TBHP), and CO₂ (1 bar) pressure were introduced simultaneously to the Schlenk, and the reaction was kept at 60°C for 24h.



Scheme 16: Reaction pathways for the direct synthesis of styrene carbonate from styrene.

¹H-NMR of the final crude after 24h, revealed no styrene carbonates was formed in none of the experiments conducted, however the styrene oxide as an intermediate was detected with a yield <10 %. Also, in the NMR we observed a signal at 9.8 ppm, that might be related to the dialdehyde formed by hydrolysis of L1 in Fe1a. That a

decomposition of the catalyst occurred. Surely, a more refined catalysis approach is needed in order to enhance the performance of this reaction.

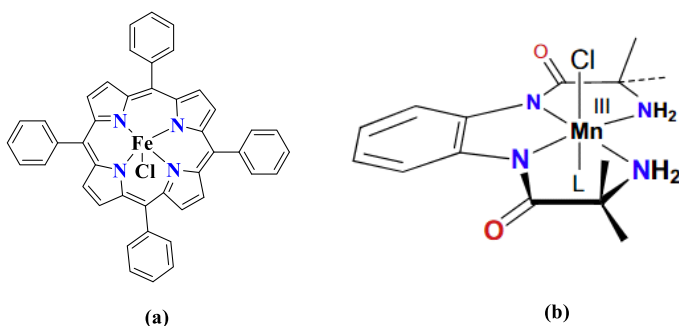


Figure 24: Catalysts employed for oxidative carboxylation.

Table 19: Synthesis of styrene carbonates from styrene.*

| Entry | Cat / Co-cat | Oxydant | P(CO ₂) | T(°C) | Conv(%) | Yield(%) | Ref |
|----------------|--------------|----------------|---------------------|-------|---------|----------|-----------|
| 1 ^a | - / TBAB | TBHP | 150 | 80 | 74 | 33 | [262] |
| 2 ^b | (a)/TBAI | O ₂ | 11 | 30 | - | 3.6 | [100] |
| 3 ^c | (b)/TBAB | TBHP | 17 | 100 | - | 34 | [263] |
| 4 ^d | Fela/TBAB | TBHP | 1 | 60 | 0 | - | This work |
| 5 ^e | Fela/TBAB | TBHP | 1 | 60 | 0 | - | This work |

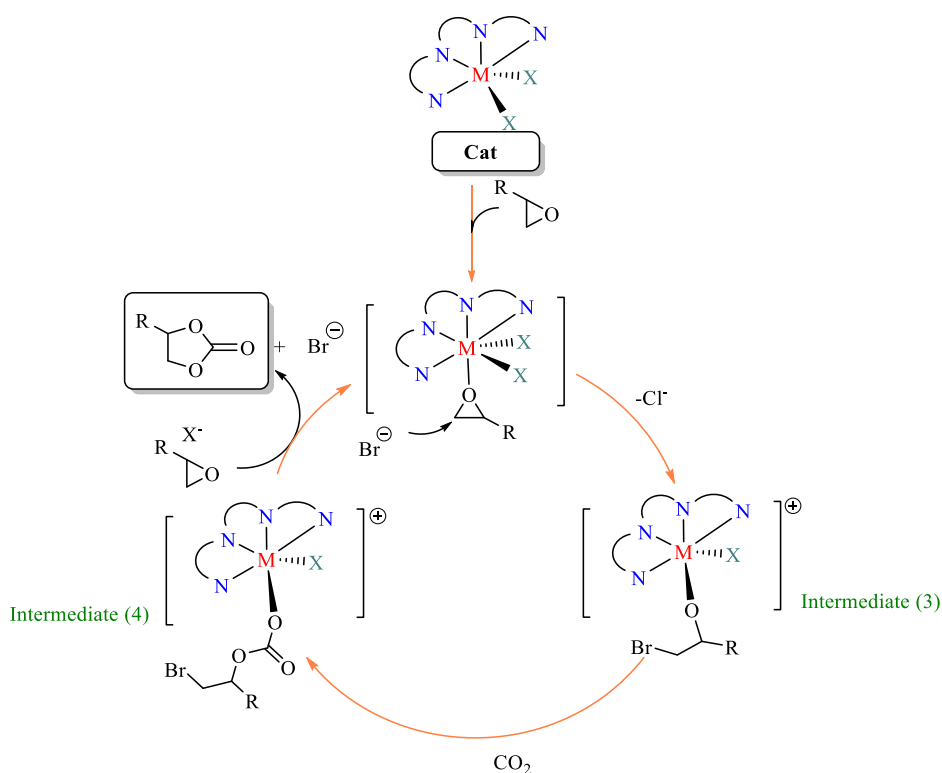
*Condition: **a:** Styrene, 17.3 mmol; TBHP, 25.4 mmol; CO₂ pressure, 150bar; temperature, 80 °C; time, 6h. **b:** Catalyst: 37.5 mg (0.05 mmol), cocatalyst 2 equivalents of catalyst, styrene 10 equivalents of catalyst, P(O₂)0.5MPa, P(CO₂)1.1MPa, CH₂Cl₂ 5ml, T:30°C, 48h. **c:** Catalyst-TBAB-alkene = 1:2:500, CO₂, oxidant :1.5 equiv. to substrate, temperature :100°C, no solvent. **d:** 2 steps in one single reactor Cat:0.0043mmol, TBAB:0.017mmol, TBHP:0.0017mmol, 2.2ml dry CH₃CN, 24h. **e:** one pot reaction: Cat:0.0043mmol, TBAB:0.017mmol, TBHP:0.0017 mmol, 2.2ml dry CH₃CN, 24h. The styrene carbonate product was determined by ¹H NMR with the mesitylene as standard reference.

It's rather complicated to compare the outcomes obtained to the previously reported ones since the reaction's conditions and the reactor setup are quietly different. However, it can be asserted that the conditions employed in the test conducted by us were significantly milder than those previously reported. It was confirmed by Arai and coworkers ^[264] that CO₂ pressure plays a crucial role in obtaining high yields of styrene carbonate. When the CO₂ pressure was varied over a wide range, yields were obtained at a maximum of 1,8 and 15 MPa. In another study conducted and reported

by Aresta et al.^[265] it was confirmed that the selectivities of the products were strongly dependent on the solvent used, the temperature, the auxiliary ligand coordinated to the metal, the molar ratio of the Cat/Co-cat and the gas pressure injected.

4.3.7. Proposed mechanism for the cycloaddition of CO₂ to epoxides.

According to the present study and the literature data in this field, the cycloaddition reaction of CO₂ to epoxides can be launched by the activation of the epoxide. The metal complex interacts with the oxygen atom of the epoxide, followed by nucleophilic attack (Br⁻) promoting the opening of the epoxide ring, resulting in an intermediate (3), followed by insertion of CO₂ into the metal-alkoxide bond of intermediate (3), producing a new intermediate (4). Ring closure of the intermediate produces a cyclic carbonate as the final product, and the nucleophile is recycled for further reactions (Scheme 18).



Scheme 17: General mechanism proposed for the CO₂/epoxides coupling.

4.4. Conclusion

Summarizing this chapter, the direct synthesis of cyclic carbonates from olefins and CO₂ by oxidative carboxylation, which formally involves the combination of the selective epoxidation of the alkenes followed by cycloaddition of CO₂ to the formed epoxide, could be a more economically viable process because it works with a cheap and readily available starting material, alkenes, and does not require the separation of the epoxide after the first step. Moreover, only one amount of catalyst could be employed in the two successive processes, performing this reaction using only CO₂ at atmospheric pressure could be a very promising idea.

Admittedly, with the catalytic systems developed in this study, the results obtained were modest. But the catalyst was active in the epoxidation as well as in the CO₂ cycloaddition separately, although the one-pot process was not effective under milder conditions. It is therefore still necessary to develop other highly efficient catalytic systems that can improve this conversion under milder conditions.

***CHAPTER 5: Metal catalyzed
photocatalytic CO₂ reduction towards
CO/H₂***

5.1. Introduction

Photocatalytic reduction of carbon dioxide using visible light energy combined with homogeneous transition metal catalysts is an exciting process ^[266–268] to use carbon dioxide as a C1-feedstock to produce useful chemicals and to close the carbone cycle.

The main focus of this study is the production of CO, although this gas is a toxic gas, but it is widely recognized as a useful gas in many industrial processes with several advantages as discussed in the general introduction.^[269,270] Carbon monoxide is used extensively in industry as a molecular building block, particularly in the form of syngas, a mixture of CO and H₂, which is usually derived from coal gasification or steam reforming of natural gas. It is in this form that it is used in the Fischer-Tropsch process ^[270] to obtain synthetic fuels or to be recycled via the hydroformylation of alkenes for the generation of aldehydes.^[271]

There have been numerous investigations dedicated to the exploration of catalysts for photocatalytic CO₂ reduction using both molecular metal complexes,^[117,118] and heterogeneous metal nanoparticles.^[82,272] The homogeneous metal complexes provide benefits for both mechanistic analysis as well as ligands tuning in the quest for catalysts for CO₂ reduction.^[273] The performance and product selectivity are frequently dependent on the choice of catalyst as well as the conditions used to conduct the reactions. Rare metals such as ruthenium, rhodium have exhibited outstanding results. However, attempting to minimize the use of precious metals but also to achieve a photocatalytic system employing non-costly transition metal complexes are the focus of the present study.

Complexes with tetradentate ligands of cobalt,^[274] nickel,^[268,275,276] and iron,^[277,278] have been employed as catalysts for the CO₂ photoreduction.^[279] In the case of homogeneous photocatalytic reduction of CO₂, for instance a Ni(II) complex bearing an S₂N₂-type tetradentate ligand (C18, Figure 25) had been reported by Hong et al.^[273] to produce CO in a photocatalytic system using [Ru(bpy)₃]²⁺ (bpy = 2,2'-bipyridine)

as photosensitizer and 1,3-dimethyl-2-phenyl-2,3-dihydro-1Hbenzo[d]imidazole (BIH) as electron donor. This complex shows a high turnover number, above 700 with a high CO selectivity of >99%.

Other systems employing Fe and Co consisting on N4-tetradentate quaterpyridine complexes (C19,C20, Figure25) were explored, using [Ru(bpy)₃]²⁺ as photosensitizer and (BIH) as a sacrificial reductant in CH₃CN/TEOA solution under visible light (blue LED) excitation. This system was capable of achieving a TON of CO as high as 2660 with 98% selectivity in the case of the cobalt catalyst, and a TON above 3000 with up to 95% selectivity in the case of iron.^[183] Further systems were spotted in the literature ^[273,280] employing N4 tetradentate ligands with non-expensive metals proved to be appealing and challenging. Thus, the outstanding outcomes have been motivated us to investigate the synthesized N4 tetradentate containing phenanthrolyl and bipyridyl ligands as catalysts for photocatalytic reduction of CO₂ under visible light irradiation.

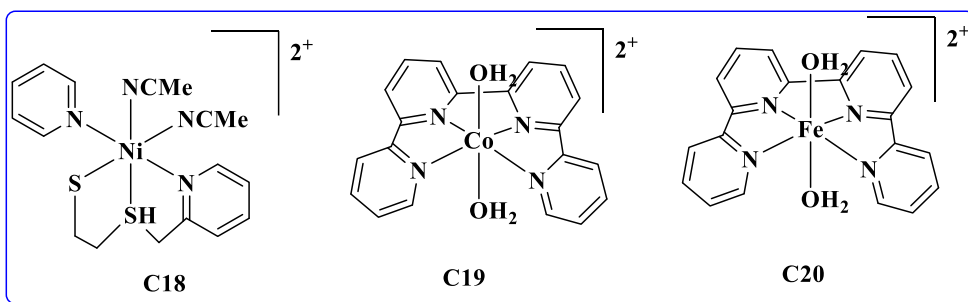


Figure 25: Tetradentate N(II), Fe(II) and Co(II) catalysts for CO₂ photoreduction.

Therefore, the series of iron (II), cobalt (II) and nickel (II) halide complexes bearing 2,9-bis(imino)-1,10-phenanthrolyl and bipyridyl ligands (Fe1a, Fe1b, Co1, Ni1, Fe4, Co4, Ni4) which were described previously in the (Chapter 4) were used as catalysts, for the photocatalytic CO₂ reduction. This allows to study the effects of chelating N4 ligand coordination on metal (II)-catalyzed photochemical conversion of CO₂ (Figure 26).

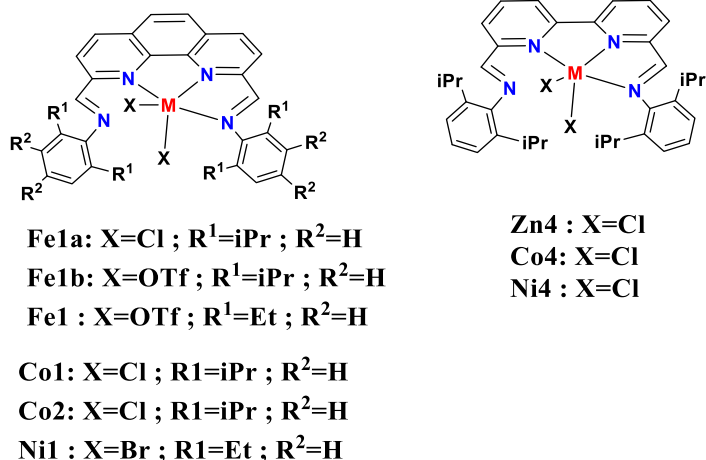


Figure 26: Fe(II), Ni(II) and Co(II) catalysts for CO₂ photoreduction.

Metalloporphyrins are of particular relevance among homogeneous catalysts.^[143] They are widely used in the photocatalytic process of CO₂, both as catalysts and as photosensitizers.^[281] Several examples in the literature have illustrated the success achieved by porphyrins in this field.^[182,282–284] Therefore, a series of iron and zinc porphyrins have been synthesized in collaboration with Prof. Pereira's group (university of Coimbra) and have been tested as catalyst or as photocatalyst (Figure 27).

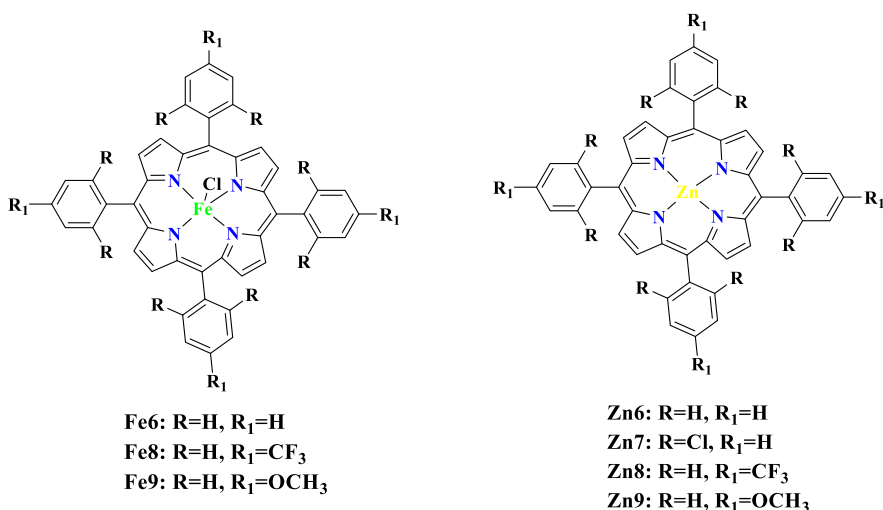


Figure 27: Zn and Fe porphyrins employed in CO₂ photoreduction.

Various photosensitizers including metal-based and organic compounds, were examined to study the effect of photosensitizer on the performance and selectivity towards CO and H₂ (Figure 28).

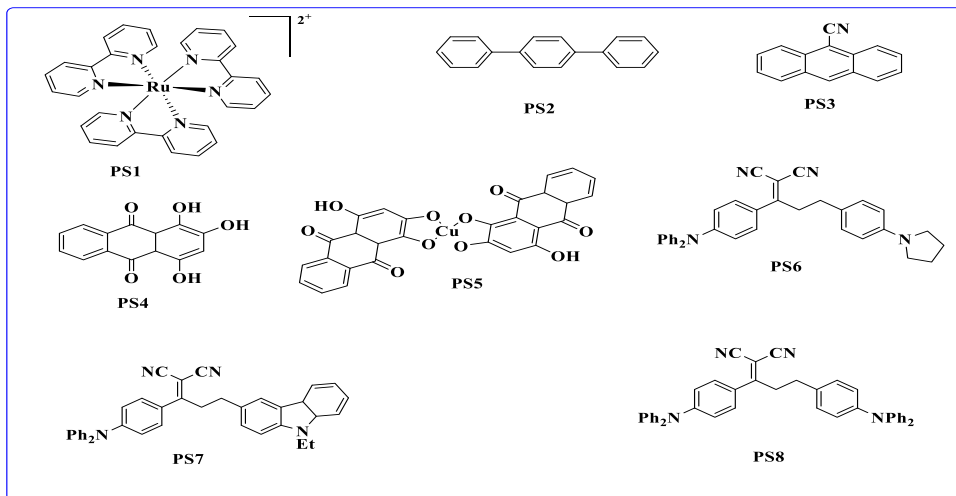


Figure 28: Photosensitizers employed in the photocatalytic CO₂ reduction.

Alcohols, amines, and some ascorbic acids are well known as Sacrificial electron donors.^[131] Using electron donors with high reducing ability should thus be favorable, based on that, the TEOA (Figure 29) which has been routinely employed as sacrificial donor and as Bronsted base providing a basic environment for accelerating the CO₂ photoreduction process,^[282] TEA (Figure 29) were experimented as well. and the BIH (Figure 29) combination to TEOA had often provided the best outcomes, and that was also checked. As solvents we used dry acetonitrile or dimethylformamide or N,N methyl-pyrrolidone solvents.

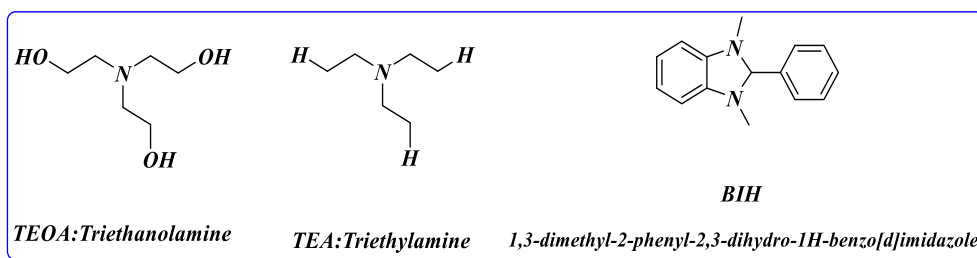


Figure 29: Sacrificial electron donors employed in the photocatalytic CO₂ reduction.

5.2. Experimental section

5.2.1. General comments

The synthesis of the complexes **Fe1a**, **Fe1b**, **Ni1**, **Co1**, **Fe4**, **Co4**, and **Ni4**, were described in chapter 4. The chemicals employed for porphyrin synthesis and used in other processes were commercially available, analytical grade reagents were all utilized with no further purification. The solvents used for the synthesis were used directly without drying or purification. With the exception of the solvents used for photocatalysis, which were dried on molecular sieves and deoxygenated before use. TEOA and TEA were stored on molecular sieves and opened in an N₂ environment. All photosensitizers are commercially supplied and employed as received. However, PS6, PS7, PS8 (Figure 28) allylidene malononitrile family were obtained by Seferoglu's group, department of chemistry, Ankara university (Turkey). Their synthesis had been described earlier.

The preparation of the photocatalytic systems is done under an inert atmosphere. Analyses for the detection of CO and H₂ produced as major products after photocatalysis are performed using gas chromatography-thermal conductivity detector (GC-TCD). The detection of formic acid as by-product was performed by HPLC chromatography. All analyses are performed in duplicate at least of until consistency of the obtained results.

The lamps used are Kessil PR160L on a kit furnished with a powerful fan to blow air from above efficiently to maintain the reactions at room temperature. It is also supplied with light shields for laboratory safety which effectively block out all uv rays and most blue light. The wavelengths of the lamps are in the visible region of λ :456nm and λ :467nm. The average intensity is about 399mW/cm² (measured at a distance of 1cm). The sample is putted 11cm far from the lamp, with a maximum power of 50W. The metal porphyrins **Fe6**, **Fe9** and **Zn6**, **Zn7**, **Zn9** were performed at the University of Coimbra (Portugal) in the framework of a 3-months internship.

5.2.2. Synthesis

5.2.2.1. Porphyrin ligands synthesis

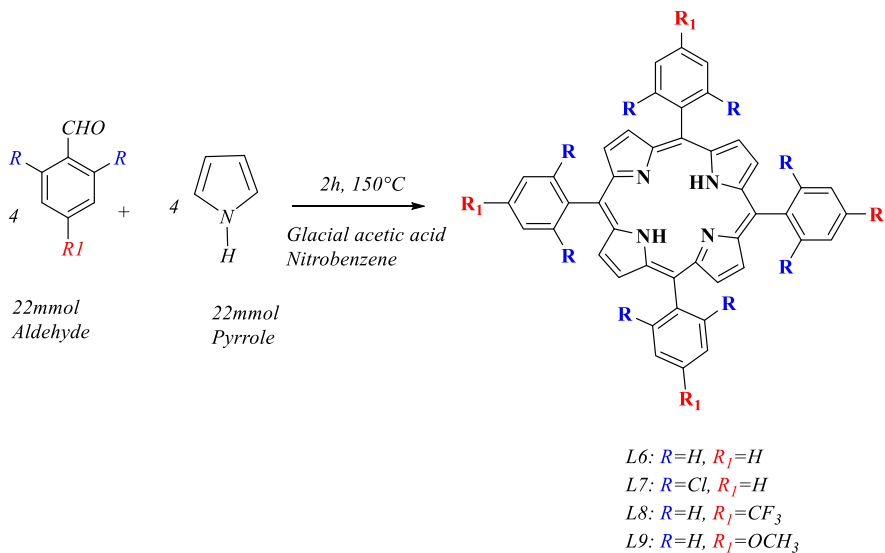
General synthesis of porphyrins L6-L9, was accomplished following similar procedure from the literature.^[285,286] The suitable aldehyde (22mmol, 1eq) was first dissolved in glacial acetic acid 80ml, then nitrobenzene 50ml was added until complete dissolution, followed by a dropwise addition of pyrrole (1,5g, 22mmol) over 30min to the first mixture (Scheme 19). The resulting reaction mixture was refluxed at 140°C for 2h. Then the solution was allowed to cool to r.t. and 150ml of cold MeOH was added to induce precipitation. After kept overnight at -30°C, the solid was filtered, and the crude product was washed three times with cold methanol. The purity of the products was verified by ¹H NMR and compared to the reported values.

L6 : Purple crystals. (Yield 50%) : ¹H NMR (400MHz, ppm, CDCl₃): δ: 8.80 (s, 8H), 8.17 (m, 8H), 7.68(m, 12H), -2.82(s, 2H).

L7 : Blue powder. (Yield 5%) : ¹H NMR (400MHz, ppm, CDCl₃): δ: 8.62 (s, 8H), 7.68 (m, 12H), -2.59(s, 2H).

L8 :Purple crystals. (Yield 35%) : ¹H NMR (400MHz, ppm, CDCl₃): δ : 8.81 (s, 8H), 8.34 (d, 8H), 8.05 (d, 8H), -2.83 (s, 2H).

L9: Purple powder (Yield 70%) : ¹H NMR (400MHz, ppm, CDCl₃): δ: 8.85 (s, 8H), 8.12 (d, 8H), 7.28 (d, 8H), 4.05 (s, 12H), -2.8 (s, 2H).



Scheme 18: Synthesis of porphyrins reaction.

5.2.2.2. Metal porphyrins synthesis

General synthesis of Zn porphyrins complexes

Following general procedure described previously in the literature.^[287] 1eq of the appropriate porphyrin was dissolved in 50ml of chloroform and 25ml of methanol, then acetate salt (10eq) of the Zn(OAc)₂ was added to the reaction mixture and stirred for 24h under reflux. After that, the mixture was allowed to cool down, then the solvent was evaporated to half of volume. Finally, cold methanol was added to induce the precipitation. After 1 night at -30°C, the product could be recovered by filtration, and washed 3 times with cold methanol to yield the complex. The ¹H NMR analysis coincides with the reported values.

Zn6. Dark purple. (Yield 85%) : ¹H NMR (400MHz, ppm, CDCl₃): δ 8.85: (s, 8H), 8.20 (m, 8H), 7.75 (m, 12H)

Zn7. Dark purple. (Yield 33%) : ¹H NMR (400MHz, ppm, CDCl₃): δ: 8.5 (s, 8H), 7.4 (m, 12H).

Zn9. Dark purple. (Yield 70%) : ¹H NMR (400MHz, ppm, CDCl₃): δ: 8.85 (s, 8H), 8.12 (d, 8H), 7.28 (d, 8H), 4.05 (s, 12H).

General synthesis of Fe6, Fe9 porphyrins complexes

The metalation of porphyrins with Fe metal precursor have been performed following a procedure from the literature.^[288] In a round flask and under nitrogen, the porphyrin (0.25 mmol) was dissolved in DMF (100 mL). Then the solution was heated to reflux with magnetic stirring. Upon dissolution of the porphyrin completely, FeCl₂·4H₂O (0.3 g, 1.5 mmol) was added into the solution in three portions over 30 min. Thin-layer chromatography (alumina, using CH₂Cl₂ as eluant), indicated no free porphyrins at this point. After that, half volume of the DMF was evaporated. The solution was cooled to -30°C and 6 M HCl (40 mL) was added into it. The solid appeared from the solution, then was filtered, and washed with 3M HCl until the filtrate is colorless. The resulting solid was vacuum-dried to afford the complex. The results of the Uv-vis correspond to those already described

Fe6. Dark green. (Yield 75%) : Uv-vis (nm), Soret band : 419, Q bands= 507 ; 572.

Fe9. Dark green. (Yield 80%) : UV-vis (nm) : Soret band : 420, Q bands 509 ; 572.

5.2.2.3. BIH Preparation

The synthesis of the sacrificial reductant BIH has already been described in the literature.^[169] In an oven dried Schlenk ,the solution of substituted N, N'-dimethyl-o-phenylenediamine (0,35g, 2,569.10⁻³mol) in a minimal amount of methanol (3ml) was added a suitable amount of benzaldehyde (0.27g, 1eq) with vigorous stirring at room temperature, followed by the addition of one drop of glacial acetic acid. After 1h, the crude product was separated from the reaction mixture by filtration, then washed with cold methanol and recrystallized from petroleum ether to give the corresponding pure product, as a white crystal. 0.41g. Yield of 70%. ¹H-NMR fit with the already reported values.

¹H NMR (400 MHz, ppm, CDCl₃) δ : 7.58 (m, 2H), 7.41 (m, 3H), 6.72 (dd, 2H), 6.43 (dd, 2H), 4.87 (s, 1H), 2.56 (s, 6H).

5.2.3. Photocatalytic experiments

A typical procedure for the photocatalysis experiment was as follows. 12ml total volume vial, fitted with a magnetic stir bar, and connected to the N₂ gas input, was charged with 1.5μmol of catalyst, 6.25μmol of photosensitizer, in CH₃CN-SD (5:1 v/v) to a 3.75mL total solution volume. The sample vial was sealed with a rubber septum, and then saturated with CO₂ gas for 20 min. Then it was placed in the lamp kit with 2 blue LED lamps on ($\lambda = 456\text{nm}$ and 467nm as light sources) positioned on both sides of the sample in opposite relative position with a distance of 11 cm each. Samples are picked up after 4h, 24h irradiation time. A volume of 100μl of the gaseous phase samples were extracted by a Hamilton glass syringe, and the CO and H₂ content were analyzed by a gas chromatograph equipped with a thermal conductivity detector (TCD). High-purity Ar was used as carrier gas, and the calibration of the GC parameters was accomplished with the use of standard CO/H₂/Ar mixtures of known concentration.

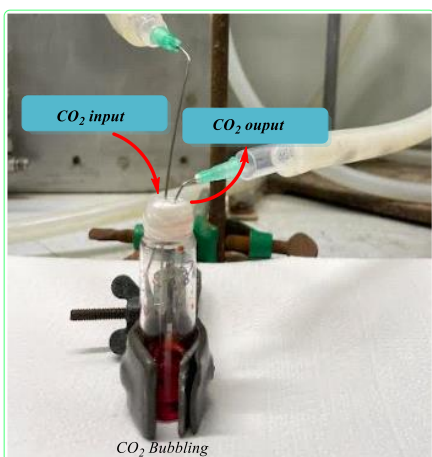


Figure 30: CO₂ bubbling to the vial cell

5.2.4. Formic acid determination method

For the quantification of formate, a procedure adopted from the literature was used.^[289] 1 ml of the crude mixture was taken, and 1 mL of water was added. then 200 μ l of 1M H₂SO₄ was also added to the mixture the reaction. Finally for extraction 2.2 ml of ethyl acetate was introduced, then the mixture was stirred vigorously for a few minutes. Finally, the extracted phase (upper phase) was analyzed by high performance liquid chromatography (HPLC).

5.2.5. Cyclic voltammetry cell preparation

Cyclic voltammetry experiments were performed at room temperature, in a compartment cell of Metrohm Autolab 302 N potentiostat equipment, fitted with a stirring bar, and conventional three-electrodes system. The electrodes were cleaned with ethanol and dried with soft paper. The glassy carbone working electrode was polished, a Pt counter electrode, and a standard calomel or Ag/AgCl (3M) as reference electrodes were used. 25mL of dry deoxygenated CH₃CN solution containing 0.5M Bu₄NPF₆ or LiClO₄ as the supporting electrolyte. 0.5mmol/L of ferrocene (0.0023g), as the external standard. The measurements were carried out in nitrogen atmosphere, or in CO₂ saturated solutions. The solution was stirred before each scan. Various scans were performed at varying potential ranges 10 and 50mV/s between to determine the different reversible reduction and oxidation steps.

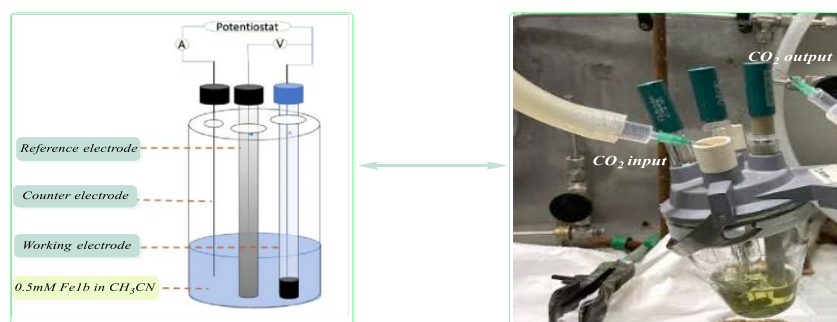


Figure 31: Cyclic voltammetry cell illustration.

5.2.6. Hydroformylation experiments attempts

The first run was conducted by combining in a 12mL vial containing 2ml of toluene, equipped with a magnetic stirrer, (1.34M, 308.08 μ L) styrene, [Rh(acac)(CO₂)] (6.7.10⁻³M, 3.46.10⁻³ g) and PPh₃ (0.01675M, 8.78.10⁻³g). The (CO/H₂) produced by the photocatalytic system is introduced through a metal cannula directly connecting the photocatalytic system vial to the hydroformylation vial. The system was agitated and heated at 80°C for 24 hours.

The second run was conducted as a single-pot reaction. In a vial of 12ml fitted with a magnetic stirrer, containing 3.12mL of CH₃CN, TEOA (1.34M, 0.625mL), **Fe1b** (0.42M, 0.0013g) as catalyst, PS1 (1.78M, 0.0055g), BIH (0.1M, 0.126g), [Rh(acac)(CO₂)] (3.46.10⁻³ g, 0.01675M), PPh₃ (0.01675M, 8.7.10⁻³ g), and styrene (1.34M, 308 μ L) were introduced. And finally, the mixture was bubbled with CO₂ gas for 20min. The vial was irradiated for 24h with visible light at room temperature, with continuous stirring, and after that, the vial was removed from the light and kept under stirring at 60°C for further 24h.

5.3. Results and Discussion

5.3.1. Synthetic aspects

The synthesis of phenanthroline and bipyridine complexes (Figure 22) employed for CO₂ photoreduction has been discussed in the preceding chapter 4. Synthesis of porphyrin and their Fe and Zn complexes is detailed in this chapter.

The metalation of porphyrins was carried out according to procedures already described in the literature.^[287,288] Generally metal porphyrins were obtained by the insertion of the metal by reaction of free base porphyrins with the appropriate metal salts. ¹H NMR and UV-Vis measurements were sufficient to ensure the purity of the synthesized compounds by comparison to the previously reported data.

The coordination of the porphyrins to Fe was checked by monitoring the reaction in the UV-Vis. The coordination is proved by decrease of the intensity and the number of Q bands, and the soret band shifted slightly, which were the characteristics of the iron porphyrin compounds formed. For **Fe6**, the disappearance of the Q bands 514nm, 585nm, 538nm, 620nm, and a slight shift in the soret band from 417nm of the L6 to 419 for the **Fe6**. Similarly, to the **Fe9**, the 4 bands of the Q bands disappeared (512, 545, 589, 643 nm), and the shift in the soret band from 417nm to 420nm revealed the coordination of the Fe metal to the porphyrin.

The coordination of the Zn metal to the porphyrins was approved by ¹H NMR, in which a slight movement in the chemical shifts, along with the disappearance of the negative chemical shifts -2.71 ppm corresponding to the N-H signal of the pyrrole was evidenced to its coordination.

5.3.2. Photocatalytic CO₂ reduction

The reaction parameters and photocatalytic system were basically selected on the basis of previous photocatalytic studies on CO₂ reduction,^[290] and adjusted upon the availability of the equipment in the purpose to achieve optimal activity and selectivity.

5.3.2.1. Fe catalyst effect on CO₂ photoreduction

Initial conditions for the CO₂ photoreduction of CO₂ were selected according to the literature reported for in situ iron catalyst,^[290] using triethanolamine (TEOA) as sacrificial donor along with a ruthenium complex as PS in N-methyl-pyrrolidone (NMP) CO₂ saturated solution. Thus, the results published by Alsabeh et al.^[290] were reproduced in our setup. After that, a catalyst free blank with PS1 (entry 1, Table 20) was conducted under this conditions giving no CO or H₂. Secondly, a run using Fe1b without photosensitizer (entry 2, Table 20) neither CO nor H₂ gas were detected even after 24h irradiation time. In the lack of PS that is in charge of triggering the photocatalytic setup, the catalyst Fe1b itself cannot initiate the photocatalytic process. In fact, the UV-vis absorption spectra measurement of Fe1b in CH₃CN showed that it absorbs in the ultraviolet area <400nm which is under the lamp wavelength employed, what renders the excitation of the catalyst impossible. These blank experiments (entries 1,2, Table 20) also (entry 3, Table 20) without CO₂ bubbling, these results revealed that no CO was formed, which confirmed that the catalyst, and photosensitizer and also CO₂ gas are required to form CO, and that the CO₂ formed is not resulting of any decomposition of the components and CO₂ is the only source of CO.

Table 20: Effect of the cat (Fe1a and Fe1b) and PS in photocatalytic CO₂ reduction.
^a

| Entry | Catalyst | PS | TON CO | TON H ₂ | Selectivity CO (%) | Selectivity H ₂ (%) |
|-------|----------|-----|--------|--------------------|--------------------|--------------------------------|
| 1 | - | PS1 | - | - | - | - |
| 2 | Fe1b | - | - | - | - | - |
| 3* | Fe1b | PS1 | - | - | - | - |
| 4 | Fe1a | PS1 | 7 | 9 | 29 | 70 |
| 5 | Fe1b | PS1 | 12 | 10 | 56 | 44 |

^a: Conditions: 1,5 μmol of catalyst, PS1(6,25 μmol), 3.5 mL of CO₂ saturated. NMP /TEOA (5 : 1, v/v), visible light >450 nm, 24h irradiation time. *: Without CO₂.

The effect of the X ligand (Cl or OTf) was first investigated. The catalyst with Fe1a (entry 3, Table 20) yielded a TON of 7 for CO and a TON of H₂ of 9 after 24h of irradiation. Replacing the Fe1a with the catalyst with Fe1b containing the triflate instead of the chloride (Entry 4, Table 20), it was noticed a slight increase in the turnover number of both CO and H₂. No HCOOH was detected in either case. The higher lability and less nucleophilicity of the triflate ion respect to the chloride might favor the interaction of CO₂ with the active species in the catalytic cycle.

5.3.2.2. Fe, Ni, Co metal effect on the conversion

Next, The screening involving the complexes as catalysts, gave the possibility to investigate the effects of the metal center, the backbone of the ligand and the steric bulk of the substituents on the photocatalytic activity was investigated under the same reaction conditions the results are presented in table 21.

The cobalt and nickel-based complexes bearing phenanthrolyl ligands Co1, Co2, Ni1 showed lower conversion than the iron analog Fe1b. Thus, it was noted that the cobalt exhibits a moderate activity (entries 2,3, Table21). Moreover, it was observed that the cobalt catalysts Co1, Co2 produce H₂ preferentially with a selectivity 86% and 90% respectively, whereas the nickel has absolutely no catalytic activity towards the products concerned (entry 4, Table 21).

Table 21: Complexes comparison on CO₂ photoreduction to CO/H₂.^a

| Entry | Catalyst | TON (CO) | TON(H ₂) | Select CO% | Select H ₂ % |
|-------|----------|----------|----------------------|------------|-------------------------|
| 1 | Fe1b | 12 | 10 | 56 | 44 |
| 2 | Co1 | 6.5 | 41 | 19 | 86 |
| 3 | Co2 | 4 | 38 | 0 | 90 |
| 4 | Ni1 | 0 | 0 | 0 | 0 |

^a:Conditions: 1.5 μmol of catalysts, PS1 (6.25 μmol), 3.5 mL of CO₂ saturated. NMP /TEOA (5 : 1, v/v), visible light >450 nm, 24h irradiation time.

5.3.2.3. Solvent effect

NMP solvent is a nonflammable, powerful dipolar aprotic solvent with high solvency power and low volatility makes it an interesting solvent with various applications. From the other side acetonitrile is a polar aprotic solvent mainly used as a solvent in purification due to its low viscosity, high chemical stability, and high elution power. Since, economically, CH₃CN is cheaper than the NMP. So, the acetonitrile was selected as an alternative solvent. Switching the solvent from the NMP to the CH₃CN resulted in a slight increase in CO and H₂ TONs, whereas the selectivity versus CO decreased (entries 1,2, Table 22) Therefore, it may be concluded that CH₃CN solvent promotes the production of H₂, as is illustrated in the table 22.

Table 22: Solvent effect on the TON and selectivity of the products in the photoreduction of CO₂ using Fe1b/PS1/TEOA catalytic system. ^a

| Entry | Solvent/SD | TON(CO) | TON(H ₂) | Select(%) CO | Select(%) H ₂ |
|-------|-------------------------|---------|----------------------|--------------|--------------------------|
| 1 | NMP/TEOA | 12 | 10 | 56 | 44 |
| 2 | CH ₃ CN/TEOA | 19 | 70 | 21 | 75 |

^a:Conditions: 1,5 μmol of Fe1b catalyst,PS1 (6,25 μmol), 3.5 mL of CO₂ saturated. Solvent /TEOA (5 : 1, v/v), visible light >450 nm, 24h irradiation time.

After that, we decided to test the bipyridyl based complexes using the acetonitrile as a solvent. The results obtained with Fe³ (entry 1, Table23) reaching a TON of CO of 10 with a selectivity up to 35%. The activity of Fe³ is lower than Fe1b but the selectivity to CO was higher with Fe³ catalyst (entry 1, Table 23). The phenanthroline

based catalysts showed more activity than the bipyridyl based ones. (Table 23). The Co₄ similar to the Co₁, Co₂ showed more selectivity towards H₂ (entry 2, Table 23).

Table 23: Metals bearing bipyridyl effects of the photocatalytic system activity. ^a

| Entry | Catalyst | TON(CO) | TON(H ₂) | Select CO % | Select H ₂ % |
|-------|-----------------|---------|----------------------|-------------|-------------------------|
| 1 | Fe ₄ | 17 | 28 | 38 | 61 |
| 2 | Co ₄ | 17 | 76 | 19 | 80 |
| 3 | Ni ₄ | 0 | 0 | 0 | 0 |

^a: Conditions: 1,5 μmol of catalysts, PS1 (6,25 μmol), 3.5 mL of CO₂ saturated. CH₃CN /TEOA (5 : 1, v/v), visible light >450 nm, 24h irradiation time.

5.3.2.4. Influence of SD on the photocatalytic activity of the system

In the majority of reported photocatalytic systems for CO₂ reduction using transition metal complexes as PS, the catalytic cycles were started by the reductive quenching process (RQ), in which an electron was injected into the PS* from the reductant (SD). Therefore, the choice of SD sometimes drastically affects the photocatalytic capabilities of the systems. The stability of SD^{•+} strongly affects the efficiency of the photocatalytic system because the return electron transfer from PS^{••} to SD^{•+} decreases the efficiency of the photocatalytic reaction. Therefore, to promote the return electron transfer, SD^{•+} must be sacrificially decomposed, for instance by deprotonation, in order to lose its oxidative power as quickly as possible. Another point to consider when selecting a SD should be the reactivity of the final oxidation products of the D, as they sometimes react with intermediates, such as PS*, PS^{••}, and Cat^{••}, and this may induce suppression of the photocatalytic reaction.^[291] Then, other SD were tested in this reaction, results are listed in table 24. TEA (entry 2, table 24) as SD was unable to effectively perform the sacrificial electron donor behavior. Previous reports have suggested that TEA performs as a better electron donor at higher pH medium. So, at lower pH, the protonation of TEA diminishes its ability to function as an electron donor.^[186] Nevertheless, working in organic solvent at the photocatalytic reaction conditional protonation of TEA is not expected. However, it was found that the TEA

and the TEOA having very similar properties, they exhibit irreversible oxidation potentials around 0.7V vs. SCE,^[131,150] making them thermodynamically able to be part of similar electron transfer processes nevertheless the alcohol groups in TEOA necessarily improve miscibility in water, and that a lower pKa for TEOA than TEA, which turns the medium system more acidic. Still, all the systems being described using TEA or TEOA^[151,153,161,162] demonstrate varying performance, which leads to confusion in selecting the optimal one between them. Hence possibly linked to the coupled components to the SD and catalyst. Interaction of TEA with the catalyst in the CH₃CN medium cannot be discarded also.

The BIH is known to be an effective reducing quencher for the excited state of PS. The BIH is two electrons, one proton source (hydride donor)^[292] which can react as well with the excited state of [Ru(bpy)₃]²⁺ as PS in a reductive quenching process, yielding PS⁻ and oxidized BIH^{•+}, this latter one is very acidic and loses a proton to a base (TEOA in this case) in the medium and generate the powerful reductant BI[•], as a strong second electron donor to the PS, (E(BI[•]/BI⁺) = 1.5 V/SCE).^[130,169] Moreover, the high reduction potential of BIH allows the use of metal complexes which have a low oxidation power in their excited states.^[177,293]

In the current work, the BIH itself (entry 3, Table 24) failed, to produce CO, which might be attributed to that reversible electron transfer process between the reduced PS⁻ and the BIH^{•+}, in the absence of a base being able to pick up the proton from the BIH inhibits the reaction.^[130] However, coupling BIH with TEOA they could achieve the optimum results (entry 4, Table 24). In this case BIH role is to quench the active state of PS while triethanolamine mainly functions as the proton acceptor for BIH^{•+}. Moreover, enhancing the concentration of BIH from 0.1M to 0.15M (Entry 5, Table 24), led to further increases in the system efficiency since the TON in CO reached 188 and decrease in the TON of H₂, along with increasing the selectivity towards CO to reach 75%. An experiment involving BIH in aqueous acetonitrile solution, could led to an increase in the TON of CO, that is slightly higher than the TON's obtained with TEOA in acetonitrile solution (entry6, Table 24). However, the presence of

water in the reaction medium, as well the protons issued from the degradation of TEOA would be involved in the increase of the increase in the (TON H₂ to 168).

Table 24: Results of SD effect on the photocatalytic CO₂ reduction.*

| Entry | SD | TON (CO ₂) | TON (H ₂) | Select(CO) % | Select(H) % |
|----------------|-----------------------|------------------------|-----------------------|--------------|-------------|
| 1 | TEOA | 19 | 25 | 43 | 56 |
| 2 | TEA | 0 | 0 | 0 | 0 |
| 3 | BIH | 0 | 0 | 0 | 0 |
| 4 ^a | BIH / TEOA | 102 | 123 | 45 | 55 |
| 5 ^b | BIH/TEOA | 188 | 63 | 75 | 25 |
| 6 ^c | BIH/TEOA | 70 | 58 | 56 | 45 |
| 7 ^d | BIH/ H ₂ O | 27 | 168 | 13 | 87 |

*:Conditions : 1,5 μmol of catalyst(Fe1b), RuBipy (6,25 μmol), V_T=3.5 mL of CO₂ saturated. CH₃CN /SD (5 : 1, v/v), Visible light >450 nm, Reaction time: 24h irradiation time. a : BIH : 0.1M .b : BIH : 0.15M. c: BIH: 0.30M. d : CH₃CN / H₂O (5:1, v/v) V_T= 3,5ml , BIH:0.1M.

5.3.2.5. Photosensitizer effect on CO₂

In the present study, [Ru(bpy)₃](PF₆)₂ (PS1, Figure 28) has been proven to be an effective and powerful photosensitizer in molecular photocatalytic CO₂ reduction. However, and in order to make the process cost-effective viable, efforts have been made to incorporate organic compounds that have previously functioned as PS into an artificially generated photocatalytic system. For that a series of metal free photosensitizers (PS2-PS7, Figure 28) were selected to be used in our photocatalytic systems.

Although the absorption band of the photosensitizers is mainly in the visible range, except for (PS2, Figure 28) p-terphenyl was reported in a previous work that its radical anion has a long lifetime in a system containing TEA/DMF, and is a very strong reducing reagent (-2.45 V vs SCE) [146] and absorbed in the uv region. It was reported previously the use of PS2 as photosensitizer coupled with Co and Fe cyclam catalysts, as well as with metalloporphyrins, using a Hg lamp > 280nm. For this reason, we tried PS2 with uv lamp (356nm), but the system was not active (entry 2, Table 25). This may be because the wavelength of the used lamp is higher or also

that the intensity of the lamps employed was weak (1,5W) compared to the more powerful lamps reported in literature.^[148,294]

The purpurin (PS4, Figure 28) used in the (entry 4, Table 25) has been reported earlier as one of the most active organic photosensitizers for CO₂ reduction when coupled with a variety of metal catalysts,^[295,296] achieving a TON CO as high as 1365 (TOF 300 h⁻¹) with respect to the catalyst.^[183] Nevertheless, the inactivity of this compound (entry 4, Table 25) in our photocatalytic system, may be related to its redox potential which is not enough to reduce the catalyst employed in this study.

The anthracene based organic dye (PS3, Figure 28) coupled with FeIb no reaction was detected (entry 3, Table 25), which constitute an upcoming group of inexpensive PSs exhibiting high molar absorption coefficients in the visible region, have demonstrated good stability in the photocatalytic reduction of CO₂.^[297] However, the activity of these photocatalytic systems is much lower than that of systems using metal-based photosensitizers, due to the inefficiency of multiple electron transfer to the catalyst.^[280,298]

Allylidenemalononitrile compounds were also employed as photosensitizers (PS6 PS7, PS8, Figure 28), but only PS6 showed a negligible TON of CO and H₂ 0.5 and 0.10 respectively (entries 5-7, Table 25).

The reducing power of the free metal PS is much lower than the metallic one, which may explain the obtained results in ruthenium PS1, possessing a more positive redox potential than the metal free ones employed.

Table 25: Photosensitizer effect on the photocatalytic system activity. ^a

| Entry | PS | TON(CO ₂) | TON(H ₂) | Select(CO ₂)% | Select (H ₂)% |
|-------|-----|-----------------------|----------------------|---------------------------|---------------------------|
| 1 | PS1 | 19 | 25 | 56 | 43 |
| 2* | PS2 | - | - | - | - |
| 3 | PS3 | - | - | - | - |
| 4 | PS4 | - | - | - | - |
| 5 | PS6 | 0.50 | 0.10 | - | - |
| 6 | PS7 | - | - | - | - |
| 7 | PS8 | - | - | - | - |

^a:Conditions: 1,5 μmol of catalysts, PS (6,25 μmol), 3.5 mL of CO₂ saturated. CH₃CN /TEOA (5:1, v/v), visible light >450 nm; 24h irradiation time. *UV lamp : λ = 365nm.

5.3.2.6. Irradiation time effect / stability of the system.

With the aim to investigate stability of the photocatalytic system over the time, it was decided to allow the reaction to proceed for a period of 72 hours. Using the Fe1b catalyst combined with PS1, BIH in CH₃CN/TEOA CO₂ saturated solution. Samples for GC injection have been taken after 4h, 24h, 48h and then 72h. The activity of the system increased from 4h to 24h. and after that the production of CO and H₂ was leveled off. which might be attributed to the degradation of the catalyst (Figure 32).

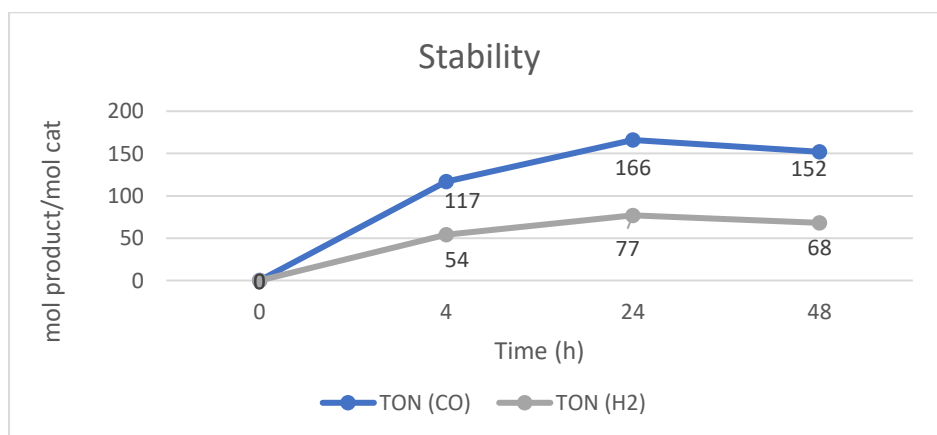


Figure 32: TONs of CO and H₂ within irradiation time (h). Conditions: 1,5 μmol of catalyst Fe1b, PS1 (6,25 μmol), 3.5 mL of CO₂ saturated. CH₃CN /TEOA (5:1, v/v), BIH (0.1M), Visible light >450 nm; 24h irradiation time.

5.3.3. Porphyrins as catalysts

The porphyrins synthesized during the internship in Portugal, were studied independently from the N₄ tetradentate complexes, based on what is already reported in the literature,^[148,282,283,284,300] regarding the use of porphyrins as electron-transfer mediators to effect photochemical reduction of CO₂ in homogeneous solutions. The porphyrins could act as photocatalysts and photosensitizers, in particular iron tetraphenyl porphyrin [iron(III) 5,10,15,20-tetraphenylporphyrin chloride (FeTPP)] and its derivatives, were found to be catalytically and efficiently capable of reducing CO₂ through electrochemical,^[283,301] and photochemical,^[148,300] processes.

In this regard, in order to study their performance, the Fe(III) (Figure 27), and Zn(II) porphyrins (Figure 27) were incorporated into our designed photocatalytic system in CH₃CN or DMF solutions, depends on the solubility of the porphyrins.

In the case of Zn porphyrins which are applied as PS, by comparing to a previous study that employed Zn(II) (TPP: 5,10,15,20-tetraphenylporphyrin) as PS,^[281] they have shown the cyclic voltammogram of this compound, it could be observed that there were two obvious reduction peaks, one at -1.05 V vs. SCE and the other at -1.65 V vs. SCE. The first peak (-1.05 V vs. SCE) stood for the reduction of ZnTPP to an excited state of ZnTPP (ZnTPP*), which was a transition form of the ZnTPP complex. The second state (-1.65 V vs. SCE) stood for the reduction of ZnTPP* to ZnTPP. Therefore a blockage of the system in this stage, so, the Zn porphyrins were not powerful enough to reduce the catalyst employed that will be discussed later.

The results obtained with the porphyrins have shown that weak or no catalytic activity has been demonstrated, this could be related to many reasons. The potency of the PS employed, since the cyclic voltammograms of FeTPP previously reported,^[302] have shown that the reduction of Fe(III) to Fe(0), occurs in a very negative potential, especially the passage from Fe(I) to Fe(0) that occurs in 1.8 V Vs SCE, so maybe a more powerful reductant is necessary, also the reduction reactions involving multiple electron transfers coupled with proton transfers, thus the employed sacrificial donors

may not be able to provide all the electrons and protons needed for this reduction. Further limitation could be related to the concentrations of the PS and sacrificial donors employed, which may be not sufficient, and they consumed rapidly during the process. A second probability could be due to the lamps used, since in the literature, the lamps used are more powerful with a power between 300 and 600 W. Otherwise, additional studies are necessary to overcome these limitations.

5.3.3.1. Fe (III) porphyrins

Herein, firstly, we studied the photochemical reduction of CO₂ with symmetrical Fe porphyrins as catalysts, and/or photocatalysts (Table 26).

In the case of Fe6 (Figure 27) which is the iron porphyrin non substituted used as photocatalyst, coupled with TEOA as SD. After 24h irradiation time under blue LEDs. No CO was detected, traces of H₂ and the formic acid was found with a TON up to 19 (entry 1, Table 26). In another experiment, using the Fe6 as photocatalyst, by introducing the BIH with TEOA, after 24h irradiation, the CO could be detected with a TON up to 9.5 and H₂ with a TON up to 5.5, but no HCOOH was formed in this case (entry 2, Table 26). Using the Fe6 as catalyst coupled with PS1 as photosensitizer, and TEOA as SD, without BIH. After 24h irradiation time, the H₂ was the main reduction product with a TON up to 49, and CO was detected with TON up to 2.5 (entry 3, Table 26). Coupling the Fe6 with the catalyst Fe1b revealed no CO production and traces of H₂ under the same reaction conditions (entry 4, Table 26). In the (entry 5, Table 26) in which we coupled the Fe8 which is the symmetrical iron porphyrin having CF₃ substituent in the para position, with the PS1 as photosensitizer and TEOA as SD. This experiment leads to the formation of H₂ with a TON of 20, however no CO or HCOOH were detected after 24h irradiation time with the blue LEDs.

Table 26: *Fe porphyrins for photochemical CO₂ reduction.**

| Entry | Cat ^a | PS | SD | TON(CO) | TON(H ₂) | HCOOH |
|----------------|------------------|-----|----------|---------|----------------------|-------|
| 1 ^a | Fe6 | | TEOA | 0 | 0.7 | 19 |
| 2 ^b | Fe6 | | TEOA/BIH | 9,5 | 5.5 | 0 |
| 3 | Fe6 | PSI | TEOA | 2.5 | 49 | 6 |
| 4 | Fe1b | Fe6 | TEOA/BIH | 0 | 0.15 | 0 |
| 5 | Fe8 | PSI | TEOA | 0 | 20 | 0 |

*Conditions: 1,5μmol Cat, 6,25μmol PS, V_T: 3.5 mL of CO₂ saturated DMF /TEOA (5 : 1, v/v), Visible light >450 nm; 24h irradiation time. BIH:0.1M. a : 0,2mM Fe6 b : 0,2mM Fe8, BIH: 0.1M.

5.3.3.2. Zn(II) porphyrins as PS

Inspired from previous studies, It was shown in many other metal catalysts that H₂O, one kind of the weak Brønsted acid, also plays an important role to help with the catalytic reaction in this process, water was a necessary reagent to acquire the catalytic activity.^[281,303] employing the Zn porphyrins complexes as photosensitizers, we decide to conduct experiments coupling the Zn porphyrins with the catalyst Fe1b. The results are presented in table 27.

In the case of Zn6 (Figure 24) as PS with Fe1b as catalyst using TEA as SD in saturated aqueous acetonitrile solution. After 24 hours of irradiation with the blue LEDs, no CO, H₂ or HCOOH was detected (entry 1, Table 27). Another experiment using only CH₃CN without the addition of H₂O, traces of H₂ were detected with a TON of 1,5 under the same reaction conditions (entry 2, Table 27). When introducing BIH into the system,(entry 3, Table 27) no CO was formed, and again, traces of H₂ were found after 24 hours of irradiation. Changing the Zn6 with Zn7 didn't show any CO or H₂ nor HCOOH formation (entry 4, table 27). Zn8 and Zn9 (Figure 23) were used under the same reaction conditions, and led to the formation of H₂ as the only product with TONs of 4 and 1.1 respectively. (entries 5,6, Table 27).

Table 27: Zn porphyrins as photosensitizers results. *

| Entry | PS | SD | Solvent | TON(CO) | TON(H ₂) |
|----------------|-----|----------|-------------------------------------|---------|----------------------|
| 1 ^a | Zn6 | TEA | CH ₃ CN-H ₂ O | 0 | 0 |
| 2 | Zn6 | TEOA | CH ₃ CN | 0 | 1.5 |
| 3 ^b | Zn6 | TEOA/BIH | CH ₃ CN | 0 | 1 |
| 4 | Zn7 | TEOA | CH ₃ CN | 0 | 0 |
| 5 | Zn9 | TEOA | CH ₃ CN | 0 | 1.1 |
| 6 | Zn8 | TEOA | CH ₃ CN | 0 | 4 |

*Conditions: : 1,5µmol Cat Fe1b; 6,25µmol PS; VT: 3.5 mL of CO₂ saturated CH₃CN/SD (5 : 1, v/v); Visible light >450 nm; 24h irradiation time. a : TEA: 0,1M; VT: 3.5 mL of CO₂ saturated CH₃CN/H₂O (20:1, v/v) . b: BIH:0.1M.

5.3.4. Fe catalysts reported for photocatalytic CO₂ reduction

It is rather complicated to compare the results obtained in this work to those reported previously since the reaction parameters and the setup are significantly varied. Nevertheless, it can be asserted that the conditions employed in the test we performed were significantly milder than those reported previously. In this section, we select some similar systems employing Fe(II) and Fe(III) as catalysts, with PS that vary between the metallic and non-metallic ones, as well as three different sacrificial donors. Takeda et al.^[184] succeeded in developing a photocatalytic system from complexes containing only abundant metals, with Cu(I): Cu(I) (dmp)(P)²⁺ (dmp = 2,9-dimethyl-1,10-phenanthroline; P = phosphine ligand) as the redox photosensitizer and Fe(II) (dmp)₂(NCS)₂ as the catalyst, using BIH as the sacrificial electron donor, could produce CO with a TON of 273 as the main product in 12h irradiation by 436 nm monochromatic light irradiation for 12 h (entry 1, Table 28). Another system developed by Rao et al.^[295] developed an iron-substituted tetraphenyl porphyrin bearing positively charged trimethylammonium groups at the para position of each phenyl ring for photoinduced CO₂ conversion. This complex selectively was able to reduce CO₂ to CO under visible light irradiation in aqueous solutions (acetonitrile: water 1:9 v:v) with the help of 1 equiv. of purpurin, in the presence of 0.1M NaHCO₃ and TEA as a sacrificial reductant. CO was produced with a catalytic selectivity of 95% and a turnover rate of 60 for an irradiation time of 47h (entry 2, Table 28) and could reach TON of 120 while adding 3 equiv. of purpurin with visible light

irradiation. A slight decrease in the TON of CO was noted while replacing TEA with TEOA (entry 3, Table28). In another essay, Bizzarri and coworkers^[304] report two photocatalytic reduction of CO₂ by employing a copper (I) as a sacrificial donor coupled to a heterocyclic Fe(II) catalyst (C22, C23, Figure 33) as well as BIH as a sacrificial donor in TEOA acetonitrile solution after 4 hours of irradiation at 420 nm, achieving a CO TON of 107 and 7.8 respectively (entries 4,5, Table 28). Later on, Guo et al.^[183] in 2016 could design a fantastic photocatalytic reduction of CO₂ combination using Fe(II) quaterperidine [Fe(qpy)(OH₂)₂]²⁺ (C20, figure 31) have been investigated. With PS1 as the photosensitizer and BIH as the sacrificial reductant in CH₃CN/triethanolamine solution under visible-light excitation (blue light-emitting diode), a turnover number (TON) for CO >3000 with up to 95% selectivity could be reached (entry 6, Table28). The non-substituted Fe(III) porphyrin have been already employed as catalyst but also as photocatalyst by Grodkowski et al.^[300] they could achieve a TON of CO up to 17 without adding any PS, only by using the Fe porphyrin coupled with TEA in acetonitrile solution, after 3h irradiation time using a strong xenon lamp (300-900W) (Entry 7, Table28). While employing the same Fe6 porphyrin (Figure 27) with TEOA in our system, employing the blue LEDs for irradiation, we could not detect CO production but 0.7 TON of H₂ was detected, and 90 TON of HCOOH as well was formed after 24h irradiation time (entry 10, Table28).

Zn porphyrins are scarcely used for the photocatalytic CO₂ reduction. It was found that Zhang et al.^[281] reported a non-substituted Zn porphyrin as photosensitizer (1equiv.) coupled with a manganese catalyst (4 equiv.) and TEOA as sacrificial reductant. After 3h irradiation time with a xenon lamp (500W), 119 TON of CO was formed also 19 TON of HCOOH was detected, however, none of the products were detected while coupling the Zn6 porphyrin to our catalyst Fe1b.

To summarize, from this preliminary study, we obtained promising results on the photoreduction of CO₂ but still the aspects of stability and selectivity must be improved.

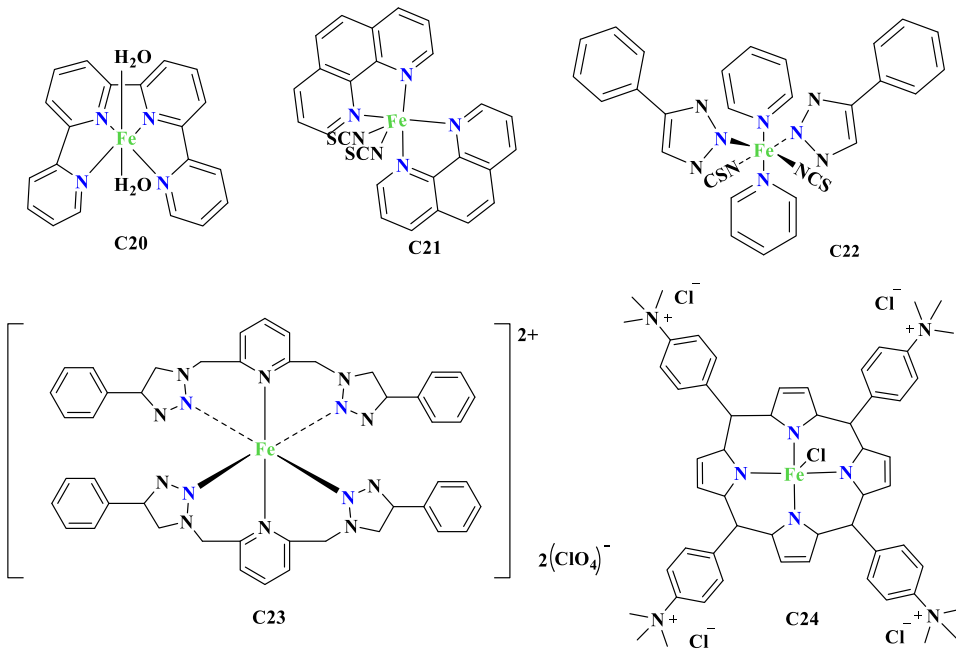


Figure 33 : Catalysts employed in the photocatalytic CO₂ reduction.

Table 28: Comparison of the results to the previously reported photocatalytic CO₂ reduction using iron cobalt and nickel catalysts in homogenous systems.*

| Entry | Cat | PS | SD | TON (CO) | TON (H ₂) | TON HCOOH | T(h) | Ref |
|----------------|------|-----|----------------------|----------|-----------------------|-----------|------|------------------|
| 1 ^a | C21 | CuI | BIH | 273 | 75 | - | 12 | [184] |
| 2 ^b | C24 | PS4 | TEA | 60 | 3 | - | 47 | [295] |
| 3 ^c | C24 | PS4 | TEOA | 42 | 4 | - | 47 | [295] |
| 4 ^d | C22 | CuI | BIH | 107 | 43 | - | 4 | [305] |
| 5 ^e | C23 | CuI | BIH | 7.8 | 2 | - | 4 | [305] |
| 6 ^f | C20 | PS1 | BIH | >3000 | 15 | - | 3 | [183] |
| 7 ^g | Fe6 | - | TEA | 17 | 37 | - | 3 | [300] |
| 8 ^h | Mn1 | Zn6 | TEA | 119 | - | 19 | 3 | [281] |
| 9 | Fe1b | Zn6 | TEOA | 0 | 0 | 0 | 24 | <i>This work</i> |
| 10 | Fe6 | - | TEOA | 0 | 0.7 | 19 | 24 | <i>This work</i> |
| 11 | Fe1b | PS1 | BIH/TEOA | 188 | 63 | - | 24 | <i>This work</i> |
| 12 | Fe1b | PS1 | TEOA | 19 | 25 | - | 24 | <i>This work</i> |
| 13** | Fe1b | PS4 | TEOA | 0 | 0 | - | 24 | <i>This work</i> |
| 12 | Fe1b | PS1 | H ₂ O/BIH | 27 | 168 | | 24 | <i>This work</i> |

*Conditions: 1,5µmol Cat Fe1b; 6,25µmol PS; V_T: 3.5 mL of CO₂ saturated CH₃CN /SD (5 : 1, v/v); SD:0.1M, Visible light >450 nm; 24h irradiation time. **: DMF/SD. **a**: 0.5mM PS, 0.05mM Cat, 10mM BIH, (CH₃CN/TEOA:5/1:v/v), High pressure xenon lamp (436nm). **b**: visible light irradiation (> 420 nm) of a CO₂-saturated ACN:H₂O (1:9, v:v) solution containing 2 µM C24, 0.2 mM PS4, 0.1 M NaHCO₃ and 0.05 M SD: TEA. **c**: visible light irradiation (> 420 nm) of a CO₂-saturated ACN:H₂O (1:9, v:v) solution containing 2 µM C24, 0.2 mM PS4, 0.1 M NaHCO₃ and 0.05 M SD:TEOA. **d**: 20 mM BIH, [CAT]=0.1 mM, 1.0 mM PS under CO₂ MeCN/TEOA (5 : 1, v/v), 8W lamp 4 h irradiation at 420 nm. **e**: 20 mM BIH, [CAT]=0.1 M, 1.0 mM PS under CO₂ MeCN/TEOA (5 : 1, v/v), 8W lamp 4 h irradiation at 420 nm. **f**: 0.005 mM Cat, 0.3 mM PS1, 0.1 M BIH, and 0.5 M TEOA, CH₃CN CO₂ saturated solution blue light-emitting diode (LED).**g**: DMF solutions, 5% TEA, and saturated with CO₂, Cat:10⁻⁵ irradiation in a Pyrex ampoule cooled by a water jacket, 300 UV lamp. **h**: cat:Mn1: fac-[Mn(phen)(CO)₃ Br]: 2 mM, Zn6: 0.5 mM, TEA (0.1 M) in a MeCN-Water (v/v = 20:1), 500w xenon lamp. (Cu(I): CuI(dmp)(P)²⁺ (dmp =2,9-dimethyl-1,10-phenanthroline; P= phosphine ligand).

5.3.1. Sequential photoreduction/ hydroformylation

With the purpose of using the in-situ CO/H₂ obtained from the photocatalytic process, two experiments were designed to couple the production of CO/H₂ mixture with the hydroformylation of alkenes. Styrene was selected as the olefin object of the transformation along with [Rh(acac)(CO)₂] / 5PPh₃ as hydroformylation catalyst.

In one experiment we connected via cannula the vial where CO/H₂ was generated to another vial containing the [Rh(acac)(CO)₂] / 5PPh₃ catalyst, and the styrene in toluene. The mixture then was heated to 60°C for 24h. In a second experiment, the components were located in one vial which was subjected to 24h irradiation after being bubbled with CO₂ and heated at 60°C for further 24h.

Unfortunately, the GC-MS analysis could not identify any of the peaks corresponding to the aldehydes. This may be mainly attributed to low pressure of the generated gases from the CO₂ photoreduction, comparing with the pressures commonly reported within this reaction.

5.3.1. Electrochemical studies

To identify the species formed under reductive conditions, cyclic voltammograms (CVs) of complexes Fe1b and Co1, were recorded. Complex Fe1b in acetonitrile (CH₃CN, 0.5mM) with tetrabutylammonium hexafluorophosphate NBu₄PF₆ (0.1 M) as electrolyte using ferrocene as external standard (Fc⁺/Fc) under nitrogen atmosphere, shows pseudo reversible three reduction processes at -1.336 V, -1.821 V and -2.061 V, which are shifted from the values of L1 (Figure 34). This indicates a participation of the ligand in the electro-reduction processes as reported for a Fe(II)-bipyridine-diimines complex^[306] and were accordingly assigned to three reductions. When CO₂ was bubbled to this solution a new pseudo reversible wave appeared at -1.73 V. The current intensity decreased, and the E_{1/2} of the ligand related reduction waves shifted close to free ligand values. These observations point that a new species is formed under CO₂ saturated solution and that the deactivation of the catalysts is due to ligand dissociation. Which may be slower under photocatalytic conditions. Similar CV was obtained for Co1 under nitrogen atmosphere, however, instead, when

CO₂ was bubbled in the solution, practically no change in the E_{1/2} value was detected suggesting that no interaction with CO₂ took place. This different behavior may explain the lower activity towards CO₂ reduction of the cobalt complexes.

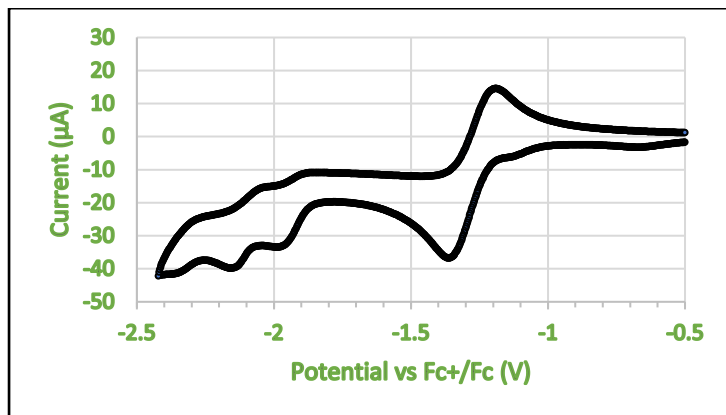


Figure 34: CV of LI in ACN (0.5 mM) with NBu₄PF₆ (0.1 M) under N₂ 50 mV·s⁻¹ scan rate. Working electrode: 3 mm diameter glassy carbon. Counter electrode: Pt wire. Reference electrode: Ag/AgCl (3M KCl). Potential (V) vs Fc⁺/Fc

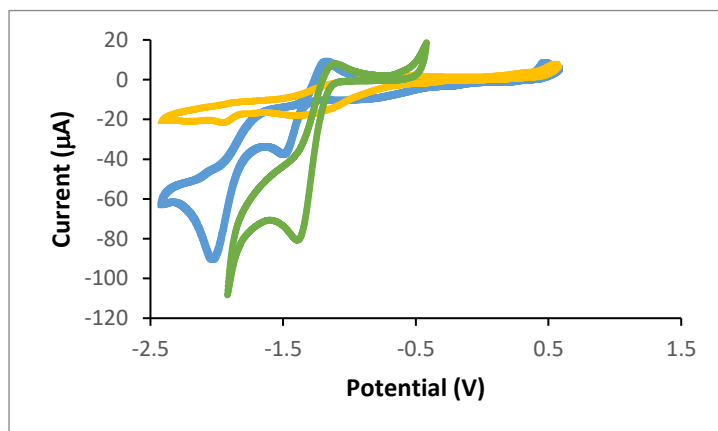


Figure 35: CV of Fe1b under nitrogen (yellow), Co1 under nitrogen (orange) and Fe1b under CO₂ atmosphere (green) in CH₃CN (0.5mM) with NBu₄PF₆ (0.1 M) at scan rate 50 mV·s⁻¹. Working electrode: 3 mm diameter glassy carbon. Counter electrode: Pt wire. Reference electrode: Ag/AgCl (3M KCl). Values referenced to Fc⁺/Fc.

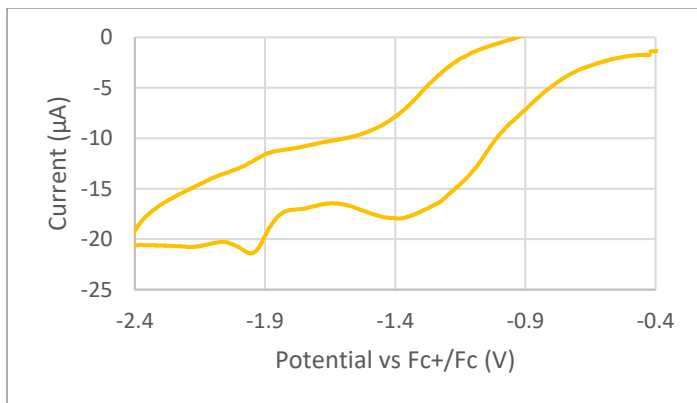
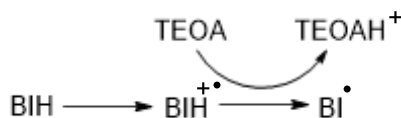


Figure 36: Extract of the cyclic voltammogram of **Fe1b** under CO₂ atmosphere in ACN (0.5mM) with NBu₄PF₆ (0.1 M) at scan rate 50 mV.s⁻¹. Working electrode: 3 mm diameter glassy carbon. Counter electrode: Pt wire. Reference electrode: Ag/AgCl (3M KCl). Values referenced to Fc⁺/Fc.

5.3.2. Proposed Mechanism of the photocatalytic CO₂ reduction

A mechanism proposal is presented herein for the photocatalytic system in which the [Ru(bpy)₃](PF₆)₂ as photosensitizer PS1, the BIH is the sacrificial electron donor, along with the Fe1b as catalyst, all together in a CO₂ saturated CH₃CN/TEOA solution in visible photons irradiation.

First of all, it's important to determine whether the excited state PS* is quenched by the catalyst (CAT) and/or by the sacrificial electron donor in order to draw the mechanistic scheme. The BIH employed as SD which has been used in various redox photosensitized reactions for organic substrates,^[307,308] and was applied to the photocatalytic reduction of CO₂.^[130] BIH has no absorption in visible region. However, it has a stronger reduction power (E) = 0.33 V vs. SCE in CH₃CN).^[280]

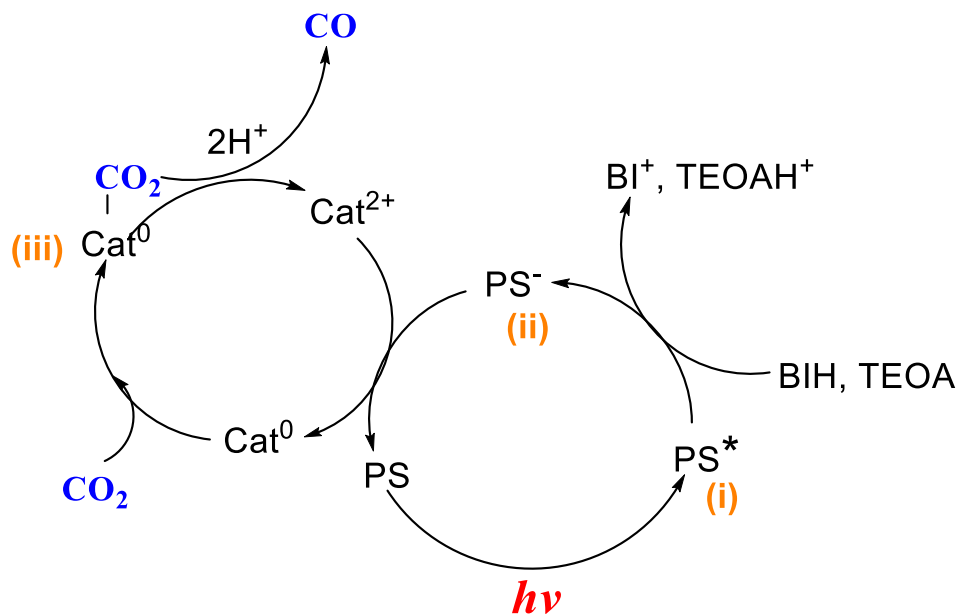


Scheme 19: BIH : electron donor oxidation

According to the previous reported literature, the PS1 is excited by the irradiation of induced light, to generate the excited state PS* (i, Scheme 20). The excited state of

PS* is reductively quenched by the powerful reductant BIH capable of getting oxidized to generating electrons. The electrons reduce the PS* to give PS⁻ and the BIH is transforming to (BIH^{•+}). The latter is rapidly deprotonated by the presence of TEOA (Scheme 20) which in this situation acts only as a base but not a sacrificial donor, capturing the proton of BIH^{•+}, to generate BI⁻ (Scheme 19) has a strong reducing power ($E_{1/2} = -1.95 \text{ V}$)^[309] sufficient to provide one more electron to reduce the catalyst and then converted to BI⁺.

The reduced PS⁻ generated from quenching of the PS* (ii, Scheme 20) is a strong reductant, The PS⁻ is then oxidized to return to its ground state and reducing the catalyst. The reduced catalyst will then be the species responsible for the reduction of CO₂. According to the cyclic voltammogram of the FeIb catalyst, the electron will be located at the ligand (Fe(I^{•-})). The latter species can then reduce CO₂ by binding to the reduced metal through carbon atom to give the CAT⁰-CO₂ adduct (iii, Scheme 20), after which additional electron and 2H⁺ are needed to break the CO₂ band and released the CO, and regenerate the catalyst, as it's illustrated in (Scheme 20). On another hand, extensive experimental and theoretical studies have indicated mechanistic processes that contribute to H₂ formation when mediated by transition metal-containing molecular catalysts. Catalytic H₂ production by molecular complexes is generally thought to proceed through metal-hydride intermediates, which are formed by reduction and protonation of a transition metal center.^[115,310,311] Alternatively, the generated H₂ may originates from the reduction of H⁺ ions produced from H₂O oxidation, through its reduction : $2\text{H}^+ + 2\text{e}^- \longrightarrow \text{H}_2$.^[312]



Scheme 20: Suggested mechanism for CO₂ photoreduction toward CO.

5.4. Conclusion

To summarize this chapter, the effects of phenanthroline and bipyridine ligand structure as well as the effect of the metal center on the photocatalytic reactivity of CO₂ were studied, using a range of metallic and organic compounds as photosensitizers, and amines as reducing quenchers. A TON of CO₂ up to 188 was achieved in a photocatalytic system with FeIb as catalyst coupled to ruthenium bipyridine (PS1) as photosensitizer, together with BIH as a sacrificial electron donor in a CH₃CN/TEOA CO₂ saturated solution under blue LEDs light irradiation ($\lambda = 467\text{nm}, 456\text{nm}$). Electrochemical studies have also been performed to better understand the reduction process of the iron complex and indices of Fe-CO₂ adducts were obtained.

Porphyrins had also been the focus of preliminary investigations as catalysts and/or as photosensitizers, but the results obtained are considerably lower compared to what has been described in the literature.

So far, the experimental studies herein, demonstrate the versatility of the synthesized complexes, which was able to prove their ability to work also in photocatalytic CO₂ reduction. However, we consider that additional investigations may be necessary in order to acquire a deeper insight into the photocatalytic system of the complexes, and to improve their catalytic activity and stability.

CHAPTER 6: General conclusions

The main objective of this doctoral thesis was the development of novel catalytic and photocatalytic metallic systems for the preparation of value-added products, having a wide application in the chemical industry, involving carbon dioxide as the main reactant.

During this work, a variety of catalytic approaches involving cost-effective metal catalysts bearing mainly N₄ donor ligands were successfully developed.

- ✓ Structural studies allow the synthesis of novel Zn N₄-donor complexes, with phenanthroline and bipyridines backbones with various substituents.
- ✓ The solid-state structures of Zn₂, Zn₅ were determined by X-ray diffraction methods showing a penta and tetra coordinated structure respectively.
- ✓ The synthesized Zn₁-Zn₅ complexes were explored in the presence of TBAB as nucleophile source for the cycloaddition of CO₂ to epoxides, and they proved to be efficient catalysts for the formation of cyclic carbonates with terminal epoxides, being the **Zn₁/TBAB** the catalytic system the most efficient achieving a conversion of 61% with an initial TOF of 207 h⁻¹ in the formation of the cyclic carbonate from epoxyhexane while working under mild conditions.
- ✓ Epoxides scope was explored using the **Zn₁/TBAB** catalytic system, the 1,2-epoxy-3-phenoxypropane showed the highest initial TOF of 228h⁻¹ in 3h reaction time.
- ✓ The **Zn₁/TBAB** system stability was studied by recycling attempts to the using the propylene oxide with a conversion of 84% in 6h during the first run. And keeping active during 3 successive runs with a slow decrease in the conversion.
- ✓ The synthesis and characterization of a variety of novel transition metal complexes including non-toxic, abundant, and cost-effective iron (II), nickel (II), and cobalt (II) metals, bearing N₄ donor tetradentate ligands, were achieved with a yield between (80-42)%. Thus, allowing to study the effect of the skeletons as well as the effect of the substituents on the catalyst activity.

- ✓ Crystals of the new metal compound **Fe1b** could not be obtained, but it was characterized by IR spectroscopy, ESI-TOF spectrometry, elemental analysis, and magnetic susceptibility, along with DFT calculations that favored its octahedral structure.
- ✓ The transition metal complexes of Fe, Co, and Ni were active for the epoxidation of a series of olefins.
- ✓ The **Fe1b** complex was active as catalyst for the epoxidation of olefins, the optimum catalytic result was obtained for the epoxidation of styrene using TBHP as the oxidation source, without the addition of any co-catalyst, resulting in a conversion of 93% and a selectivity of 49% towards styrene oxide, in a temperature of 60°C.
- ✓ The scope of olefins substrates was investigated, using **Fe1a** as catalyst and tertbutylhydroperoxide (TBHP) as oxidizing agent, with (T:60°C, 24h). Cis-stilbene and trans-stilbene gave interesting results: 50% cis-stilbene oxide yield, with 75% selectivity. On the other hand, trans-stilbene gave 39% trans-stilbene oxide, with a selectivity of 83%.
- ✓ The Fe(II), Co(II) and Ni(II) were further investigated for the cycloaddition of CO₂ to epoxides to generate selective cyclic carbonates.
- ✓ Conversions up to 84%, 53% were obtained by **Ni1/TBAB**, and **Fe1a/TBAB** respectively, with 10 bar CO₂, 60°C temperature, and 24 reaction time.
- ✓ Ni1 proved to be active at the lower pressure of 1 bar, giving a conversion of 34% in 24h and 60°C.
- ✓ Ni1 exhibits activity in the absence of the nucleophile source, reaching a conversion of 22% in 3h at 60°C.
- ✓ Preliminary study of the direct oxidative carboxylation of styrene olefins to styrene cyclic carbonates with CO₂ at atmospheric pressure using Fe(II) complexes with the chelating ligand N4 tetradentate, failed to generate the desired carbonates.
- ✓ In the last part, the screening of transition metal complexes with N4-donor ligands, was explored in different photocatalytic systems, yielding an activity following this order Fe(II)>Co(II)>Ni(II) .

- ✓ A photocatalytic system without BIH, probing the efficiency of TEOA as a sacrificial donor coupled with **Fe1b** as a catalyst and PS1 as a photosensitizer, yielded a modest TON of CO up to 19 and a TON of H₂ up to 70.
- ✓ The **Fe1b** catalyst coupled to PS1, BIH in TEOA/CH₃CN medium exhibited good TON and selectivity, up to 188 and 75% selectivity towards CO respectively. Herein, the advantageous role of the integration of BIH in the photocatalytic system has been proven.
- ✓ Further photocatalytic studies by trying different photosensitizers, including free metal compounds and sacrificial donors were carried out but no products were detected.
- ✓ Initial electrochemical studies for a deeper understanding of the photocatalytic CO₂ process, and to be able to propose a suitable reaction mechanism were performed.

- ✓ The initial tests with Zn and Fe porphyrins have been carried out for the photocatalytic reduction of CO₂ under irradiation with visible light, but the activities were low, and the major product formed was HCOO⁻/HCOOH.

- ✓ Regrettably, the attempt to recycle the CO/H₂ generated by photocatalysis for olefin hydroformylation was not successful, neither with subsequent system, nor in a one-pot system as explained in the experimental section.

Altogether this may prove the polyvalency of such N₄ tetradentate metal compounds synthesized and their efficiency for various catalytic pathways.

CHAPTER 7: Bibliography list

Bibliography list

- [1] H. Balat, C. Öz., *Energy Explor. Exploit.*, 2007, 25, 357–392.
- [2] M. Mikkelsen, M. Jørgensen, F. C. Krebs., *Energy Environ. Sci.*, 2010, 3, 43–81.
- [3] J. Yu, L. X. Chen., *Environ. Sci. Technol.*, 2008, 42, 6961–6966.
- [4] Mauna Loa Observatory, “CO₂.earth. (NOAA) Preliminary data released March 5,” 2023.
- [5] J. Rogelj, M. Elzen, N. Höhne, T. Fransen, H. Fekete., *Nature.*, 2016, 534, 631–639.
- [6] J. Cheon, J.Y. Yang, M. Koper, O. Ishitani., *Acc. Chem. Res.*, 2022, 55, 931–932.
- [7] F. M. Baena-moreno, M. Rodríguez-Galán, F. Vega, B. Alonso-Fariñas, L. F. Vilches Arenas, B. Navarrete., *Energ. Source Part A.*, 2019, 41, 1403–1433.
- [8] G. Fiorani, W. Guoa, A. W. Kleij., *Green Chem.*, 2015, 17, 1375–1389.
- [9] P. Bhanja, A. Modak, A. Bhaumik., *Chem. Eur. J.*, 2018, 29, 7278–7297.
- [10] M. Chihiro, M. Yuki, E. Tadashi., *Catal. Sci. Technol.*, 2014, 4, 1482–1497.
- [11] A. Rafiee, K. R. Khalilpour, D. Milani, M. Panahi., *J. Environ. Chem. Eng.*, 2018, 6, 5771–5794.
- [12] Q-W. Song, Z-H. Zhou, L-N. He., *Green Chem.*, 2017, 19, 3707–3728.
- [13] A. J. Kamphuis, F. Picchioni, P. P. Pescarmona., *Green Chem.*, 2019, 21, 406–448.
- [14] S. Samanta, R. Srivastava., *Mater. Adv.*, 2020, 1, 1506–1545.
- [15] C. Hepburn, E. Adlen, J. Beddington, E. A. Carter, S. Fuss, et al. *Nature.*, 2019, 575, 87–97.
- [16] B. Rego de Vasconcelos, J-M. Lavoie., *Front. Chem.*, 2019, 7, 392.

- [17] R-P Ye, J. Ding, W. Gong, M. D. Argyle, Q. Zhong, et al. *Nat. Commun.*, 2019, 10, 5698.
- [18] G. Centi, E. A. Quadrelli, S. Perathoner., *Energy Environ. Sci.*, 2013, 6, 1711–1731.
- [19] K. Malik, S. Singh, S. Basu, A. Verma., *Wiley Interdiscip, WIREs Energy Environ.*, 2017, 6, e244.
- [20] J. Wu, Y. Huang, W. Ye, Y. Li., *Advanced Science.*, 2017, 4, 1700194.
- [21] Y. Zheng, W. Zhang, Y. Li, J. Chen, B. Yu, et al. *Nano Energy.*, 2017, 40, 512–539.
- [22] J. Kothandaraman, A. Goepfert, M. Czaun, G. A. Olah, G. K. Surya Prakash., *J. Am. Chem. Soc.*, 2016, 138, 778–781.
- [23] Z. Liu, Z. Deng, S. J. Davis, C. Giron, P. Ciais., *Nat. Rev. Earth Environ.*, 2022, 3, 217–219.
- [24] A. D. N. Kamkeng, M. Wang, J. Hu, W. Du, F. Qian., *Chem. Eng. J.*, 2021, 409, 128138.
- [25] M. North, R. Pasquale, C. Young., *Green Chem.*, 2010, 12, 1514–1539.
- [26] N. MacDowell, N. Florin, A. Buchard, J. Hallett, A. Galindo, G. Jackson, et al. *Energy Environ. Sci.*, 2010, 3, 1645–1669.
- [27] M. Aresta, CHEMRAWN-XVII and ICCDU-IX, Kingston, Canada, Buncel, E., Ed. Kingston 2007, 123–149.
- [28] Laia Cuesta Aluja, Doctoral thesis, Rovira i Virgili University, 2015.
- [29] T. Sakakura, K. Kohno., *Chem. Commun.*, 2009, 11, 1312–1330.
- [30] R. Zevenhoven, S. Eloneva, S. Teir., *Catal. Today.*, 2006, 115, 73–79.
- [31] M. Aresta, A. Dibenedetto., *Energy and Fuels.*, 2001, 15, 269–273.
- [32] M. Aresta, A. Dibenedetto, A. Angelini., *J. CO₂ Util.*, 2013, 3–4, 65–73.
- [33] H. Arakawa, M. Aresta, J. N. Armor, M. A. Barteau, E. J. Beckman, et al. *Chem. Rev.*, 2001, 101, 953–960.
- [34] X. Xiaoding, J. A. Moulijn., *Energy & Fuels*, 1996, 10, 305–325.

- [35] M. Aresta, E. Quaranta., *Chem. Tech.*, 1997, 27, 32–40.
- [36] M. Aresta, *Carbon Dioxide as Chemical Feedstock*, Wiley-VCH Verlag GmbH & Co. KGaA, 2010.
- [37] J. Wang, C-S. Jia, C-J. Li, X-L. Peng, L-H. Zhang., *ACS Omega.*, 2019, 4, 19193–19198.
- [38] T. Sakakura, J-C. Choi, H. Yasuda., *Chem. Rev.*, 2007, 107, 2365–2387.
- [39] H-J Buysch, *Carbonic Esters*. In *Ullmann’s Encyclopedia of Industrial Chemistry*, Wiley-VCH Verlag GmbH & Co. KGaA, Weinheim, Germany, 2000, 45–71.
- [40] A-A. G. shaikh., *Chem. Rev.*, 1996, 96, 951–976.
- [41] W. Natongchai, J. A. Luque-Urrutia, C. Phungpanya, M. Solà, V. D’Elia., *Org. Chem. Front.*, 2021, 8, 613–627.
- [42] A. Monfared, R. Mohammadi, A. Hosseinian, S. Sarhandia, P. D. Kheirollahi Nezhad., *RSC Adv.*, 2019, 9, 3884–3899.
- [43] S. Fukuoka, M. Kawamura, K. Komiya, M. Tojo, H. Hachiya., *Green Chem.*, 2003, 5, 497–507.
- [44] T. Ogasawara, A. Débart, M. Holzapfel, P. Novák, P. G. Bruce., *J. Am. Chem. Soc.*, 2006, 128, 1390–1393.
- [45] A. S. Hawkins, P. M. McTernan, H. Lian, R. M. Kelly, M. W. Adams., *Curr. Opin. Biotechnol.*, 2013, 24, 376–384.
- [46] J. Sun, L. Han, W. Cheng, J. Wang, X. Zhang, S. Zhang., *ChemSusChem.*, 2011, 4, 502–507.
- [47] M. Liu, L. Liang, X. Li, X. Gao, J. Sun. *Green Chem.*, 2016, 18, 2851–2863.
- [48] R. R. Kuruppathparambil, R. Babu, H. M. Jeong, G-Y. Hwang, G. S. Jeong, et al. *Green Chem.*, 2016, 18, 6349–6356.
- [49] M. North, R. Pasquale., *Angew. Chem. Int. Ed.*, 2009, 48, 2946–2948.
- [50] Y. Du, F. Cai, D-L, Konga, L-N. He., *Green Chem.*, 2005, 7, 518–523.
- [51] V. Caló, V. A. Nacci, A. Monopoli, A. Fanizzi., *Org. Lett.*, 2002, 4, 2561–2563.

- [52] M. Cokoja, M. E. Wilhelm, M. H. Anthofer, W. A. Herrmann, F. E. Kühn., *ChemSusChem*, 2015, 8, 2436-2454.
- [53] J. Sun, S-I Fujita, M. Arai., *J. Organomet. Chem.*, 2005, 690, 3490–3497.
- [54] Q. He, J. W. O'Brien, K. A. Kitselman, L. E. Tompkins, G. C. T. Curtisa, F. M. Kerton., *Catal. Sci. Technol.*, 2014, 4, 1513-1528.
- [55] L. Martínez-Rodríguez, J. O. Garmilla, A. W. Kleij., *ChemSusChem*, 2016, 9, 749–755.
- [56] S. Sopeña, C. Martín, A. W. Kleij., *ChemSusChem*, 2015, 8, 3248-3254.
- [57] P. P. Pescarmona, M. Taherimehr., *Catal. Sci. Technol.*, 2012, 2, 2169-2187.
- [58] K. Yamaguchi, K. Ebitani, T. Yoshida, H. Yoshida, K. Kaneda., *J. Am. Chem. Soc.*, 1999, 121, 4526-4527.
- [59] L. Cuesta-Aluja, J. Castilla, A. M. Masdeu-Bultó., *Dalton Trans.*, 2016, 45, 14658–14667.
- [60] S. Iksi, A. Aghmiz, R. Rivas, M. D. González, L. Cuesta-Aluja, et al. *J. Mol. Catal. A : Chem.*, 2014, 383-384, 143–152.
- [61] X. Li, A. K. Cheetham, J. Jiang., *Mol. Catal.*, 2019, 463, 37–44.
- [62] M. Y. Wani, A. Kumar, C. T. Arranja, C. M. F. Días, A. J. F. N. Sobral., *New J. Chem.*, 2016, 40, 4974–4980.
- [63] Y. Ren, Y. Shi, J. Chen, S. Yang, C. Qi, H. Jiang., *RSC Adv.*, 2013, 3, 2167–2170.
- [64] F. Nasirov, E. Nasirli, M. Ibrahimova., *J. Iran. Chem. Soc.*, 2022, 19, 353–379.
- [65] L. Cuesta-Aluja, A.M. Masdeu-Bultó., *ChemistrySelect*, 2016, 1, 2065–2070.
- [66] J. Zhou, W. Yan, Z. Gan, C. Shu, Z. Zheng., *ACS Appl. Energy Mater.*, 2023, 6, 2954–2961.
- [67] M. D. Burkart, N. Hazari, C. L. Tway, E. L. Zeitler. *ACS Catal.*, 2019, 9, 7937–7956.

- [68] F. Zhou, Q. Deng, N. Huang, W. Zhou, W. Deng., *ChemistrySelect*, 2020, 5, 10516–10520.
- [69] A. Decortes, A. W. Kleij., *ChemCatChem.*, 2011, 3, 831–834.
- [70] H. Vignesh Babu, K. Muralidharan., *Dalton Trans.*, 2013, 42, 1238–1248.
- [71] R. Ma, L-N. He, Y-B. Zhou., *Green Chem.*, 2016, 18, 226–231.
- [72] M.S. Salga, H. Mohd Ali, M. A. Abdulla, S. I Abdelwahab., *Int. J. Mol. Sci.*, 2012, 13, 1393–1404.
- [73] M. Adolph, T. A. Zevaco, C. Altesleben, S. Staudt, E. Dinjus., *J. Mol. Catal. A : Chem.*, 2015, 400, 104–110.
- [74] E. Mercadé, E. Zangrando, C. Claver, C. Godard., *ChemCatChem*, 2016, 8, 234–243.
- [75] A. Decortes, M. M. Belmonte, J. Benet-Buchholza, A. W. Klei., *Chem. Commun.*, 2010, 46, 4580–4582.
- [76] M. A. Fuchs, S. Staudt, C. Altesleben, O. Walter, T. A. Zevaco, E. Dinjus., *Dalton Trans.*, 2014, 43, 2344–2347.
- [77] L. M. Plum, L. Rinkand, H. Haase., *Int. J. Environ. Res. Public Health*, 2010, 7, 1342–1365.
- [78] D. J. Darensbourg, M. W. Holtcamp., *Coord. Chem. Rev.*, 1996, 153, 155–174.
- [79] D.J. Darensbourg, S. A. Niezgoda, J. D. Draper, J. H. Reibenspies., *J. Am. Chem. Soc.*, 1998, 120, 4690-4698.
- [80] A. Angeloff, J. Daran, J. Bernadou, B. Meunier., *Eur. J. Inorg. Chem.*, 2000, 1985–1996.
- [81] L.F. Hernández-Ayala, M. Flores-Álamo, S. Escalante-Tovar, R. Galindo-Murillo, J. C. García-Ramos, et al. *Inorg. Chim. Acta*, 2018, 470, 187–196.
- [82] S. Wang, Z. Ding, X. Wang., *Chem. Commun.*, 2015, 51, 1517–1519.
- [83] A. Decortes, A. M Castilla, A. W Kleij., *Angew. Chem. Int. Ed.*, 2010, 49, 9822–9837.

- [84] M. Alonso de La Peña, L. Merzoud, W. Lamine, A. Tuel, H. Chermette., et al. *J. CO₂ Util.* 2021, 44, 101380.
- [85] Z. Wang, Z. Bu, T. Cao, T. Ren, L. Yang, et al. *Polyhedron*, 2012, 32, 86–89.
- [86] D. Ji, X. Lu, R. Hei., *Appl. Catal. A : Gen.*, 2000, 203, 329–333.
- [87] L. Jin, H. Jing, T. Chang, X. Bu, L. Wang., et al. *J. Mol. Catal A: Chem.*, 2007, 261, 262–266.
- [88] A. Buchard, M. R. Kember, K. G. Sandeman, C. K. Williams., *Chem. Commun.*, 2011, 47, 212–214.
- [89] J. E. Dengler, M. W. Lehenmeier, S. Klaus, C. E. Anderson, E. Herdtweck, et al. *Eur. J. Inorg. Chem.*, 2011, 336–343.
- [90] X. Sheng, L. Qiaoa, Y. Qina, X. Wanga, F. Wang., *Polyhedron*, 2014, 74, 129–133.
- [91] M. A. Fuchs, T. A. Zevaco, E. Ember, O. Walter, I. Held, et al. *Dalton Trans.*, 2013, 42, 5322–5329.
- [92] J. Honores, D. Quezada, G. Chacón, O. Martínez-Ferraté, M. Isaacs., *Catal. Lett.*, 2019, 149, 1825–1832.
- [93] A. L. Girard, N. Simon, M. Zanatta, S. Marmitt, P. Gonçalves, et al. *Green Chem.*, 2014, 16, 2815–2825.
- [94] J. P. Hallett, T. Welton., *Chem. Rev.*, 2011, 111, 3508–3576.
- [95] M. Alves, B. Grignard, R. Mereau, C. Jerome, T. Tassaing, e al. *Catal. Sci. Technol.*, 2017, 7, 2651–2684.
- [96] G. W. Coates, D. R. Moore., *Angew. Chem. Int. Ed.*, 2004, 43, 6618–6639.
- [97] R. Dalpozzo, N. Della, B. Gabriele, R. Mancuso., *Catalysts*, 2019, 9, 511.
- [98] R. R. Shaikh, S. Pornpraprom, V. D'Elia., *ACS Catal.*, 2018, 8, 419–450.
- [99] C. Martín, G. Fiorani, A. W. Kleij., *ACS Catal.*, 2015, 5, 1353–1370.
- [100] D. Bai, H. Jing., *Green Chem.*, 2010, 12, 39–41.
- [101] Y-Y. Wu, X-G. Meng, W-W. Yu, H. Huang, L-Y. Chen, et al. *ChemSelect.*, 2021, 6, 6132–6136.

- [102] A. F. Tai, L. D. Margerum, J. S. Valentine., *J. Am. Chem. Soc.*, 1986, 108, 5006–5008.
- [103] D. D. Agarwal, R. P. Bhatnagar, R. Jain, S. Srivastava., *J. Chem. Soc., Perkin Trans.*, 1990, 2, 989–992.
- [104] Y. Zhu, Q. Wang, R. G. Cornwall, Y. Shi., *Chem. Rev.*, 2014, 114, 8199–8256.
- [105] P. Le Maux, H. F. Srour, G. Simonneaux., *Tetrahedron*, 2012, 68, 5824–5828.
- [106] C. Wang, H. Yamamoto., *Chem. Asian J.*, 2015, 10, 2056–2068.
- [107] M. Mitra, O. Cusso, S. S. Bhat, M. Sun, M. Cianfanelli, et al. *Dalton Trans.*, 2019, 48, 6123–6131.
- [108] B. Wang, S. Wang, C. Xia, W. Sun., *Chem. Eur. J.*, 2012, 18, 7332–7335.
- [109] M. S. Batra, R. Dwivedi, R. Prasad., *ChemistrySelect*, 2019, 4, 11636–11673.
- [110] J. Tan, T. Zheng, Y. Yu, K. Xu., *RSC Adv.*, 2017, 7, 15176–15180.
- [111] Y. Kon., *J. Jpn. Petrol. Inst.*, 2017, 60, 159–169.
- [112] G. Grigoropoulou, . H. Clark, J. A. Elings., *Green Chem.*, 2003, 5, 1–7.
- [113] M. Aresta, A. Dibenedetto, I. Tommasi., *Appl. Organomet. Chem.*, 2000, 14, 799–802.
- [114] B. Kumar, M. Llorente, J. Froehlich, T. Dang, A. Sathrum, et al. *Annu. Rev. Phys. Chem.*, 2012, 63, 541–569.
- [115] S. Berardi, S. Drouet, L. Franca`s, C. Gimbert-Surin`ach, M. Guttentag, et al. *Chem. Soc. Rev.*, 2014, 43, 7501–7519.
- [116] Y. Sakuragi, D. A. Bryant., *Photosystem I*, 2006, 24, 205–222.
- [117] R. J. Cogdell, T. HP. Brotsudarmo, A. T. Gardinera, P. M Sanchez, L. Cronin. *Biofuels*, 2010, 1, 861–876.
- [118] G. Sahara, O. Ishitani., *Inorg. Chem.* 2015, 54, 5096–5104.
- [119] S. Zhang, X. Yin, Y. Zheng., *Chem. Phys. Lett.*, 2018, 693, 170–175.
- [120] X. Cheng, R. Chena, X. Zhua, Q. Liao, L. An, et al. *Energy*, 2017, 120, 276–282.

- [121] Q. H. Zhang, W-D. Han, Y-J. Hong, J-G. Yu., *Catal. Today*, 2009, 148, 335–340.
- [122] M. Ming, L. Kai, S. Jie, K. Recep, S. Wilson A., *ACS Energy Lett.*, 2018, 3, 1301–1306.
- [123] E. E. Benson, C. P. Kubiak, A. J. Sathrum, J. M. Smieja., *Chem. Soc. Rev.*, 2009, 38, 89–99.
- [124] M. Aresta, A. Dibenedetto, A. Angelin., *Chem. Rev.*, 2014, 114, 1709–1742.
- [125] M. E. Dry. *Catal. Today.*, 2002, 71, 227–241.
- [126] M. Schwartz, M. E. Vercauteren, A. F. Sammells., *J. Electrochem. Soc.*, 1994, 141, 3119.
- [127] X. Chen, R-T. Guo, L-F. Hong, Y. Yuan, W-G. Pan., *Energy and Fuels*, 2021, 35, 19920–19942.
- [128] X. Yang, D. Wang., *ACS Appl. Energy Mater.*, 2018, 1, 6657–6693.
- [129] Y. Chen, C. Xu, B. Xu, Z. Mao, J-An. Li, et al. *Mater. Chem. Front.*, 2019, 3, 1800–1806.
- [130] Y. Tamaki, K. Koikeb, T. Morimoto, O. Ishitani., *Catal.*, 2013, 304, 22–28.
- [131] Y. Pellegrin, F. Odobel., *C. R. Chim.*, 2017, 20, 283–295.
- [132] H. Hori, F-P. A. Johnson, K. Koike, K. Takeuchi, T. Ibusuki., *J. Chem. Soc., Dalton trans.*, 1997, 1019–1024.
- [133] T. C. Pham, V-N. Nguyen, Y. Choi, S. Lee, J. Yoon., *Chem. Rev.*, 2021, 121, 13454–13619.
- [134] Y. Tamaki, T. Morimoto, K. Koike, O. Ishitani., *Proc. Natl. Acad. Sci. U. S. A.*, 2012, 109, 15673–15678.
- [135] Y. Kuramochi, J. Itabashi, K. Fukaya, A. Enomoto, M. Yoshida, et al. *Chem. Sci.*, 2015, 6, 3063–3074.
- [136] J. Hawecker, J-M. Lehn, R. Ziessel., *Helv. Chim. Acta*, 1986, 69, 1990–2012.
- [137] J. M. Lehn, R. Ziessel., *J. Organomet. Chem.*, 1990, 382, 157–173.
- [138] K. Mochizuki, S. Manaka, I. Takeda, T. Kondo., *Inorg. Chem.*, 1996, 35, 5132–5136.

- [139] A. H. A. Tinnemans, T. P. M. Koster, D. H. M. W. Thewissen, A. Mackor., *Recl. Trav. Chim. Pays-Bas*, 1984, 103, 288–295.
- [140] J. L. Grant, K. Goswami, L. O. Spreer, J. W. Otvos, M. Calvin., *J. Chem. Soc., Dalton Trans.*, 1987, 2105–2109.
- [141] A. Rosas-Hernández, C. Steinlechner, H. Junge, M. Beller., *Green Chem.*, 2017, 19, 2356–2360.
- [142] H. Yuan, B. Cheng, J. Lei, L. Jiang, Z. Han., *Nat. Commun.*, 2021, 12, 1835-
- [143] K. Kiyosawa, N. Shiraishi, T. Shimada, D. Masui, H. Tachibana, S. Takagi, O. Ishitani, D. A. Tryk, H. Inoue, *J. Phys. Chem. C*, 2009, 113, 11667–11673.
- [144] S. D. Choudhury, S. Muralidharan, H. Pal, *Phys. Chem. Chem. Phys.*, 2014, 16, 11509–11518.
- [145] S. Yanagida, T. Ogata, Y. Kuwana, Y. Wada, K. Murakoshi, A. Ishidat, S. Takamuku, M. Kusaba, N. Nakashima, *J. Chem. Soc., Perkin Trans.*, 1996, 2, 1963–1969.
- [146] E. Fujita, B. S. Brunshwig, T. Ogata, S. Yanagida, *Coord. Chem. Rev.*, 1994, 132, 195–200.
- [147] C. D. Windle, M. V. Câmpian, A-K. Duhme-Klair, E. A. Gibson, R. N. Perutz, J. Schneider, *Chem. Commun.*, 2012, 48, 8189–8191.
- [148] T. Dhanasekaran, J. Grodkowski, P. Neta, P. Hambright, E. Fujita, *J. Phys. Chem. A*, 1999, 103, 7742–7748.
- [149] H. Cui, J. Brooks, D. Graf, Y. Okano, H. Sun, H. Kobayashi, *Inorg. Chem.*, 2009, 48, 4268–4270.
- [150] Y. L. Chow, W. C. Danen, S. F. Nelson, D. H. Rosenblatt, *Chem. Rev.*, 1978, 78, 243–274.
- [151] E. D. Cline, S. E. Adamson, S. Bernhard, *Inorg. Chem.*, 2008, 47, 10378–10388.
- [152] J. Hawecker, J. M. Lehn, R. Ziessel, *J. Chem. Soc., Chem. Commun.*, 1983, 536–538.
- [153] V. S. Thoi, N. Kornienko, C. G. Margarit, P. Yang, C. J. Chang, *J. Am. Chem. Soc.*, 2013, 135, 14413–14424.

- [154] J. Kiwi, M. Grätzel., *Nature*, 1979, 281, 657–658.
- [155] M. S. Lowry, J. I. Goldsmith, J. D. Slinker, R. A. Pascal Jr, G. G. Malliaras, S. Bernhard, *Chem. Mater.*, 2005, 17, 5712–5719.
- [156] M. G. Pfeffer, B. Schfer, G. Smolentsev, J. Uhlig, E. Nazarenko, J. Guthmuller, C. Kuhnt, M. Wächtler, B. Dietzek, V. Sundström, S. Rau, *Angew. Chem. Int. Ed.*, 2015, 54, 5044–5048.
- [157] P. Kumar, S. Kumar, S. Cordier, S. Paofai, R. Boukherroub, S. L. Jain, *RSC Adv.*, 2014, 4, 10420–10423.
- [158] T. W. Ebbesen, G. Levey, L. K. Patterson, *Nature*, 1982, 298, 545–548.
- [159] P. Du, J. Schneider, F. Li, W. Zhao, U. Patel, F. N. Castellano, R. Eisenberg, *J. Am. Chem. Soc.*, 2008, 130, 5056–5058.
- [160] L. L. Tinker, S. Bernhard, *Inorg. Chem.*, 2009, 48, 10507–10511.
- [161] P. N. Curtin, L. L. Tinker, C. M. Burgess, E. D. Cline, S. Bernhard, *Inorg. Chem.*, 2009, 48, 10498–10506.
- [162] Y. J. Yuan, J. Y. Zhang, Z. T. Yu, J. Y. Feng, W. J. Luo, J. H. Ye, Z. G. Zou, *Inorg. Chem.*, 2012, 51, 4123–4133.
- [163] S. S. Jayanthi, P. Ramamurthy, *Phys. Chem. Chem. Phys.*, 1999, 1, 4751–4757.
- [164] M. Haga, E. S. Dodsworth, G. Eryavec, P. Seymour, A. B. P. Lever, *Inorg. Chem.*, 1985, 24, 1901–1906.
- [165] H. B. Kim, N. Kitamura, Y. Kawanishi, S. Tazuke., *J. Phys. Chem. C* 1989, 93, 5757–5764.
- [166] C. V. Krishnan, N. Sutin., *J. Am. Chem. Soc.* 1981, 103, 2141–2142.
- [167] M.M. Taqui Khan, R.S. Shukla., *Inorganica Chim. Acta* 1988, 149, 89–94.
- [168] C. Hidenori, H. Ide, K. Itoh., *J. Org. Chem.* 1986, 51, 5400–5405.
- [169] X. Q. Zhu, M-T. Zhang, A. Yu, C-H. Wang, J-P. Cheng., *J. Am. Chem. Soc.* 2008, 130, 2501–2516.
- [170] Z. Guo, F. Yu, Y. Yang, C-F. Leung, S-M. Ng, C-C. Ko, C. Cometto, T-C. Lau, M. Robert., *ChemSusChem* 2017, 10, 4009–4013.

- [171] E. Boutin, L. Merakeb, B. Ma, B. Boudy, M. Wang, J. Bonin, E. Anxolabéhère-Mallart, M. Robert., *Chem. Soc. Rev.* 2020, 49, 5772–5809.
- [172] S. T. Bai, G. De Smet, Y. Liao, R. Sun, C. Zhou, M. Beller, B. U. W. Maes, B. F. Sels., *Chem. Soc. Rev.* 2021, 50, 4259–4298.
- [173] F. Jameel, M. Stein, *J Catal* 2022, 405, 24–34.
- [174] Z. Han, W. R. McNamara, M-S. Eum, P. L. Holland, R. Eisenberg., *Angew. Chem. Int. Ed.* 2012, 51, 1667–1670.
- [175] T. Lazarides, T. McCormick, P. Du, G. Luo, B. Lindley, R. Eisenberg., *J. Am. Chem. Soc.* 2009, 131, 9192–9194.
- [176] K. Iwai, M. Uesugi, F. Takemura., *Polymer* 1985, 17, 1005–1011.
- [177] A. M. Masdeu-Bultó, M. Reguero, C. Claver., *Eur. J. Inorg. Chem.* 2022, 14, e202100975.
- [178] K. E. Dalle, J. Warnan, J. J. Leung, B. Reuillard, I. S Karmel , E. Reisner., *Chem. Rev.* 2019, 119, 2752–2875.
- [179] H. Kumagai, Y. Tamaki, O. Ishitani., *Acc Chem Res* 2022, 55, 978–990.
- [180] J. Qiao, Y. Liu, F. Hong, J. Zhang., *Chem Soc Rev* 2014, 43, 631–675.
- [181] J. Bonin, M. Robert, M. Routier., *J Am Chem Soc* 2014, 136, 16768–16771.
- [182] T. Morimoto, T. Nakajima, S. Sawa, R. Nakanishi, D. Imori, O. Ishitani., *J Am Chem Soc* 2013, 135, 16825–16828.
- [183] J. Agarwal, B. C. Sanders, E. Fujita, H. F. Schaefer III, T. C. Harrop, J. T. Muckerman., *Chem Comm* 2012, 48, 6797–6799.
- [184] A. Nakada, K. Koike, K. Maedaa, O. Ishitani., *Green Chemistry* 2015, 18, 139–143.
- [185] A. Rosas-Hernández, P. G. Alsabeh, E. Barsch, H. Junge, R. Ludwig, M. Beller., *Chem. Comm.* 2016, 52, 8393–8396.
- [186] M. Bourrez, F. Molton, S. Chardon-Noblat, A. Deronzier., *Angew. Chem. Int. Ed.* 2011, 50, 9903–9906.
- [187] M. S. Jeletic, M. T. Mock, A. M. Appel, J. C. Linehan., *J. Am. Chem. Soc.* 2013, 135, 11533–11536.

- [188] J. D. Froehlich, C. P. Kubiak., *Inorg Chem* 2012, 51, 3932–3934.
- [189] J. Bonin, M. Chaussemier, M. Robert, M. Routier., *ChemCatChem* 2014, 6, 3200–3207.
- [190] Guo Z, S. Cheng, C. Cometto, E. Anxolabéhère-Mallart, S-M. Ng, C-C. Ko, G. Liu, L. Chen, M. Robert, T-C. Lau., *J Am Chem Soc* 2016, 138, 9413–9416.
- [191] H. Takeda, K. Ohashi, A. Sekine, O. Ishitani., *J Am Chem Soc* 2016, 138, 4354–4357.
- [192] G. G. Stanley., *Kirk-Othmer Encyclopedia of Chemical Technology* 2017, 1, 1–19.
- [193] X. Chen, K. Ding, L. Jun., *Dyes and Pigments* 2015, 123, 404–412.
- [194] G. M. Rodriguez, S. Atsumi., *Metab Eng* 2014, 25, 227-237.
- [195] Z. Zhang, S-Y. Panb, H. Lic, J. Caid, A. G. Olabi, E. J. Anthony, V. Manovic., *Renewable and Sustainable Energy Rev* 2020, 125, 109799.
- [196] S. Dabral, T. Schaub., *Adv Synth Catal* 2019, 361, 223–246.
- [197] A. Rehman, F. Saleem, F. Jave, A. Ikhlaq, S. W. Ahmad, A. Harvey., *J. Environ. Chem. Eng.* 2021, 9, 2213-3437.
- [198] Tapan K. Pal, D. Deb, P. K. Bharadwaj., *Coord Chem Rev* 2020, 408, 213173.
- [199] A. Centeno-Pedraza, J. Perez-Arce, Z. Freixa, P. Ortiz, E. J. Garcia-Suarez., *Ind Eng Chem Res* 2022, 62, 3428-3443.
- [200] S. Manoja, S. K. Mishra, A. Saidi, J-M. Basset., *J Organomet Chem* 2021, 945, 121864.
- [201] P. Rollin, L. K. Soares, A. M. Barcellos, D. R. Araujo, E. J. Lenardão, R.G. Jacob, G. Perin., *Appl. Sci.* 2021, 11, 5024.
- [202] P. P. Pescarmona, *CurrOpin Green Sustain Chem* 2021, 29, 100457.
- [203] J. Gascon., *Chem* 2019, 5, 3015–3016.
- [204] A. Brege, B. Grignard, R. Méreau, C. Detrembleur, C. Jerome, T. Tassaing., *Catalysts* 2022, 12, 124.
- [205] A. Rehman, V. C. Eze, M.F.M. Gunam Resul, A. Harvey., *Green Process. Synth.* 2019, 8, 719–729.

- [206] C. J. Whiteoak, A. Nova, F. Maseras, A. W. Kleij, *ChemSusChem* 2012, 5, 2032-2038.
- [207] J. Song, H. Fan, J. Ma, B. Han, *Green Chem* 2013, 15, 2619-2635.
- [208] K. R. Roshan, T. Jose, D. Kim, K. A. Cherian, D. W. Park., *Catal Sci Technol* 2014, 4, 963-970.
- [209] K. Naveen, H. Ji, T. S. Kim, D. Kim, D-H Cho, *Appl Catal B* 2021, 280, 1193-1195.
- [210] M. Cavalleri, N. Panza, A. di Biase, G. Tseberlidis, S. Rizzato, G. Abbiati, A. Caselli., *European J Org Chem* 2021, 2021, 2764-2771.
- [211] R. Arevalo, R. López, L. R. Falvello, L. Riera, J. Perez. *Chem. Eur. J.* 2021, 27, 379-389.
- [212] M. B. Yeamin, Doctoral thesis, Rovira i Virgili, 2021.
- [213] C. L. Redondo, Doctoral thesis, Rovira i Virgili, 2015.
- [214] F. W. Lewis, L. M. Harwood, M. J. Hudson, M. B. Drew, J. F. Desreux, G. Vidick, N. Bouslimani, G. Modolo, A. Wilden, M. Sypula, T-H Vu, J-P. Simonin., *J Am Chem Soc* 2011, 133, 13093-13102.
- [215] L. Wang, W-H, Suna, L. Hana, H. Yanga, Y. Hua, X. Jin., *J Organomet Chem* 2002, 658, 62-70.
- [216] V. Subramaniam, H. A. Goodwin., *J Agric Food Chem* 1988, 36, 1326-1329.
- [217] G. R. Newkome, H. W. Lee., *J Am Chem Soc* 1983, 311, 5956-5957.
- [218] S. Gouthaman, S. Periyaraja, P. Shanmugam., *Tetrahedron Lett* 2015, 56, 5920-5923.
- [219] P. D. Beer, J. P. Danks., *J. Org. Chem.* 1994, 476, 63-72.
- [220] G. A. Griffith, M. J. Al-Khatib, K. Patel, K. Singh, G. A. Solan., *Dalton Trans.* 2009, 2, 185-196.
- [221] S. Zai, H. Gao, Z. Huang, H. Hu, H. Wu, Q. Wu., *ACS Catal* 2012, 2, 433-440.
- [222] A. S. A. Technologies, Rigaku Oxford Difraccion. Agilent Tecnologies 2018, 1.171.40.35a.

- [223] M. C. Burla, R. Caliandro, B. Carrozzini, G. L. Cascarano, C. Cuocci, C. Giacobazzo, M. Mallamo, A. Mazzone, G. Polidori., *J Appl Crystallogr* 2015, 48, 306–309.
- [224] G. M. Sheldrick., *Acta Crystallogr. C Struct. Chem.* 2015, 71, 3–8.
- [225] C. B. Hübschle, G. M. Sheldrick, B. Dittrich, *J Appl Crystallogr* 2011, 44, 1281–1284.
- [226] H. H. Perkampus, W. Rother, *Spectrochim Acta A* 1974, 30, 597–610.
- [227] A. Begum, O. Seewald, I. Florke, G. Henke., *Chem Select* 2016, 1, 2257-2264.
- [228] A. B. Charette, R. Chinchilla, C. Nájera, Tetrabutylammonium Bromide. In *Encyclopedia of Reagents for Organic Synthesis*, (Ed.) 2007.
- [229] B. C. Ranu, S. S. Dey, A. Hajra., *Tetrahedron* 2003, 59, 2417–2421.
- [230] V. Calò, A. Nacci, A. Monopoli, A. Fornaro, L. Sabbatini, N. Cioffi, N. Ditaranto., *Organometallics* 2004, 23, 5154–5158.
- [231] V. Calò, A. Nacci, L. Lopez, V. L. Lerario., *Tetrahedron Lett* 2000, 41.8977-8980.
- [232] B. J. Orlińska, J. M. Zawadiak., *Cent. Eur. J. Chem.* 2010, 8, 285–290.
- [233] F. Wang, X. Li, Z. Li, S. Zhou, W. Zhang., *ACS Omega* 2019, 4, 331–343.
- [234] P. Fontaine, A. Chiaroni, G. Masson, J. Zhu., *Org Lett* 2008, 10, 1509–1512.
- [235] D. Fang, J-Q. Liu, X-S. Wang., *Res. Chem. Intermed.* 2018, 44, 5271–5283.
- [236] J. Tharun, K. R. Roshan, A. C. Kathalikkattil, D-H. Kang, H-M. Ryu, D-W. Park., *RSC Adv* 2014, 40, 41266–41270.
- [237] H. Kisch, R. Millini, I-J. Wang., *Chem Ber* 1986, 119, 1090–1094.
- [238] J. Sun, S-I. Fujita, F. Zhao, M. Arai., *Appl Catal A Gen* 2005, 287, 221–226.
- [239] L. Cuesta-Aluja, A. Campos Carrasco, J. Castillaa, M. Reguero, A. M. Masdeu-Bultó, A. Aghmiz., *J. CO₂ Util.* 2016, 14, 10–22.
- [240] H. Vignesh Babu, K. Muralidharan., *Dalton Trans.*, 2013, 42, 1238–1248.
- [241] N. Eghbali, et al., *Green chemistry.* 2007, 213–215.

- [242] B. Wang, X-Y. Wu, O. A. Wong, B. Nettles, M-X. Zhao, D. Chen, Y. Shi., *J. Org. Chem.* 2009, 3986–3989.
- [243] S. Enthaler, K. Junge, M. Belle., *Angew. Chem. Int. Ed.* 2008, 47, 3317–3321.
- [244] M. B. Francis, E. N. Jacobsen., *Angew Chem Int Ed Engl* 1999, 38, 937–941.
- [245] K. A. Andrea, F. M. Kerton, *Polym J* 2021, 53, 29–46.
- [246] Britovsek George J.P, et al., *InorganicaChim. Acta* 2003, 345, 279–291.
- [247] R. Haddad, E. Yousif, A. Ahmed., *Springerplus* 2013, 2, 1–6.
- [248] A. Bencini, V. Lippolis., *Coord. Chem. Rev.* 2010, 254, 2096–2180.
- [249] N. C. Thacker, P. Ji, Z. Lin, A. Urban, W. Lin., *Faraday Discuss* 2017, 201, 303–315.
- [250] R. Thenarukandiyil, E. Paenurk, A. Wong, N. Fridman, A. Karton, R. Carmieli, G. Ménard, R. Gershoni-Poranne, G. de Ruiter., *Inorg. Chem.* 2021, 60, 18296–18306.
- [251] M. Reguero, Rovira i Virgili, 2023.
- [252] M. M. R. Bhuiyan, M. L. Mohammed, B. Saha et al., *Reactions* 2022, 3, 537–552.
- [253] C. Dinoi, M. Ciclosi, E. Manoury, L. Maron, L. Perrin, R. Poli., *Chem. Eur. J.* 2010, 16, 9572–9584.
- [254] L. Li, H-J. Song, X-G. Meng, R-Q. Yang, N. Zhang., *Tetrahedron Lett* 2018, 59, 2436–2439.
- [255] D. Prasetyoko, H. Fansuri, Z. Ramli, S. Endud, H. Nur., *Catal Letters* 2009, 128, 177–182.
- [256] A. M. Zima, O. Y. Lyakin, R. V. Ottenbacher, K. P. Bryliakov, E. P. Talsi., *ACS Catal* 2017, 7, 60–69.
- [257] H. Su, Z. Li, Q. Huo, J. Guan, Q. Kan, *RSC Adv* 2014, 4, 9990–9996.
- [258] A. A. Kori, F. M. Kerton., *Polym J* 2021, 53, 29–46.
- [259] J. Dongfeng, et al., *Appl Catal A Gen* 2000, 203, 329–333.

- [260] A. J. Kamphuis, F. Milocco, L. Koiter, P. Pescarmona, E. Otten., *ChemSusChem* 2019, 12, 3635–3641.
- [261] F. Chen, N. Liu, B. Dai., *ACS Sustain Chem Eng* 2017, 5, 9065–9075.
- [262] J. Sun, S-I. Fujita, B. M. Bhanage, M. Arai., *Catal Comm* 2004, 5, 83–87.
- [263] P. Ramidi, C.M.Felton, B.P. Subedic, H. Zhou, Z.R. Tian, Y. Gartiaa, B.S. Piercec, A. Ghosh., *J.CO₂ Util.* 2015, 9, 48–57.
- [264] Sun J, S-I Fujita, B. M. Bhanage, M. Arai., *Catal Today* 2004, 93–95, 383–388.
- [265] M. Aresta, A. Dibenedetto., *J Mol Catal* 2002, 182–183, 399–409.
- [266] C. Wang, Z. Sun, Y. Zheng, Y. Hang Hu., *J Mater Chem A Mater* 2019, 7, 865–887.
- [267] Y. Rambabu, U. Kumarb, N. Singhal, M. Kaushalb, M. Jaiswal, S. L. Jain, S. C. Roy., *Appl Surf Sci* 2019, 485, 48–55.
- [268] T. Kojima., *ChemPhotoChem* 2021, 5, 512–520.
- [269] X. Wu, J. Lang, Z. Sun, F. Jin, Y. Hang Hu., *Appl Catal B* 2021, 295, 120312
- [270] S. Fujimori, S. Inoue., *J Am Chem Soc* 2022, 144, 2034–2050.
- [271] R. Pruet, J. Smith., *J. Org. Chem.* 1969, 34, 327–330.
- [272] W. Itamar, D. Mandler, A. Riklin., *J Chem Soc Chem Commun* 1986, 1022–1024.
- [273] D. Hong, Y. Tsukakoshi, H. Kotani, T. Ishizuka, T. Kojima., *J Am Chem Soc* 2017, 139, 6538–6541.
- [274] S. L. Fung Chan, T. Lung Lam, C. Yang, S.C Yan, N. Man Cheng., *Chem Comm* 2015, 51, 7799–7801.
- [275] S. Muthuramalingam, M. Velusamy, R. Mayilmurugan., *Dalton Trans.* 2021, 50, 7984–7994.
- [276] Y. M. Albkuri, A. B. Rangu Magar, A. Brandt, H. A. Wayland, B. P. Chhetri, C. M. Parnell, P. Szwedo, A. Parameswaran-Thankam, A. Ghosh., *Catal Lett* 2020, 150, 1669–1678.

- [277] M. A. Bernd, F. Dyckhoff, B. J. Hofmann, A. D. Böth, J. F. Schlagintweit, J. Oberkofler, R. M. Reich, F. E. Kühn., *J Catal* 2020, 391, 548–561.
- [278] U. Herber, K. Hegner, D. Wolters, R. Siris, K. Wrobel, A. Hoffmann, C. Lochenie, B. Weber, D. Kuckling, S. Herres-Pawlis., *Eur J Inorg Chem* 2017, 2017, 1341–1354.
- [279] N. A. Carmo Dos Santos, M. Natali, E. Badetti, K. Wurst, G. Licini, C. Zonta., *Dalton Trans.* 2017, 46, 16455–16464.
- [280] Y. Yamazaki, H. Takeda, O. Ishitani., *J. Photochem. Photobiol. C* 2015, 25, 106–137.
- [281] J. X. Zhang, C-Y. Hu, W. Wang, H. Wang, Z-Y. Bian., *Appl Catal A Gen* 2016, 522, 145–151.
- [282] N. Sadeghi, M. Sillanpää., *Photochem. Photobiol. Sci.* 2021, 20, 391–399.
- [283] I. Bhugun, D. Lexa, J-M. Saveant., *J Am Chem Soc* 1996, 118, 1769–1776.
- [284] S. Lian, M. S. Kodaimati, E. A. Weiss., *ACS Nano* 2018, 12, 568–575.
- [285] M. Silva, A. Fernandes, Suse S. Bebiano, M. J. F. Calvete, M. F. Ribeiro, H. D. Burrowsa, M. M. Pereira., *Chem Comm* 2014, 50, 6571–6573.
- [286] R. A. W. Johnstone, M. G. Nunes, M. M. Pereira, A. M. d'A. Rocha Gonsalves, A. C. Serra., *Heterocycles* 1996, 43, 1423–1437.
- [287] M. Pineiro, A. L. Carvalho, M. M. Pereira, A. M. d'A. Rocha Gonsalves, L. G. Arnaut, S. J. Formosinho., *Chemistry - A European Journal* 1998, 4, 2299–2307.
- [288] Z. C. Sun, Y-B. She, Y. Zhou, X-F. Song, K. Li., *Molecules* 2011, 16, 2960–2970.
- [289] Y. Kuramochi, M. Kamiya, H. Ishida., *Inorg Chem* 2014, 53, 3326–3332.
- [290] P. G. Alsabeh, A. Rosas-Hernández, E. Barsch, H. Junge, R. Ludwig, M. Beller., *Catal Sci Technol* 2016, 6, 3623–3630.
- [291] P. J. DeLaive, T. K. Foreman, C. Giannotti, D. G. Whitten ., *J. Am. Chem. Soc.* 1980, 102, 5627–5631.
- [292] Y. Yamazaki, T. Onoda, J. Ishikawa, S. Furukawa, C. Tanaka, T. Utsugi, T. Tsubomura., *Front Chem* 2019, 7, 1–12.

- [293] Y. Tamaki, K. Koikec, O. Ishitani., *Chem Sci* 2015, 6, 7213–7221.
- [294] S. Matsuoka, K. Yamamoto, T. Ogata, M. Kusaba, N. Nakashima, E. Fujita, S. Yanagida., *J Am Chem Soc* 1993, 115, 601–609.
- [295] H. Rao, J. Bonin, M. Robert., *ChemSusChem* 2017, 10, 4447–4450.
- [296] L. Chen, Y. Qin, G. Chen, M. Li, L. Cai, Y. Qiu, H. Fan, M. Robert, T-C. Lau., *Dalton Trans.* 2019, 48, 9596–9602.
- [297] G. Klaus, S. Held., *Photochem. Photobiol.* 1993, 70, 135–145.
- [298] Z. Han, R. Eisenberg., *Acc Chem Res* 2014, 47, 2537–2544.
- [299] N. Sadeghi, M. Sillanpää., *Photochem. Photobiol. Sci.* 2021, 20, 391–399.
- [300] J. Grodkowski, D Behar, Pedatsur Neta, P G. Hambright., *J. Phys. Chem. A* 1997, 101, 248-254.
- [301] A. Gennaro, A. A. Isse, J-M. Savéant, M-G. Severin, E. Vianello., *J Am Chem Soc* 1996, 118, 7190–7196.
- [302] I. Bhugun, D. Lexa, J-M. Saveant., *J Am Chem Soc* 1994, 116, 5015–5016.
- [303] T. Arai, S. Sato, K. Uemura, T. Morikawa, T. Kajino, T. Motohiro., *Chem Comm* 2010, 46, 6944–6946.
- [304] L-L. Gracia, L. Luci, C. Bruschi, L. Sambri, P. Weis, O. Fuhr, C. Bizzarri., *Chem. Eur. J.* 2020, 26, 9929–9937.
- [305] L. Lou Gracia, E. Barani, J. Braun, A. B. Carter, O. Fuhr, A. K. Powell, K. Fink, C. Bizzarri., *ChemCatChem* 2022, 14, e202201163.
- [306] P. Krumholz, H. Li Chum, M. A. De Paoli, T. Rabockai., *J. electroanal. chem. Interfacial electrochem.* 1974, 51, 465–468.
- [307] E. Hasegawa, T. Seida, N. Chiba, T. Takahashi, H. Ikeda., *J. Org. Chem.* 2005, 70, 9632–9635.
- [308] E. Hasegawa, S. Takizawa, T. Seida, A. Yamaguchi, N. Yamaguchi, N. Chiba, T. Takahashi, H. Ikeda, K. Akiyama., *Tetrahedron* 2006, 62, 6581–6588.
- [309] C. Zhu, M. Gore, E S. Buckler, J. Yu., *Plant Genome* 2008, 1, 5–20.

[310] V. S. Thoi, Y. Sun, J. R. Long, C. J. Chang., *Chem Soc Rev* 2013, 42, 2388–2400.

[311] W. T. Eckenhoff, R. Eisenberg., *Dalton Trans.* 2012, 41, 13004–13021.

[312] S. Yin, X. Zhao, E. Jiang, Y. Yan, P. Zhou, P. Huo., *Energy Environ Sci* 2022, 15, 1556–1562.

CHAPTER 8: Appendix

8.1. Publications

- Nassima El Aouni, Claudia Lopez Redondo, Md Bin Yeamin, Ali Aghmiz, Mar Reguero, Anna M. Masdeu-Bulto: *Influence of structural properties of zinc complexes with N4-donor ligands on the catalyzed cycloaddition of CO₂ to epoxides into cyclic carbonates*'. J. Molecular Catalysis 538 (2023) 112992. Contents lists available at ScienceDirect.

8.2. Abbreviation lists

A

| | |
|-------|------------------------------|
| ACAN: | 9-Amino-10-cyanoanthracene |
| Ar: | Argon |
| Ap: | Artificial photosynthesis |
| atm: | Atmosphere |
| Al: | Aluminum |
| ATR: | Attenuated total reflection. |

B

| | |
|-------|---|
| BarF: | Tetrakis(3,5-bis(trifluoromethyl)phenyl)borate) |
| BIH: | 1,3-dimethyl-2-phenyl-2,3-dihydro-1H- benzo[d]imidazole |
| Bipy: | Bipyridine |

C

| | |
|---------------------|----------------------------|
| Cat : | Catalyst |
| CC : | Cyclic carbonate |
| CV : | Cyclic voltammetry |
| CO ₂ : | Carbon dioxide |
| Co-Cat: | Co-catalyst |
| CdCl ₃ : | Deuterated chloroform |
| CdCl ₂ : | Deuterated dichloromethane |
| Conv : | Conversion |
| Cl ₂ : | Chloride |
| CO: | Carbon monoxide |
| Co : | Cobalt |
| °C: | Celsius |
| cm: | Centimeter |
| Cu: | Copper |

D

| | |
|-------|----------------------|
| DMF: | Dimethylformamide |
| DMSO: | Dimethyl sulfoxide |
| DMA : | Dimethyl acetamide |
| d: | Doublet (NMR) |
| dd: | Double doublet (NMR) |
| DCM: | Dichloromethane |
| DME: | Dimethyl ether |

E

| | |
|---------|---|
| Esi-MS: | Electrospray ionization-Mass spectrometry |
| EtOH: | Ethanol |
| ED: | Electron Donor |
| EA: | Elemental analysis |

F

| | |
|--------|---|
| Fe: | Iron |
| FT-IR: | Fourier transform infrared spectroscopy |

G

| | |
|-----|--------------------|
| GC: | Gas chromatography |
|-----|--------------------|

H

| | |
|---------------------------------|--|
| H: | Hour |
| HPLC: | High-performance liquid chromatography |
| HCl: | Hydrochloric acid |
| H ₂ : | Dihydrogen |
| H ₂ O ₂ : | Hydrogen peroxide |

I

| | |
|-----|-----------------------|
| IR: | Infrared spectroscopy |
|-----|-----------------------|

L

| | |
|-----|------------|
| LA: | Lewis acid |
|-----|------------|

M

| | |
|-------|------------------|
| MeCN: | Acetonitrile |
| Mn: | Manganese |
| MHz: | Megahertz |
| MeOH: | Methanol |
| mmol: | Millimole |
| MW: | Molecular weight |
| M: | Molar |
| m: | Multiplet (NMR) |

N

| | |
|------------------|----------------------------|
| NMR : | Nuclear magnetic resonance |
| NMP: | N-methyl pyrrolidone |
| Ni: | Nickel |
| N ₂ : | Nitrogen |
| nm: | Nanometer |
| Nu: | Nucleophile |

O

| | |
|-------|----------|
| OTf : | Triflate |
|-------|----------|

P

| | |
|-------|-------------------|
| P : | Pressure |
| PP : | Porphyrin |
| PS: | Photosensitizer |
| ppm: | Parts per million |
| Phen: | Phenanthroline |
| Pd: | Palladium |

R

| | |
|----------|---|
| rt°: | Room temperature |
| RuBipy : | [Ru(bpy) ₃](PF ₆) ₂ : Tris(2,2'-bipyridine)ruthenium bis(hexafluorophosphate) |

S

| | |
|----------|-------------------|
| Subs: | Substrate |
| Select : | Selectivity |
| SD: | Sacrificial donor |
| SO: | Styrene oxide |
| s: | Singlet (NMR) |

T

| | |
|----------|-------------------------------------|
| TEA : | Triethylamine |
| TEOA : | Triethanolamine |
| THF : | Tetrahydrofuran |
| T° : | Temperature |
| TCD: | Thermal chromatography detector |
| t: | Time |
| TBAB : | Tetrabutylammonium bromide |
| TBAI : | Tetrabutylammonium iodide |
| TBHP : | Tert-butyl hydroperoxide |
| TPP : | Tetraphenyl porphyrin |
| TBuOOH : | Tertbutyl hydroperoxide |
| TOF : | Turn-over frequency Tetrahydrofuran |
| TON : | Turn-over number |

U

| | |
|----------|---------------------|
| Uv-vis : | Ultraviolet-visible |
|----------|---------------------|

Z

| | |
|-----------------------|--|
| Zn: | Zinc |
| ¹ H NMR : | Proton nuclear magnetic resonance |
| ¹³ C NMR : | Carbon nuclear magnetic resonance Aluminum |
| Λ _M : | Molar conductivity |
| δ : | Chemical shift (NMR) |



UNIVERSITAT
ROVIRA i VIRGILI